EFFECTS OF SILVER NANOPARTICLES ON *STAPHYLOCOCCUS AUREUS* ATCC 25923 AND *ESCHERICHIA COLI* ATCC 25922 PROTEIN PROFILES

Miss Hathaichanok Tamiyakul

A Dissertation Submitted in Partial Fulfillment of the Requirements
for the Degree of Doctor of Philosophy Program in Nanoscience and Technology
(Interdisciplinary Program)
Graduate School
Chulalongkorn University
Academic Year 2014

ผลของอนุภาคเงินนาโนต่อรูปแบบโปรตีนของ *Staphylococcus aureus* ATCC 25923 และ *Escherichia coli* ATCC 25922

นางสาวหทัยชนก เตมียกุล

วิทยานิพนธ์นี้เป็นส่วนหนึ่งของการศึกษาตามหลักสูตรปริญญาวิทยาศาสตรดุษฎีบัณฑิต
สาขาวิชาวิทยาศาสตร์นาโนและเทคโนโลยี (สหสาขาวิชา)
บัณฑิตวิทยาลัย จุฬาลงกรณ์มหาวิทยาลัย
ปีการศึกษา 2557

Thesis Title	EFFECTS OF SILVER NANOPARTICLES ON *STAPHYLOCOCCUS AUREUS* ATCC 25923 AND *ESCHERICHIA COLI* ATCC 25922 PROTEIN PROFILES
By	Miss Hathaichanok Tamiyakul
Field of Study	Nanoscience and Technology
Thesis Advisor	Associate Professor Warangkana Warisnoicharoen, Ph.D.
Thesis Co-Advisor	Professor Somboon Tanasupawat, Ph.D.
	Sittiruk Roytrakul, Ph.D.

Accepted by the Graduate School, Chulalongkorn University in Partial Fulfillment of the Requirements for the Doctoral Degree

.....Dean of the Graduate School
(Associate Professor Sunait Chutintaranond, Ph.D.)

THESIS COMMITTEE

.....Chairman
(Associate Professor Vudhichai Parasuk, Ph.D.)

.....Thesis Advisor
(Associate Professor Warangkana Warisnoicharoen, Ph.D.)

.....Thesis Co-Advisor
(Professor Somboon Tanasupawat, Ph.D.)

.....Thesis Co-Advisor
(Sittiruk Roytrakul, Ph.D.)

.....Examiner
(Associate Professor Pornthep Sompornpisut, Ph.D.)

.....Examiner
(Ratthapol Rangkupan, Ph.D.)

.....External Examiner
(Anon Thammasittirong, Ph.D.)

หทัยชนก เตมียกุล : ผลของอนุภาคเงินนาโนต่อรูปแบบโปรตีนของ *Staphylococcus aureus* ATCC 25923 และ *Escherichia coli* ATCC 25922 (EFFECTS OF SILVER NANOPARTICLES ON *STAPHYLOCOCCUS AUREUS* ATCC 25923 AND *ESCHERICHIA COLI* ATCC 25922 PROTEIN PROFILES) อ.ที่ปรึกษาวิทยานิพนธ์หลัก: รศ. ดร.วรางคณา วารีสน้อยเจริญ, อ.ที่ปรึกษาวิทยานิพนธ์ร่วม: ศ. ดร.สมบูรณ์ ธนาศุภวัฒน์, ดร.สิทธิรักษ์ รอยตระกูล, 113 หน้า.

อนุภาคเงินนาโนถูกสังเคราะห์ขึ้นจากปฏิกิริยารีดักชันทางเคมีโดยมีโซเดียมโบโรไฮไดรด์เป็นตัวรีดิวซ์ ในการศึกษานี้ ตัวปกคลุม 3 ชนิด (พอลิสไตรีน ซัลโฟนิก แอสิด โค มาเลอิก แอสิด, อัลจิเนต และคาราจีแนน) ถูกใช้ในการสังเคราะห์อนุภาคเงินนาโนเพื่อเปรียบเทียบคุณสมบัติของอนุภาคอีกทั้งคุณสมบัติการต้านแบคทีเรียเทียบกับอนุภาคเงินนาโนที่ไม่มีตัวปกคลุม การศึกษาพบว่าอนุภาคเงินนาโนที่มีตัวปกคลุมด้วยพอลิสไตรีน ซัลโฟนิก แอสิด โค มาเลอิก แอสิด ให้ผลการต้านแบคทีเรียที่ดีกว่าแบบอื่นๆ อนุภาคเงินนาโนชนิดนี้จึงถูกนำมาใช้ศึกษาคุณสมบัติการต้านแบคทีเรียและกลไกการต้านแบคทีเรียในเชื้อแบคทีเรียต้นแบบประเภท สแตฟฟีโลคอคคัส ออเรียส ซึ่งเป็นตัวแทนของแบคทีเรียแกรมบวกและเอสเชอริเชีย โคไล ซึ่งเป็นตัวแทนของแบคทีเรียแกรมลบด้วยเทคนิคโปรติโอมิกส์ เทคนิคโซเดียมโดดีซิลซัลเฟตพอลิอะคริลาไมด์เจลอิเล็กโตรโฟรีซิสและเทคนิคลิควิดโครมาโทกราฟี-แทนเดม แมสส์สเปกโทรเมตรี ถูกนำมาใช้ในการระบุรูปแบบโปรตีนและการบอกชนิดของโปรตีนตามลำดับ ผลการศึกษาพบว่าอนุภาคเงินนาโนที่สังเคราะห์ขึ้นออกฤทธิ์ในการฆ่าและทำลายเชื้อแบคทีเรียทั้งสองชนิดในระยะเวลาอันสั้น อย่างไรก็ตามหลังจากที่โปรตีนของแบคทีเรียต้นแบบทั้งแบบที่ทดสอบและไม่ได้ทดสอบด้วยอนุภาคเงินนาโนผ่านกระบวนการแยกโปรตีนด้วยวิธีอิเล็กโตรโฟรีซิสและย้อมสีแล้ว พบว่าทั้งสองแบบมีความแตกต่างกันของรูปแบบโปรตีนและการแสดงออกของโปรตีนอันเนื่องมาจากอนุภาคเงินนาโน ซึ่งสามารถตรวจสอบได้จากการระบุชนิดของโปรตีนและยีนออนโทโลยีจากฐานข้อมูลเอ็นซีบีไอและยูนิพร็อต ผลของการประมวลวิเคราะห์ข้อมูลและชีวสารสนเทศด้วยสตริงซอฟแวร์สรุปได้ว่า ความเป็นไปได้ของกลไกการต้านแบคทีเรียของอนุภาคเงินนาโนจากการศึกษานี้เกิดขึ้นจาก 6 กลไกหลัก ได้แก่ การแปรสัญญาณ การขนส่งโมเลกุล กระบวนการเมแทบอลิซึม การจำลองดีเอ็นเอ การสังเคราะห์อาร์เอ็นเอ และ การสังเคราะห์โปรตีน

สาขาวิชา วิทยาศาสตร์นาโนและเทคโนโลยี ลายมือชื่อนิสิต .....

ปีการศึกษา 2557 ลายมือชื่อ อ.ที่ปรึกษาหลัก .....

ลายมือชื่อ อ.ที่ปรึกษาร่วม .....

ลายมือชื่อ อ.ที่ปรึกษาร่วม .....

5387868520 : MAJOR NANOSCIENCE AND TECHNOLOGY
KEYWORDS: SILVER NANOPARTICLES / CAPPING AGENTS / ANTIBACTERIAL ACTIVITY / PROTEOMICS TECHNIQUE / BACTERIAL PROTEIN PROFILES / ANTIBACTERIAL MECHANISM

HATHAICHANOK TAMIYAKUL: EFFECTS OF SILVER NANOPARTICLES ON *STAPHYLOCOCCUS AUREUS* ATCC 25923 AND *ESCHERICHIA COLI* ATCC 25922 PROTEIN PROFILES. ADVISOR: ASSOC. PROF. WARANGKANA WARISNOICHAROEN, Ph.D., CO-ADVISOR: PROF. SOMBOON TANASUPAWAT, Ph.D., SITTIRUK ROYTRAKUL, Ph.D., 113 pp.

AgNPs were synthesized by the reductive sodium borohydride ($NaBH_4$) method. Three capping agents (4-styrenesulfonic acid – co – maleic acid (PSSMA), alginate, carrageenan) were used and compared with non-capping agent for characterization of particle properties and antibacterial testing. PSSMA capped AgNPs presented a better antibacterial susceptibility than AgNPs capped with others. The antibacterial activity and mechanism of PSSMA capped AgNPs on *Staphylococcus aureus* (*S. aureus*) and *Escherichia coli* (*E. coli*) were then investigated using proteomics technique. Sodium dodecyl sulfate polyacrylamide gel electrophoresis (SDS-PAGE) and liquid chromatography-tandem mass spectrometry (LC-MS/MS) were used for protein pattern observation and protein identification. From the result, the action of AgNPs against *S. aureus* and *E. coli* were determined to be bactericidal. SDS-PAGE gels after staining showed different bacterial protein profiles and protein expression between bacteria exposed and unexposed to AgNPs, which was further confirmed by protein identification and gene ontology based on NCBI and UniProt databases. In addition, data analysis and bioinformatics pathways analysis (String software) concluded that the possible antibacterial mechanism of AgNPs were based on 6 main functions i.e., signal transduction, molecular transport, metabolic process, DNA replication, transcription, and translation.

Field of Study:	Nanoscience and Technology	Student's Signature .....
		Advisor's Signature .....
Academic Year:	2014	Co-Advisor's Signature .....
		Co-Advisor's Signature .....

ACKNOWLEDGEMENTS

My sincerest gratitude would go my thesis advisor, Assoc. Prof. Dr. Warangkana Warisnoicharoen, and my thesis co-advisors, Prof. Dr. Somboon Tanasupawat and Dr. Sittiruk Roytrakul for their extensive support, valuable suggestion and assistance. It was my great pleasure to be one of their graduate students. They trained me to be a scientist, gave me lots of knowledge, skills and experiences, and also provided me many valuable opportunities to broaden my scientific life.

I would like to give my gratitude to my Ph.D. thesis examination committee members, Assoc. Prof. Dr. Vudhichai Parasuk, Assoc. Prof. Dr. Pornthep Sompornpisut, Dr. Ratthapol Rangkupan and Dr. Anon Thammasittirong, for their precious advices and time spent on my thesis and examination.

I would like to gratefully thank to the financial support from The 90th Anniversary of Chulalongkorn University Fund, Center of Innovative Nanotechnology (CIN) Research Fellowship, and Nanoscience and Technology Research Fund. Furthermore, I am grateful to Program of Nanoscience and Technology, Faculty of Graduate School, Chulalongkorn University for the valuable knowledge and experience. I also would like to thank the members of Proteomics Research Lab at National Center for Genetic Engineering and Biotechnology (BIOTEC), Microbiology lab at Faculty of Phamaceutical Sciences and Polyelectrolyte multilayer (PEM) lab at Chulalongkorn University and my friends for their valuable discussion and technical support. It was my pleasure to work with them.

Finally, I would like to express my deepest gratitude to my beloved family for their unconditional love, entirely care, understanding and encouragement. Without them, today would not come. Thank you my parents to be the greatest role model for my brother and me. Thank you for all of your support. Thank you for making my day!

CONTENTS

Page

THAI ABSTRACT iv

ENGLISH ABSTRACT v

ACKNOWLEDGEMENTS vi

CONTENTS vii

LIST OF TABLES xii

LIST OF FIGURES xiii

LIST OF ABBREVIATIONS xviii

CHAPTER I INTRODUCTION 1

1.1 Overview 1

1.2 Objectives 4

CHAPTER II THEORY AND LITERATURE REVIEW 5

2.1 Nanotechnology and nanoparticles 5

2.2 Silver nanoparticles 6

2.3 Synthesis of silver nanoparticles 8

2.3.1 Synthesis of silver nanoparticles using chemical reduction method 10

2.3.1.1 Reducing agents 10

2.3.1.2 Capping agents 11

2.3.1.2.1 Poly (4-styrenesulfonic acid – co – maleic acid) 11

2.3.1.2.2 Alginic acid or alginate 12

2.3.1.2.3 Carrageenan 12

2.4 Characterization of silver nanoparticles 13

Page

2.4.1 Ultraviolet-visible spectroscopy or ultraviolet-visible spectrophotometry 13
2.4.2 Zetasizer 15
2.4.2.1 Particle size 15
2.4.2.2 Zeta potential 15
2.4.3 Transmission electron microscopy (TEM) 18
2.5 Microorganisms 19
2.5.1 Bacteria 19
2.5.1.1 Staphylococcus aureus 21
2.5.1.2 Escherichia coli 22
2.6 Bacterial growth curve 23
2.6.1 Lag phase 24
2.6.2 Log phase 24
2.6.3 Stationary phase 25
2.6.4 Death phase 25
2.7 Silver nanoparticles and their antibacterial activity 25
2.8 Proteomics technique 27
2.8.1 Gel electrophoresis 28
2.8.1.1 One-dimensional gel electrophoresis technique 29
2.8.1.2 Two-dimensional gel electrophoresis technique 29
2.8.2 Mass spectrometry (MS) 30
2.8.2.1 Tandem mass spectrometry (MS/MS or Tandem MS) 31
2.8.3 Bioinformatics 32

Page

CHAPTER III EXPERIMENTAL 33
3.1 Preparation of silver nanoparticles 33
3.1.1 Chemicals and materials 33
3.1.2 Synthesis of silver nanoparticles 33
3.1.2.1 Non-capping agents 33
3.1.2.2 Capping agents (PSSMA, alginate and carrageenan) 34
3.1.3 Characterization of silver nanoparticles 36
3.1.3.1 Ultraviolet-visible spectroscopy 36
3.1.3.2 Zetasizer 37
3.1.3.3 Transmission electron microscopy (TEM) 37
3.2 Investigation of the antibacterial activity of silver nanoparticles 38
3.2.1 Chemicals and materials 38
3.2.2 Disc diffusion method 39
3.2.3 Bacterial growth curve 39
3.2.3.1 Preparation of bacteria 40
3.2.3.2 Preparation of silver nanoparticles 40
3.3 Studying of protein expression by sodium dodecyl sulfate polyacrylamide gel electrophoresis (SDS-PAGE) 41
3.3.1 Chemicals and materials 41
3.3.2 Collection and extraction of bacterial proteins 42
3.3.3 Protein determination by Lowry assay 43
3.3.4 Protein separation by SDS-PAGE 43
3.3.4.1 Preparation of samples for SDS-PAGE analysis 43

Page

3.3.4.2 Preparation of SDS-PAGE slab gel 43
3.3.4.3 Running condition 44
3.3.4.4 Gel staining 44
3.3.4.4.1 Silver staining 45
3.3.4.4.2 Coomassie brilliant blue G staining 46
3.4 Protein identification by liquid chromatography tandem mass spectrometry (LC-MS/MS) 47
3.4.1 Chemicals and materials 47
3.4.2 Excision of protein bands 47
3.4.3 In-gel digestion 48
3.4.4 LC-MS/MS analysis 49
3.4.5 Protein quantitation and identification 49
3.4.5.1 Protein quantitation 49
3.4.5.2 Protein identification and gene ontology 50
CHAPTER IV RESULTS & DISCUSSIONS 51
4.1 Synthesis and characterization of silver nanoparticles 51
4.1.1 Ultraviolet-visible Spectroscopy 51
4.1.2 Zetasizer 53
4.1.3 Transmission electron microscopy (TEM) 54
4.1.4 Particle size distribution 55
4.2 Investigation of antibacterial activity of silver nanoparticles 57
4.2.1 Disc diffusion method 57
4.2.2 Bacterial growth curve 59

Page

4.3 Protein separation by sodium dodecyl sulfate polyacrylamide gel electrophoresis (SDS-PAGE) 67
4.4 Protein identification by liquid chromatography tandem mass spectrometry (LC-MS/MS) 69
4.4.1 LC-MS/MS analysis 69
4.4.2 Protein identification and gene ontology 70
4.4.3 Bioinformatics pathways analysis 76
CHAPTER V CONCLUSIONS 84
REFERENCES 86
APPENDICES 103
VITA 113

LIST OF TABLES

Page

Table 2.1 Product categories with examples of products containing silver nanoparticles 7

Table 3.1 Characterization techniques of AgNPs. 36

Table 3.2 Preparation of SDS-PAGE separating and stacking gel for 90 x 80 x 1 mm mini-slab format gel size (proportion for 2 gels). 44

Table 3.3 Silver staining procedure for 90 x 80 x 1 mm gel. 45

Table 3.4 Coomassie brilliant blue G staining procedure for 90 x 80 x 1 mm gel. 46

Table 4.1 Effect of capping agents on zeta potential and average size of AgNPs (mean ± S.D., n =3). 53

Table 4.2 The identified proteins by LC-MS/MS with known functions. 73

Table A-1 Zone of inhibition (mm) of colloidal AgNPs prepared at different conditions against various kind of bacteria. (mean ± S.D., n= 3). 104

Table A-2 The effect of PSSMA on *S. aureus* ATCC 25923 growth 106

Table A-3 The effect of PSSMA on *E. coli* ATCC 25922 growth 107

Table A-4 Standard curve using BSA (OD 750 nm) by Lowry assay 108

Table A-5 Protein concentrations of *S. aureus* ATCC 25923 and *E. coli* ATCC 25922 after unexposed (control) and exposed to AgNPs with different time intervals. 110

Table A-6 Protein concentration of *S. aureus* ATCC 25923 and *E. coli* ATCC 25922 after unexposed to AgNPs (control) and amount of each component for SDS-PAGE analysis 111

Table A-7 Protein concentration of *S. aureus* ATCC 25923 and *E. coli* ATCC 25922 after exposed to AgNPs and amount of each component for SDS-PAGE analysis 112

LIST OF FIGURES

Page

Figure 1.1 The central dogma of biology and the omics trilogy (genomics, proteomics, metabolomics)..... 2

Figure 2.1 Nanomaterials dimensions on the metric scale (in nm)..... 5

Figure 2.2 Silver nanoparticles applications..... 6

Figure 2.3 The illustration of synthetic techniques of silver nanoparticles 9

Figure 2.4 The physical appearance and chemical structure of PSSMA..... 11

Figure 2.5 The physical appearance and chemical structure of alginate 12

Figure 2.6 The physical appearance and chemical structure of carrageenans..... 13

Figure 2.7 Zeta potential and related potential of a liquid particle 16

Figure 2.8 Operation of the Zetasizer Nano: Zeta potential measurements..... 16

Figure 2.9 Position of the basic components in a TEM 18

Figure 2.10 Evolutionary tree showing the common ancestry of all three domains of life, bacteria (blue color), eukaryotes (red color), and archaea (green color) and relative positions of some phyla are shown around the tree.... 19

Figure 2.11 Gram staining mechanism..... 20

Figure 2.12 (a) Scanning electron micrograph (SEM) of *S. aureus*, (b) Gram stain of *S. aureus* cells..... 21

Figure 2.13 (a) Scanning electron micrograph (SEM) of *E. coli*, (b) Gram stain of *E. coli* cells..... 22

Figure 2.14 Different phases of bacterial growth curve (kinetic curve). 23

Figure 2.15 Overview of experimental design for mass spectrometry-based proteomic studies..... 28

Page

Figure 2.16 Schematic graph of mass spectrometry (MS) 30

Figure 2.17 Schematic of tandem mass spectrometry (MS/MS) 31

Figure 3.1 Experimental setup for AgNPs synthesis with non-capping agents 34

Figure 3.2 Schematic of synthesis of silver nanoparticles by the chemical reduction method 35

Figure 3.3 Excision of protein bands 47

Figure 4.1 UV-vis absorbance spectra of AgNPs capped with three kinds of capping agents (PSSMA, alginate, carrageenan) and without capping agents 52

Figure 4.2 Transmission electron micrograph of the AgNPs with difference kinds of capping agents: (a) non-capping agent, (b) PSSMA, (c) alginate, and (d) carrageenan. Scale bar: 50 nm 54

Figure 4.3 Particle size distributions of the AgNPs with three kinds of capping agents: (a) PSSMA, (b) alginate, (c) carrageenan, (n = 250, of each sample) 56

Figure 4.4 The antibacterial susceptibility of *E. coli* ATCC 25922, *S. aureus* ATCC 25923, *L. salivarius* ATCC 11741, and *K. rhizophila* ATCC 9341 after tested with $AgNO_3$ (control) and AgNPs with capping agents, i.e., PSSMA, alginate, and carrageenan. Each bar represents mean ± S.D. of inhibition zone (mm) in each group 57

Figure 4.5 The bacterial growth of 0.05 OD (OD 600 nm) of *S. aureus* ATCC 25923 after exposed to AgNPs (solid line) compared with control (dashed line). The values for bacterial growth curve are the means of 6 replicates. Error bars indicate standard deviations of the means 59

Page

Figure 4.6 The bacterial growth of 0.05 OD (OD 600 nm) of *E. coli* ATCC 25922 after exposed to AgNPs (solid line) compared with control (dashed line). The values for bacterial growth curve are the means of 6 replicates. Error bars indicate standard deviations of the means..... 60

Figure 4.7 The antibacterial susceptibility of *Staphylococcus aureus* strains, (a) *S. aureus* ATCC 25923, (b) *S. aureus* ATCC 6538p and (c) *S. aureus* ATCC 43300, after exposed to AgNPs (solid line) compared with untreated control (dashed line). The values for bacterial growth curve are the means of 6 replicates. Error bars indicate standard deviations of the means 61

Figure 4.8 The antibacterial susceptibility of Gram-positive bacteria, (a) *S. epidermidis* ATCC 12228 and (b) *B. subtilis* ATCC 6633, after exposed to AgNPs (solid line) compared with untreated control (dashed line). The values for bacterial growth curve are the means of 6 replicates. Error bars indicate standard deviations of the means 62

Figure 4.9 The antibacterial susceptibility of Gram-negative bacteria, (a) *E. coli* ATCC 25922, (b) *En. aerogenes* ATCC 13048 and (c) *Ps. aeruginosa* ATCC 27853, after exposed to AgNPs (solid line) compared with untreated control (dashed line). The values for bacterial growth curve are the means of 6 replicates. Error bars indicate standard deviations of the means..... 63

Figure 4.10 The S-shaped growth of 0.1 OD (OD 600 nm) of *S. aureus* ATCC 25923 and *E. coli* ATCC 25922 after up-scaled study..... 64

Page

Figure 4.11 The bacterial growth of 0.1 OD (OD 600 nm) of *S. aureus* ATCC 25923 after exposed (solid line) and unexposed (dashed line) to AgNPs. The values for bacterial growth curve are the means of 4 replicates. Error bars indicate standard deviations of the means 65

Figure 4.12 The bacterial growth of 0.1 OD (OD 600 nm) of *E. coli* ATCC 25922 after exposed (solid line) and unexposed (dashed line) to AgNPs. The values for bacterial growth curve are the means of 4 replicates. Error bars indicate standard deviations of the means 66

Figure 4.13 Pattern of total protein extracted from *S. aureus* ATCC 25923 after (a) unexposed and (b) exposed to AgNPs at 7 different incubation times 67

Figure 4.14 Pattern of total protein extracted from *E. coli* ATCC 25922 after (a) unexposed and (b) exposed to AgNPs at 7 different incubation times 68

Figure 4.15 The 11 excised ranges (follow the horizontal lines) of protein expression extracted from (a) *S. aureus* ATCC 25923 and (b) *E. coli* ATCC 25922 after unexposed to AgNPs (control). 69

Figure 4.16 The 11 excised ranges (follow the horizontal lines) of protein expression extracted from (a) *S. aureus* ATCC 25923 and (b) *E. coli* ATCC 25922 after exposed to AgNPs. 70

Figure 4.17 Identified proteins from *E. coli* ATCC 25922 and *S. aureus* ATCC 25923 after exposed to AgNPs analyzed by LC-MS/MS (*: free areas of *E. coli*_control, *E. coli*_AgNPs, *S. aureus*_control, *S. aureus*_AgNPs, and $^{+}$: intersection areas of free areas of *E. coli*_control and AgNPs, and *S. aureus*_control and AgNPs). 71

Page

Figure 4.18 Significant identified proteins from (a) *S. aureus* ATCC 25923 and (b) *E. coli* ATCC 25922 after exposed to AgNPs (excluding unknown protein symbols and functions) 76

Figure 4.19 Interaction network of matched categories for *S. aureus* ATCC 25923. Thicker lines indicate higher confidence and higher number of interactions described by String database 77

Figure 4.20 Interaction network of matched categories for *E. coli* ATCC 25922. Thicker lines indicate higher confidence and higher number of interactions described by String database 79

Figure 4.21 Schematic representation of antibacterial mechanism of AgNPs 82

Figure A-1 The bacterial growth curve of *S. aureus* ATCC 25923 after exposed to PSSMA and AgNPs compared with control 106

Figure A-2 The bacterial growth curve of *E. coli* ATCC 25922 after exposed to PSSMA and AgNPs compared with control 107

Figure A-3 The BSA standard curve (OD 750 nm) 108

LIST OF ABBREVIATIONS

^{o}C	Degree celsius
µg/µL	Microgram per microliter
µL	Microliter
µL/min	Microliter per minute
%	Percentage
λ_{max}	The maximum wavelength
2D-PAGE	Two-dimensional gel electrophoresis
ACN	Acetonitrile
$AgNO_3$	Silver nitrate
AgNPs	Silver nanoparticles
Ambic	Ammonium bicarbonate
APS	Ammonium persulfate
BSA	Bovine serum albumin
CID	Collision-induced dissociation
cm	Centimeter (s)
DLS	Dynamic light scattering
d. nm.	The diameter in nanometer
DTT	Dithiothreitol
et al.	et alii
EtOH	Ethanol
FA	Formic acid
g	Gram (s)

LIST OF ABBREVIATIONS (CONT.)

GO	Gene ontology
h	Hour (s)
IAA	Iodoacetamide
i.e.	id est (that is)
IEF	Isoelectric focusing
kV	Kilovolts
LC	Liquid chromatography
LC-MS/MS	Liquid chromatography tandem mass spectrometry
LDE	Laser Doppler electrophoresis
LDV	Laser Doppler velocimetry
MeOH	Methanol
min	Minute (s)
ml	Milliliter (s)
mm^3	Cubic millimeter
mm	Millimeter (s)
mM	Millimolar (s)
MRSA	de Man, Rogosa and Sharpe agar
MRSA	Methicillin-resistant *Staphylococcus aureus*
MS	Mass spectrometry
mV	Millivolt (s)
m/z	Mass to charge ratios
$NaBH_4$	Sodium borohydride

LIST OF ABBREVIATIONS (CONT.)

NaCl	Sodium chloride
NCBI	The National Center for Biotechnology Information
ng	Nanogram (s)
nm	Nanometer (s)
O_2	Oxygen
OD	Optical density
pH	Potential of hydrogen ion
pI	Isoelectric points
PSSMA	Poly (4-styrenesulfonic acid-co-maleic acid)
rpm	Revolutions per minute
SDS	Sodium dodecyl sulfate
SDS-PAGE	Sodium dodecyl sulfate polyacrylamide gel electrophoresis
SPR	Surface plasmon resonance
STRING	The Search Tool for the Retrieval of Interacting Genes/Proteins
TEM	Transmission electron microscopy
TEMED	Tetramethylethylenediamine
TOF	Time of flight
TSA	Tryptic (trypticase) soy agar
TSB	Tryptic (trypticase) soy broth
VRSA	Vancomycin-resistant *Staphylococcus aureus*

CHAPTER I
INTRODUCTION

1.1 Overview

Nowadays, the growing of nano-products on the markets around the world continues increasing. More than 1,300 nanotechnology-based consumer products, produced by about 580 companies located in 30 countries have been reported [1]. Especially, the silver-embedded products have been popularly used because of the distinctive antibacterial properties of AgNPs.

Silver nanoparticles (AgNPs) are classified as metal nanoparticles with sizes in between 1 - 100 nm. There are two main methods to synthesize AgNPs. The first one is a physical method such as laser ablation, gamma-irradiation, and arc-discharge method [2]. The second one is a chemical method such as chemical reduction [3], photochemical method [4], and sonochemical method [5]. However, the most common method to synthesize AgNPs is the chemical reduction of silver salt by using a reducing agent such as hydrazine, citrate, and sodium borohydride. Moreover, a capping agent or a stabilizing agent such as polyelectrolytes or other polymers is used to protect the nanoparticle agglomeration [2].

AgNPs have gained much interest as they show deviating physico-chemical properties and biological activities compared to regular silver metal. AgNPs have been used in a vast range of applications because of their distinctive properties, such as good conductivity, chemical stability, catalytic and especially antimicrobial activities [6]. AgNPs represent a new generation of antibacterial and their activity appears significantly high. AgNPs have a broad range of antibacterial activity for both Gram-negative and Gram-positive bacteria, including *Escherichia coli*, *Staphylococcus aureus*, *Bacillus subtilis*, *Streptococcus mutans*, and *Staphylococcus epidermidis* [7].

That is the reason why AgNPs are applied in numerous consumer products including food storage containers, textiles, cosmetics, home appliances, paints, and etc. [8].

However, up to now, there have been no clear pathways for AgNPs affecting bacterial growth. Four possible antimicrobial mechanisms have been proposed: (1) interference with cell wall synthesis [9-12], (2) inhibition of protein synthesis [11, 12], (3) interference with nucleic acid synthesis [11, 12], and (4) inhibition of a metabolic pathway [11-13]. In order to get a better insight how AgNPs affect bacterial growth and bacterial protein profiles, the proteomics approach is concerned.

Proteomics is the second part of the omics trilogy. Normally, the omics trilogy is based on the central dogma of biology: genomics, proteomics, metabolomics as shown in Figure 1.1 [14]. Proteomics is a molecular tool that is a large scaled study of protein properties, for example expression level, post-translational modification, and interactions. The study can obtain a global, integrated view of disease processes, cellular processes and networks at the protein level [15]. With the complete genome-sequencing project, proteomics can be defined as the systematic analysis of proteome. This technology allows the global analysis of gene products in various tissues and physiological states of cells [16].

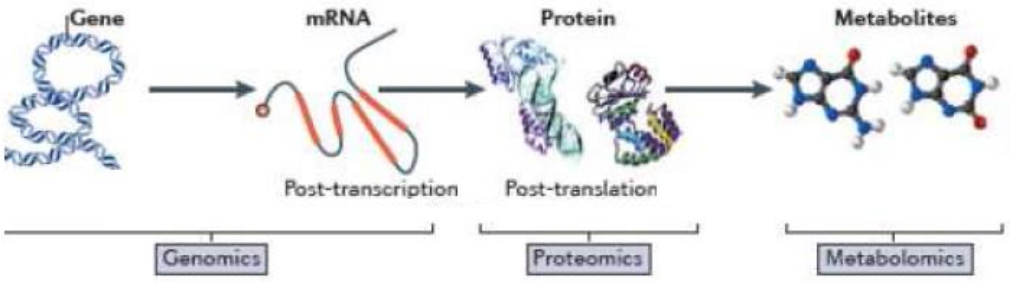

Figure 1.1 The central dogma of biology and the omics trilogy (genomics, proteomics, metabolomics) [14].

The proteomics technique facilitates the investigation of the global protein expression profile usually by using gel electrophoresis, two-dimensional gel electrophoresis (2D-PAGE) technique and one-dimensional gel electrophoresis (SDS-PAGE) technique, to separate the mixtures of proteins coupled with protein identification by mass spectrometry (MS) [17, 18]. Furthermore, protein information done in a real laboratory can be complemented by virtual experiments performed on computers (bioinformatics). These studies provide not only identification of proteins but also further characterization ranging from the calculation of basic physicochemical properties to the prediction of potential post-translational modifications and three-dimensional structures [19, 20]

Although there are few researches [7, 21] studying antibacterial effect of AgNPs by proteomics approach, there are still limited data on protein profiles of bacteria after exposed to AgNPs and the antibacterial mechanisms of AgNPs. The reasons probably are that bacterial proteins profiles depend on many factors such as kinds of bacteria and AgNPs, laboratory protocol, time consuming and costliness. Therefore, systematical investigation on proteins profiles of treated bacteria relevant to antibacterial mechanisms of AgNPs was performed in this study. The bacterial protein profiles after exposed and unexposed to AgNPs were observed. This research leads to further understand the antibacterial mechanism of AgNPs which could be applied on the design of nanoparticles for antibacterial purposes.

1.2 Objectives

1.2.1 To synthesize silver nanoparticles.

1.2.2 To characterize silver nanoparticles by using UV-vis spectroscopy, laser Doppler electrophoresis, dynamic light scattering and transmission electron microscopy.

1.2.3 To investigate the antibacterial activity of silver nanoparticles on Gram-positive and Gram-negative bacteria.

1.2.4 To investigate and compare the bacterial protein profiles between exposed and unexposed to silver nanoparticles.

1.2.5 To determine the effect of silver nanoparticles on bacterial protein profiles of *Staphylococcus aureus* ATCC 25923 and *Escherichia coli* ATCC 25922.

CHAPTER II

THEORY AND LITERATURE REVIEW

2.1 Nanotechnology and nanoparticles

Since 1959, the concept of nanotechnology have been introduced by Richard Feynman in the lecture ‘‘There is Plenty of Room at the Bottom’’ at a meeting of the American Physical Society [21]. Since then, nanotechnology becomes the tremendous field which well known in many studies area.

Nanotechnology is a disciplinary field, usually based on chemistry, physics, engineering and biology. It is defined as the understanding and manipulation of matter on an atomic or molecular scale, at dimensions of roughly 1–100 nm (Figure 2.1) [22], where unique physical properties make novel applications possible [23].

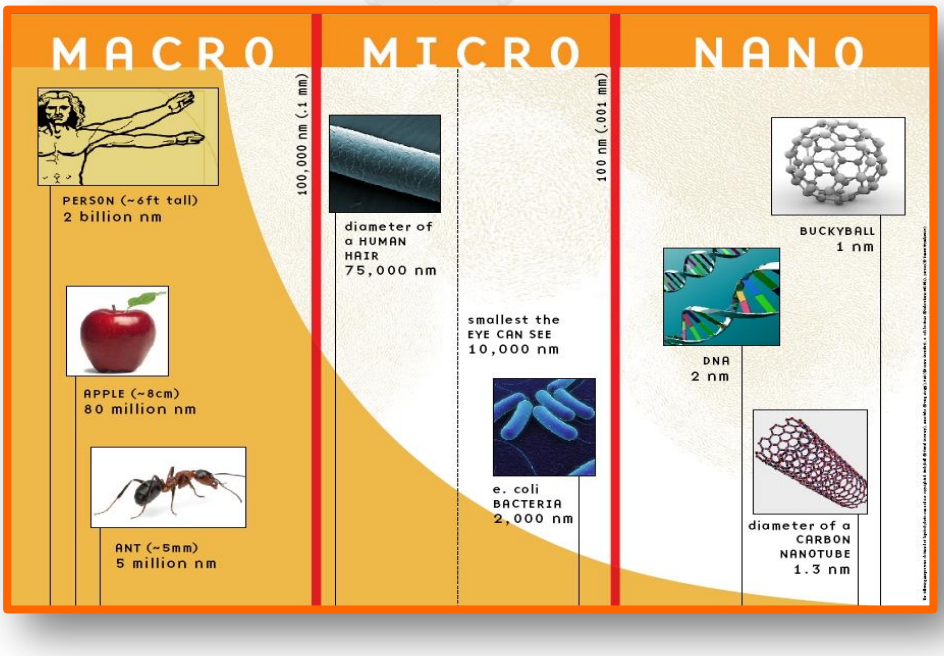

Figure 2.1 Nanomaterials dimensions on the metric scale (in nm) [22].

Therefore, nanoparticles are particles that have at least one dimension in the range of 1 to 100 nm. Nanoparticles are classified based on their size, and may or may not exhibit size-related properties that differ significantly from those observed in bulk materials [24, 25]. These kind of particle can be spherical, tubular, or irregularly shaped and can exist in fused, aggregated, or agglomerated forms [23].

2.2 Silver nanoparticles

Silver nanoparticles (AgNPs) are fine particles of metallic silver that have at least one dimension less than 100 nm. In the nanoscale, AgNPs have unique features compared with regular silver metal or bulk silver metal. According to their small size, there are the higher surface area per mass and the ability to adsorb and carry other compounds [24]. AgNPs is not a new discovery; it has been known for over 100 years, and nowadays it is being used in numerous technologies and incorporated into a wide array of consumer products that take advantages of their desirable optical, conductive, diagnostic and especially antibacterial properties as shown in Figure 2.2.

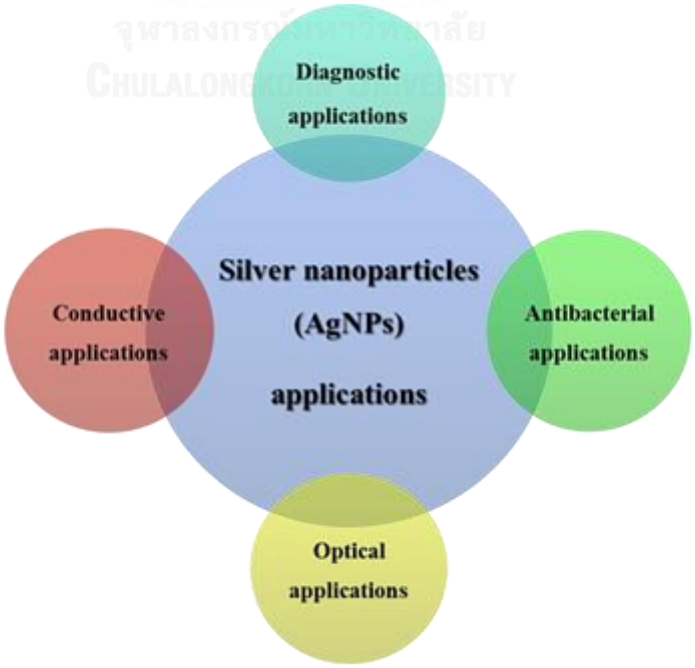

Figure 2.2 Silver nanoparticles applications.

As mentioned above, AgNPs are interesting because of the unique properties (e.g., size and shape dependent optical, electrical, and magnetic properties) which can be incorporated into antimicrobial applications, composite fibers, biosensor materials, cosmetic products, cryogenic superconducting materials and electronic components. The products are categorized according to their applications as presented in Table 2.1 [26].

Table 2.1 Product categories with examples of products containing silver nanoparticles [26].

Categories	Subcategories	Examples
Personal care and cosmetics	Skin care	(Body) cream, hand sanitizer, hair care products, beauty soap, face masks
	Oral hygiene	Tooth brush, teeth cleaner, toothpaste
	Hair care	Hair brush, hair masks
	Cleaning	Elimination wipes and spray
	Coating	Make-up instrument, watch chain
	Baby care	Pacifier, teeth developer
	Over the counter health products	Foam condom
Textile and shoes	Clothing	Fabrics and fibers, socks, shirts, caps, jackets, gloves, underwear
	Other textiles	Sheets, towels, shoe care, sleeves and braces
	Toys	Plush toys

Categories	Subcategories	Examples
Electronics	Personal care	Hair dryers, wavers, irons, shavers
	Household appliances	Refrigerators, washing machines
	Computer hardware	Notebooks, (laser) mouse, keyboards
	Mobile devices	Mobile phones
Household products/home improvement	Cleaning	Cleaning products for bathrooms, kitchens, toilets, detergents, fabric softener
	Coating	Spray, paint supplements
	Furnishing	Pillows
	Furnishing/coating/flooring	Showerheads, locks, water taps, floors, tiles
Filtration, purification, Neutralization, sanitation	Filtration	Air filters, ionic sticks
	Cleaning	Disinfectant and aerosol sprays

2.3 Synthesis of silver nanoparticles

The antibacterial activity of colloid silver particles is influenced by the dimensions of the particles in that the smaller the particles, the greater antibacterial effect [9, 27, 28]. Therefore, the main challenge in AgNPs synthesis is the control of their characteristics such as shape, stability and specially particle size distribution [29]. Basically, there are two broad areas of synthetic techniques for AgNPs (Figure 2.3), namely, physical method and chemical method.

Figure 2.3 The illustration of synthetic techniques of silver nanoparticles [30].

Physical method is currently in use for the synthesis of commercial production of nanostructure materials. Most importantly physical approaches include evaporation-condensation and laser ablation [31]. The advantages of physical over chemical methods are the uniformity of nanoparticle distribution and the relative absence of solvent contamination. However, its disadvantages are needs of expensive instrument for diminishing of sampled particles and its imperfection of the surface structure [29, 31].

Chemical method typically involves wet chemistry techniques. The popular chemical approaches, including chemical reduction, photochemical method, sonochemical method, and etc. The primary advantages of chemical method over physical methods are more homogeneous and stable suspensions of AgNPs with the ability to tune their size and shape as well as to functionalize with capping ligands for specific applications [29, 32].

2.3.1 Synthesis of silver nanoparticles using chemical reduction method

The most common and popular approach for synthesis of AgNPs is chemical reduction method. The chemical reduction method usually starts with silver ion precursor (silver nitrate, $AgNO_3$), which is reduced in a chemical reaction with a reducing agent and capping agent, then nanoparticles are formed through nucleation and growth [33].

2.3.1.1 Reducing agents

The reducing agents can refer to any chemical agents, biological agents or even plant extracts that can provide free electrons to reduce silver ions and lead to the formation of AgNPs [34]. For the AgNPs synthesis, various reducing agents are reported, for example; sodium citrate, hydrazine, sodium borohydride ($NaBH_4$), ethanol, Tollens reagent, N, N-dimethylformamide (DMF) and ethylene glycols [35-37].

Sodium borohydride ($NaBH_4$) is extensively used as reducing agent for synthesis of AgNPs because of its strong reductant. Nikolaj and coworkers [38] revealed that the strong and fast reducing agents cause the formation of numerous silver seeds at the beginning of the synthesis process, reducing the time of growth and preventing the formation of larger particles [9]. With these processes, the sizes of AgNPs are relatively small and monodisperse [9, 31, 38]. However, for the chemical reduction, capping agents or stabilizing agents are needed to stabilize the nanoparticles in suspension [29].

2.3.1.2 Capping agents

The capping agents or stabilizing agents are used to provide nanoparticle stability. Capping agents can stabilize dispersive nanoparticles during the course of metal nanoparticle preparation, protect each nanoparticles from being absorbed or bound onto other nanoparticle surfaces, and finally avoid AgNPs agglomeration [39].

The capping agents including surfactants, such as sodium dodecyl sulfate (SDS), ligands and especially polymers such as poly (vinyl alcohol), poly (vinylpyrrolidone), poly (ethylene glycol), etc. [40, 41] are extensively used for prevention of the aggregation and agglomeration of AgNPs.

2.3.1.2.1 Poly (4-styrenesulfonic acid – co – maleic acid)

Poly (4-styrenesulfonic acid – co – maleic acid) (PSSMA, sodium salt) is anionic polyelectrolyte which is a copolymer of styrenesulfonic acid and maleic acid. The physical appearance and chemical structure of PSSMA are shown in Figure 2.4 [42]. Due to their weak polyelectrolytes which contain both strong (sulfonate) and weak (carboxylate) negatively charging units [43], PSSMA comes to be adjustable polyelectrolytes that are widely developed polyelectrolytic multilayer thin films for biomaterial or drug releasing.

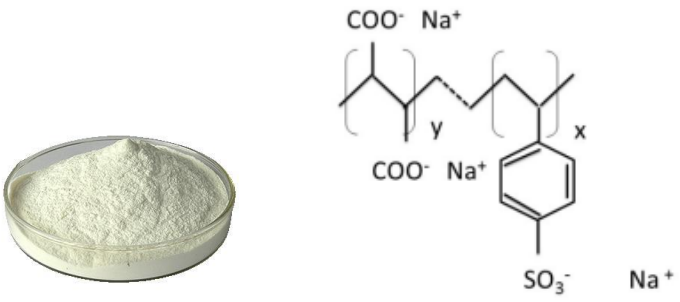

Figure 2.4 The physical appearance and chemical structure of PSSMA [42].

2.3.1.2.2 Alginic acid or alginate

Alginate is anionic polysaccharides which are the natural polysaccharide from the cell walls of brown algae. Moreover, alginate is biocompatible, non-toxic, inexpensive, and biodegradable. The structure of alginate is a linear copolymer with homopolymeric blocks of mannuronic acid (M) and guluronic acid (G), covalently linked together in different sequences or blocks. The physical appearance and chemical structure of alginate are shown in Figure 2.5 [42].

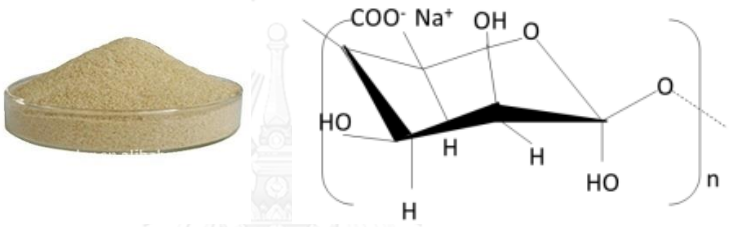

Figure 2.5 The physical appearance and chemical structure of alginate [42].

2.3.1.2.3 Carrageenan

Carrageenan is anionic polysaccharides which are a family of linear sulfated polysaccharides extracted from red seaweeds. Typically, there are three kinds of carrageenan, according to the degree of sulfation: 1) kappa (K)-carrageenan has one sulfate per disaccharide, 2) iota (I)-carrageenan has two sulfates per disaccharide, and 3) lambda (**λ**)-carrageenan has three sulfates per disaccharide. The primary differences among them are the number and position of the ester sulfate groups on the repeating galactose units.

Higher levels of ester sulfate lower the solubility temperature of the carrageenan and produce lower strength gels, or contribute to gel inhibition [44]. The physical appearance and chemical structure of carrageenans are shown in Figure 2.6 [45]. Carrageenans are large and flexible molecules so they have the ability to form various gels at room temperature and are used as thickening and stabilizing agents.

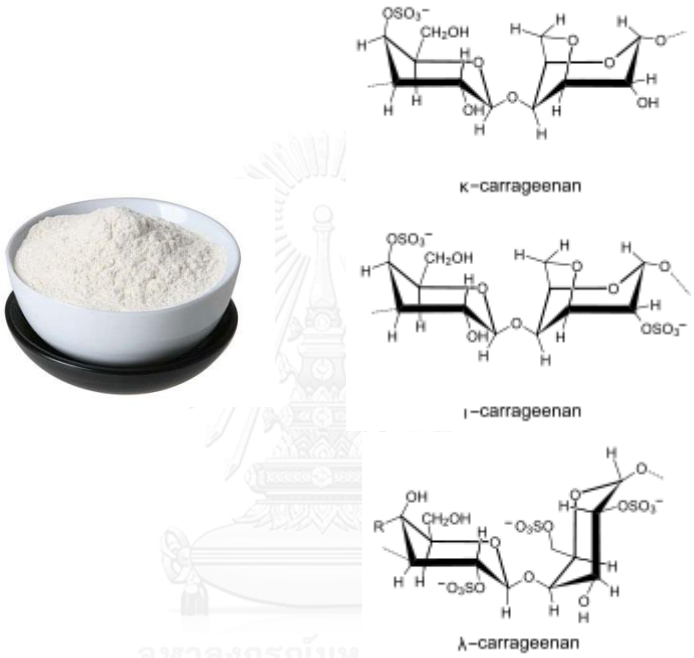

Figure 2.6 The physical appearance and chemical structure of carrageenans [45].

2.4 Characterization of silver nanoparticles

2.4.1 Ultraviolet-visible spectroscopy or ultraviolet-visible spectrophotometry

Ultraviolet-visible spectrophotometry or UV-vis spectrophotometry refers to absorption spectroscopy or reflectance spectroscopy in the ultraviolet-visible spectral region. As its name, UV-vis spectrophotometry automatically scans all the components, with the light sources range from 200 to 400 nm for ultraviolet (UV)

regions or from 400 to 800 nm for visible (VIS) regions [46]. The functioning of UV-vis spectrophotometry starts from a beam of light (UV or VIS lights) from a light source separating into its component wavelengths by a prism or diffraction grating. Then, each monochromatic beam which has a single wavelength splits into two equal intensity beams by a half-mirrored device. The reference beam passes through an identical cuvette containing the solvent, as well as one another beam, the sample beam, passes through a cuvette containing a sample solution. The intensities of both two light beams are then measured by electronic detectors and then compared [47].

When molecules of sample are exposed to light having energy which are matched a possible electronic transition within the molecule, molecules will absorb the energy in the form of ultraviolet or visible light to excite these electrons to higher energy orbitals [48]. An optical spectrometer records the wavelengths at which absorption occurs, together with the degree of absorption at each wavelength. The resulting spectrum is presented as a graph of absorbance (A) versus wavelength (**λ**), and the wavelength of maximum absorbance is a characteristic value of each compound, designated as λ_{max} [46, 49].

The applications of UV-vis spectrophotometry are extensive. It is a physical technique that routinely used in analytical chemistry for quantitative determination of different analytes, such as transition metal ions, biological macromolecules, and highly conjugated organic compounds. Also, the absorbance can be used to measure the concentration of a solution by using Beer-Lamberts Law.

Typically, solutions of colloidal AgNPs have distinctive yellow color according to their oscillation of electrons on the nanoparticles surface which is called surface plasmon resonance (SPR) [50]. The spherical AgNPs has unique property of SPR peak wavelength (λ_{max}) around 400 nm, and can be tuned by the size and shape of nanoparticles [51].

2.4.2 Zetasizer

The Zetasizer provides the ability to measure the average size of nanoparticles and the zeta potential or surface charge of the nanoparticles [52]. Moreover, these parameters can be measured over a wide range of concentrations.

2.4.2.1 Particle size

Particle size is the diameter of the sphere that diffuses at the same speed as the particle which is being measured. Particle size influences many properties of particulate nanomaterials as valuable as indicator of quality and performance of nanoparticles. Normally, the particles in a liquid move randomly and their speed of movement is used to determine the size of the particle. Therefore, the zetasizer system determines the size of nanoparticles by measuring the Brownian motion or diffusion of the particles in a sample using dynamic light scattering (DLS) [29, 53, 54].

2.4.2.2 Zeta potential

Zeta potential is a scientific term for electrokinetic potential in colloidal systems [55]. It is a measure of the magnitude of the repulsion or attraction between particles. Figure 2.7 shows the zeta potential which is a potential exists between the particle surface and the dispersing liquid which varies according to the distance from the particle surface [52].

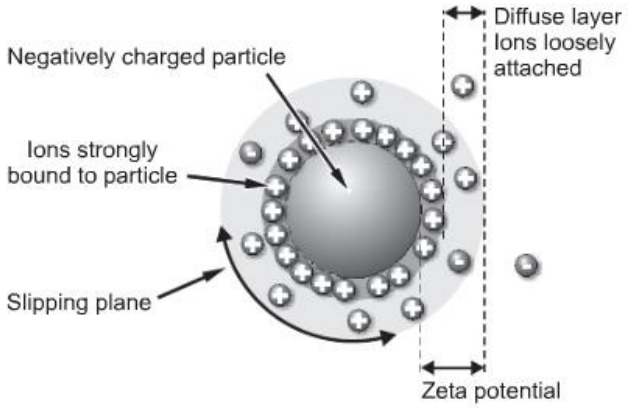

Figure 2.7 Zeta potential and related potential of a liquid particle [52].

Typically, colloidal AgNPs contain ions that can be negatively and positively charges called anions and cations, respectively. In order to get zeta potential or surface charge of nanoparticles, zetasizer is working for the data according to Figure 2.8.

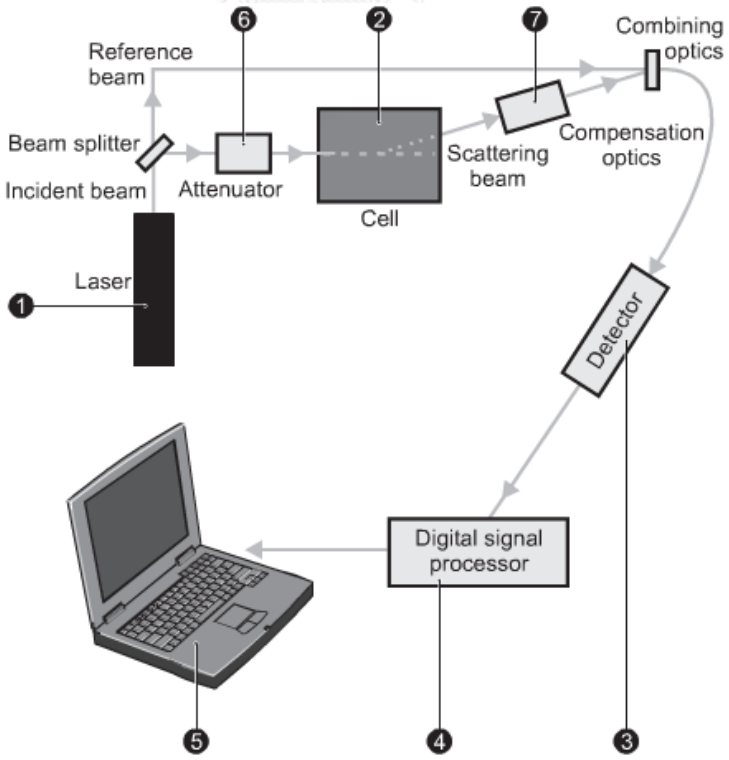

Figure 2.8 Operation of the Zetasizer Nano: Zeta potential measurements [52].

Zetasizer using a combination of the two measurements techniques both electrophoresis and laser Doppler velocimetry (LDV) namely laser Doppler electrophoresis to measure zeta potential [53, 56]. An electric field is first applied to the nanoparticles, resulting in the acceleration of the particles [38]. Light, scattered by moving particles, alters frequency. The interference between the scattered light and original beam provides a modulated signal. After that the frequency analysis leads to electrophoretic mobility (U_E), and zeta potential of the particle can be obtained by application of the Henry equation [52, 57]. The Henry equation is:

$$U_E = \frac{2\varepsilon z\, f(ka)}{3h} \qquad (1)$$

U_E = electrophoretic mobility

z = zeta potential (millivolt; mV)

ε = dielectric constant (Farads per meter; F/m)

h = viscosity (Pascal second; Pa s)

$f(ka)$ = Henry's function

Two values are generally used as approximations for the f (Ka) determination - either 1.5 or 1.0.

Duzgunes [58] revealed that nanoparticles with a zeta potential above (±) 30 mV have been shown to be stable in suspension, as the surface charge prevents aggregation of the particles. Therefore, the zeta potential of the sample will frequently determine whether particles within a liquid will tend to flocculate or remain stable or not [58].

2.4.3 Transmission electron microscopy (TEM)

Transmission electron microscopy or TEM operates on the same basic principles as light microscopy; however, it uses electrons instead of light. From this technique, a high energy electron beam is transmitted through a specimen to image and analyze materials with atomic scale resolution. The electrons are focused with electromagnetic lenses and then an image (formed from the interaction of the electrons with the sample) is magnified and focused onto an imaging device, such as a fluorescent screen, a photographic film or detected by a CCD camera as shown in Figure 2.9 [59, 60]. Due to the electrons are accelerated at several hundred kV, giving wavelengths much smaller than that of light, TEM is possible to get higher resolution than light microscopes [59].

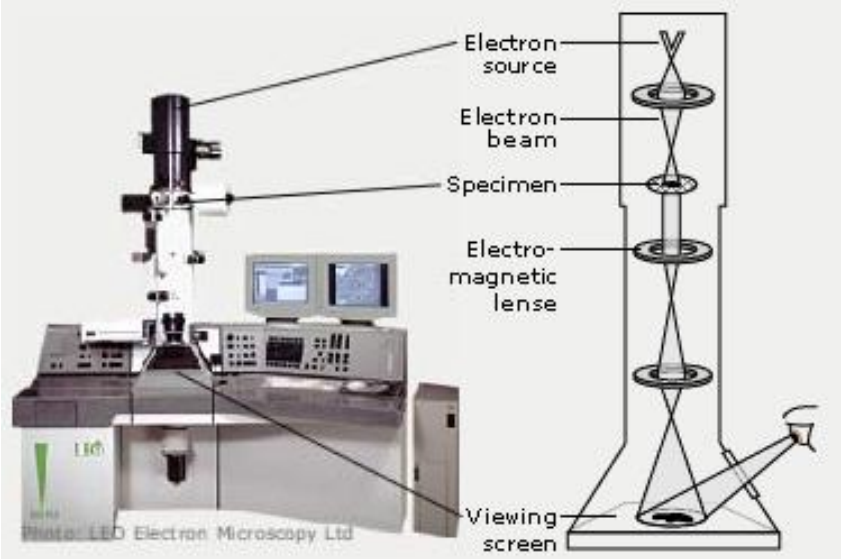

Figure 2.9 Position of the basic components in a TEM [61].

TEM has been used in biological and biomedical areas for investigations because of its ability to view the finest cell structures. It is also used as a diagnostic tool in hospital pathology labs. Furthermore, metallurgists use it to image atoms and identify the elements in material research.

2.5 Microorganisms

Microorganism or microbe is an organism that is unicellular or lives in a colony of cellular organisms. Microorganisms are very diverse, including bacteria, fungi, yeast, protist, microscopic plants such as algae and also in animals such as plankton, etc. as shown in the three domains of life's tree (Figure 2.10).

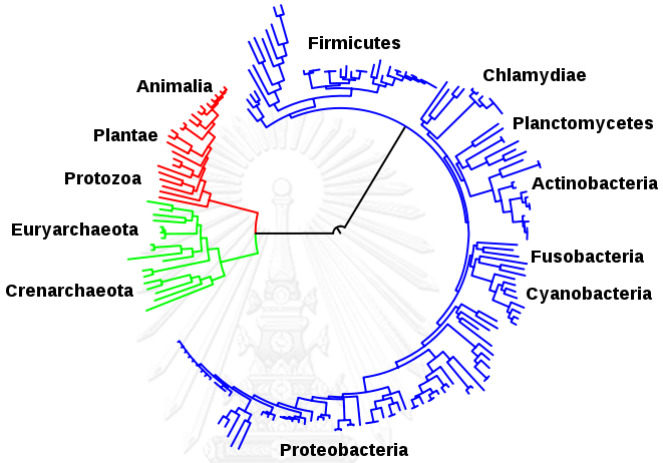

Figure 2.10 Evolutionary tree showing the common ancestry of all three domains of life, bacteria (blue color), eukaryotes (red color), and archaea (green color) and relative positions of some phyla are shown around the tree [62].

2.5.1 Bacteria

Bacteria are single celled microbes which is a main group of prokaryote microorganisms. They have a wide range of shapes, ranging from spheres to rods and spirals, and they are ubiquitous in every habitat on earth. Some bacteria live in or on other organisms, including plants, animals, humans and even soil. Some types cause food spoilage and crop damage but others are incredibly useful in the production of fermented foods. Relatively few bacteria are parasites or pathogens that cause disease in animals and plants [63].

The different types of bacteria can be classified on the basis of bacteria responses to Gram stain. Gram staining technique has been developed since 1884 by Hans Christian Gram, and it remains an important and useful technique to classify either Gram positive or negative based on their morphology and differential staining properties [64].

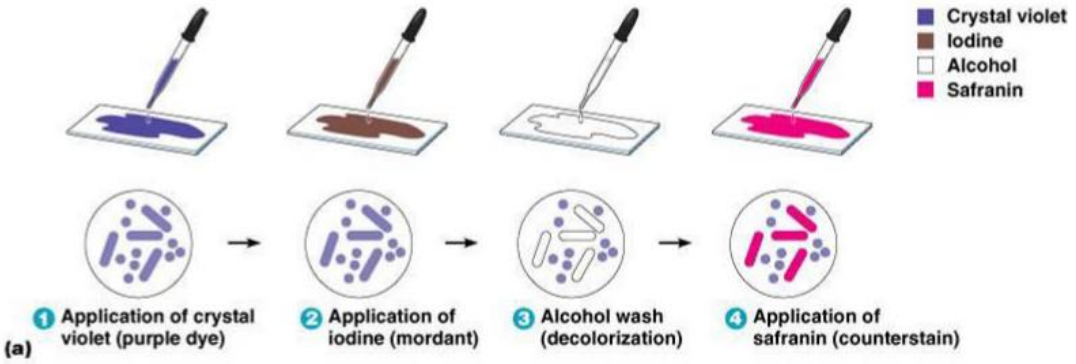

Figure 2.11 Gram staining mechanism [65].

Figure 2.11 shows that sampled slides are stained with crystal violet, iodine, then destained with alcohol and counter-stained with safranin. According to the Gram-positive bacteria stain blue-purple color and Gram-negative bacteria stain red color, it is believed that these are because of difference amount of peptidoglycan (cell wall) in bacteria [65].

The cell wall of Gram-positive bacteria contains a peptidoglycan layer that is ~30 nm thick, which has an effect on the precipitation from iodine and crystal violet, and cannot be eluted by alcohol. Unlike the Gram-positive cell wall, the Gram-negative cell wall has only a thin peptidoglycan layer that is ~2-3 nm thick, so it is easily eluted crystal violet, and restained again by safranin. In addition to the peptidoglycan layer, the Gram-negative cell wall has an additional membrane, the outer cytoplasmic membrane composed of phospholipids and lipopolysaccharides, which create an additional permeability barrier for transportation [64-66].

2.5.1.1 *Staphylococcus aureus*

Staphylococcus aureus or *S. aureus* is Gram-positive bacteria. They form spherical colonies which are immobile and form grape-like clusters [65] as shown in Figure 2.12a and 2.12b. Normally, *S. aureus* colony form is yellow colony on rich medium. *S. aureus* and their genus Staphylococci are facultative anaerobes which means they grow by aerobic respiration or fermentation that produces lactic acid [67].

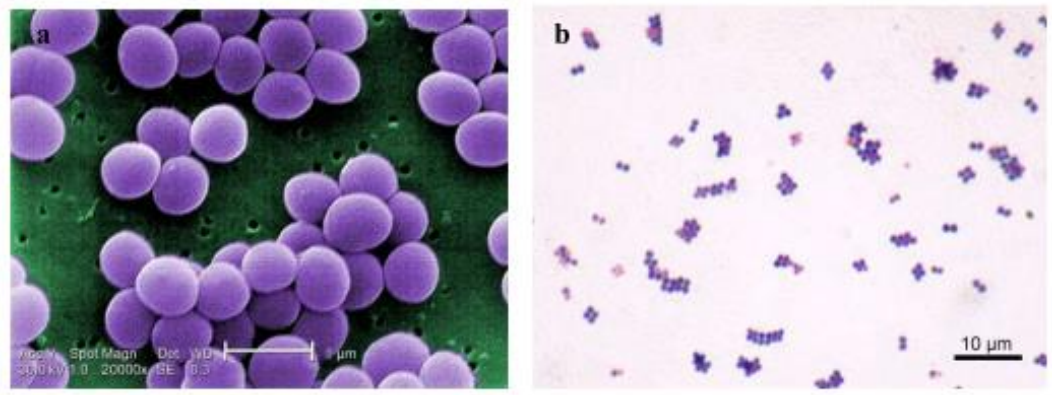

Figure 2.12 (a) Scanning electron micrograph (SEM) of *S. aureus* [68],
(b) Gram stain of *S. aureus* cells [69].

S. aureus can grow at a temperature range from 15 $^{\circ}$C to 45 $^{\circ}$C and at NaCl concentrations as high as 16%, and reproduce asexually by binary fission [70]. It is a normal flora of humans on nasal passages, skin, oral cavity, mucous membranes and gastrointestinal tract. *S. aureus* is among the most common hospital acquired pathogens that causes a wide range of suppurative infections, also various diseases including mild skin infections (impetigo), invasive diseases (wound infections), and toxin mediated diseases (food poisoning) [71].

2.5.1.2 *Escherichia coli*

Escherichia coli or *E. coli* has rod-shape (Figure 2.13a) and is a Gram-negative bacteria (Figure 2.13b) [65, 66]. *E. coli* are facultative anaerobes which can grow in the presence or absence of O_2. Under anaerobic (absence of O_2) conditions it will grow by means of fermentation, producing characteristic "mixed acids and gas" as end products.

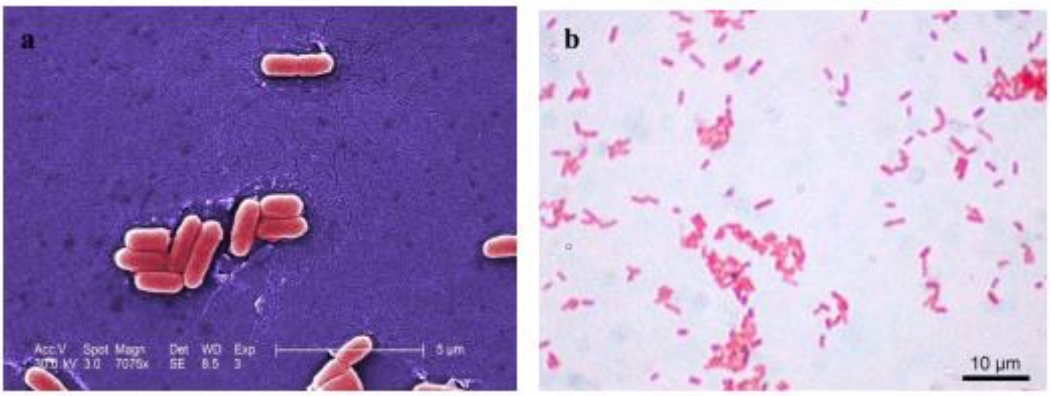

Figure 2.13 (a) Scanning electron micrograph (SEM) of *E. coli* [72],
(b) Gram stain of *E. coli* cells [73].

E. coli grow easily at the temperature around 37°C with a neutral pH around 7 (pH 7), and reproduce themselves by two means method that are cell division and conjugation. Their cells are able to survive outside the body for a limited amount of time. This makes them as markers for water contamination and ideal indicator organisms to test environmental samples for fecal contamination [74]. *E. coli* is a normal flora of human's gastrointestinal tracts, and intestine of endothermal animals. Most *E. coli* are harmless and actually are an important part of a healthy human intestinal tract. However, some *E. coli* are pathogenic, meaning they can cause illness, for example diarrhea, urinary tract infections, respiratory illness and pneumonia [75, 76].

2.6 Bacterial growth curve

Bacterial growth is the binary fission which refers the division process of a bacterial cell to duplicate itself into two daughter cells. For prokaryotes, binary fission is the primary method of asexual reproduction in which the process starts on an organism duplicates its genetic material or deoxyribonucleic acid (DNA), and then divides into two parts (cytokinesis), with each offspring receiving a complete copy of its essential genetic material [77].

Typically under optimum condition, bacterial growth in a closed system (batch culture) can be modeled with four different phases: lag phase, log phase or exponential phase, stationary phase, and death phase as shown in Figure 2.14 [78]. The dynamics of the bacterial growth can be studied by plotting the cell growth (absorbance) versus the incubation time or log of cell number versus time. An increase in the cell mass of the organism is measured by using the spectrophotometer, which measures the turbidity or optical density of the amount of light absorbed by a bacterial suspension [79]. The degree of turbidity in the broth culture is directly related to the number of bacteria.

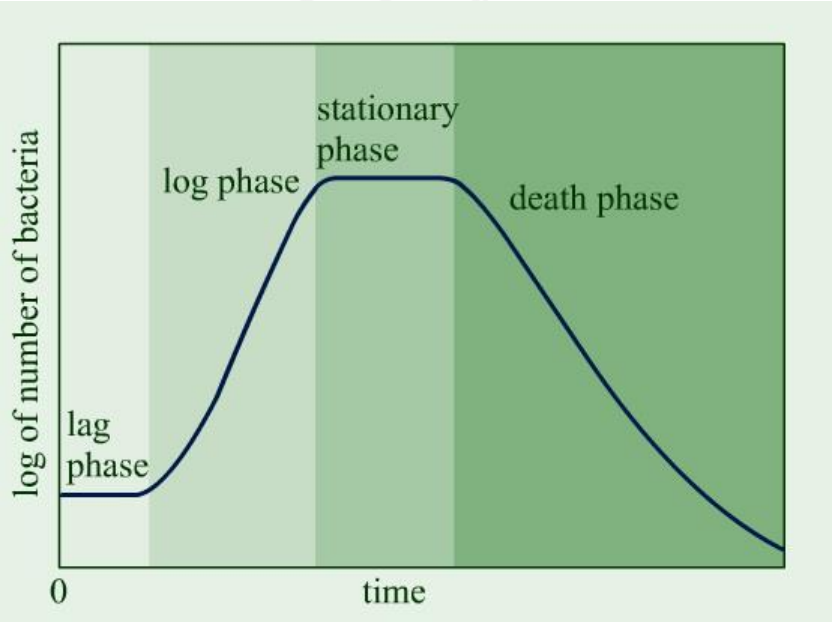

Figure 2.14 Different phases of bacterial growth curve (kinetic curve) [80].

2.6.1 Lag phase

Lag phase is the initial phase of bacterial growth curve. Bacteria is first transferred into the fresh medium, and then bacteria takes some time to adjust itself with the new environment. During the lag phase, there is no obvious cell division occurring; however, cellular metabolism (synthesis of RNA, enzymes and other molecules) exists.

2.6.2 Log phase

Log phase, logarithmic phase, or exponential phase is a period characterized by cell doubling. During this phase, bacterial cells are rapidly growing and dividing by binary fission. The growth medium is exploited at the maximal rate as the bacterial metabolic activity increases, which later affects the maximum growth rate and the logarithmically (exponentially) increases number of bacteria. The rate of exponential growth of a bacterial culture is expressed as generation time, also the doubling time of the bacterial population [81].

$$G = t / n$$

G = generation time

t = time (minutes or hours)

n = number of generations

The generation time depends on strains of bacteria. Different strain of bacteria have different generation time, for example, generation time of *E. coli* is 17 minutes whereas *S. aureus* is 27-30 minutes [81].

2.6.3 Stationary phase

Stationary phase is the phase of the limited bacterial growth. In this phase, bacteria from the log phase are rapidly growing, the depletion of essential nutrient and biological space, and the formation of an inhibitory product such as an organic acid occurs. This results in a situation that growth rate and death rate are equal, horizontal linear part of the curve during the stationary phase.

2.6.4 Death phase

Death phase is following after the population reaches stationary phase. During the death phase, the number of viable cells decreases exponentially because of the unfavourable conditions. Finally, the number of dead cells exceeds the number of living cells.

2.7 Silver nanoparticles and their antibacterial activity

From centuries, there is quite evident that some of the metallic compounds possess antimicrobial property. Silver has been widely used for treating burns and chronic wounds [82-84], and copper has been used to make water potable. Recently, nanotechnology has surprisingly brought many metals in the form of nanoparticles, for example copper, aluminium, gold, silver, magnesium, zinc and titanium nanoparticles, as potential antimicrobial agents [85]. Nanoparticles have unique and well defined physical and chemical properties which can be manipulated suitably for desired applications. In addition, their potent antimicrobial efficacy due to the high surface area to volume ratio.

Among various antimicrobial nanoparticles, AgNPs serve as the most potent antibacterial agent due to their acting against an exceptionally broad spectrum of bacteria, fungi and viruses while exhibiting low toxicity to mammalian cells [86]. For bacteria, AgNPs are an effective killing agent against a broad spectrum of genera both Gram-positive bacteria (*Bacillus*, *Enterococcus*, *Staphylococcus,* and *Streptococcus*) and Gram-negative bacteria (*Escherichia*, *Pseudomonas*, *and Salmonella*) [26, 29, 87], including antibiotic-resistant strains such as methicillin-resistant *Staphylococcus aureus* (MRSA) and vancomycin-resistant *Staphylococcus aureus* (VRSA) [88, 89]. This is the reason for the rasing of nanosilver containing products around the world (Table 2.1). Zhao and Stevens [90] revealed that consumer products that contain nanomaterials, roughly 25% are claimed to contain AgNPs, and they are well accepted universally [90, 91].

However, up to now the researches on the antibacterial effects of AgNPs are still in infant stage. There have been no clear pathways for AgNPs affecting bacterial growth. The first paper on the study of bactericidal property of nanostructured metal has been proposed by Sondi and Salopek-Sondi [92], who reported the antibacterial property of AgNPs against *E. coli*, which is a Gram-negative bacteria [83, 92]. Since then, there are several papers revealed the possible antibacterial mechanisms of AgNPs.

Morones and coworkers [27] and Pal and coworkers [93] presented that AgNPs attach to and penetrate the cell wall of bacteria, causing structural changes and damage, this could disturb vital cell functions, such as affecting permeability, depressing the activity of respiratory chain enzymes, causing pits and gaps on bacterial cells, and ultimately leading to cell death [27, 92, 93]. Also, it has been proposed that the antibacterial mechanism of AgNPs is related to the formation of free radicals and subsequent free radical-induced membrane damage [37, 94].

Furthermore, Percival and coworkers [95] presented that silver ions can lead to denaturing of protein, by reaction with nucleophilic amino acid residues and attachment to sulfhydryl, amino, phosphate, imidazole and carboxyl groups of membrane or enzyme proteins, and cause cell death [95].

Finally, Yang and coworkers [96] presented that AgNPs probably prevent bacterial cell division and interfere with microbial DNA replication within bacteria and fungi [96]. Other studies have been suggested that the phosphotyrosine profile of putative bacterial peptides that could affect cellular signaling might be modulated by AgNPs, and, therefore, inhibit the growth of bacteria [29].

In conclusion, there are four possible antimicrobial mechanisms of AgNPs that are (1) interference with cell wall synthesis, (2) inhibition of protein synthesis, (3) interference with nucleic acid synthesis, and (4) inhibition of a metabolic pathway [9-13]. In order to get a better insight about AgNPs affecting bacterial growth and bacterial protein profiles, the proteomics approach is concerned.

2.8 Proteomics technique

Proteomics is a prominent technology for the high-throughput analysis of proteins on a genome-wide scale. Proteomics defines as the systematic analysis of proteome, the protein complement of genome (an organelle, cell, tissue or an entire organism) [15, 16, 97]. Proteomics is a molecular tool that is a large scaled identification of all protein species in a cell or tissue. Their applications are currently varied to analyze various functional aspects of proteins such as protein expression, post-translational modifications, protein-protein interactions, functions and structures [98].

In order to complete of profiling proteins in biological samples, proteomics has been associated with the techniques of gel electrophoresis, i.e.; one-dimensional gel electrophoresis (SDS-PAGE) technique and two-dimensional gel electrophoresis (2D-PAGE) technique, and mass spectrometry (MS) [16, 99] as shown in Figure 2.15.

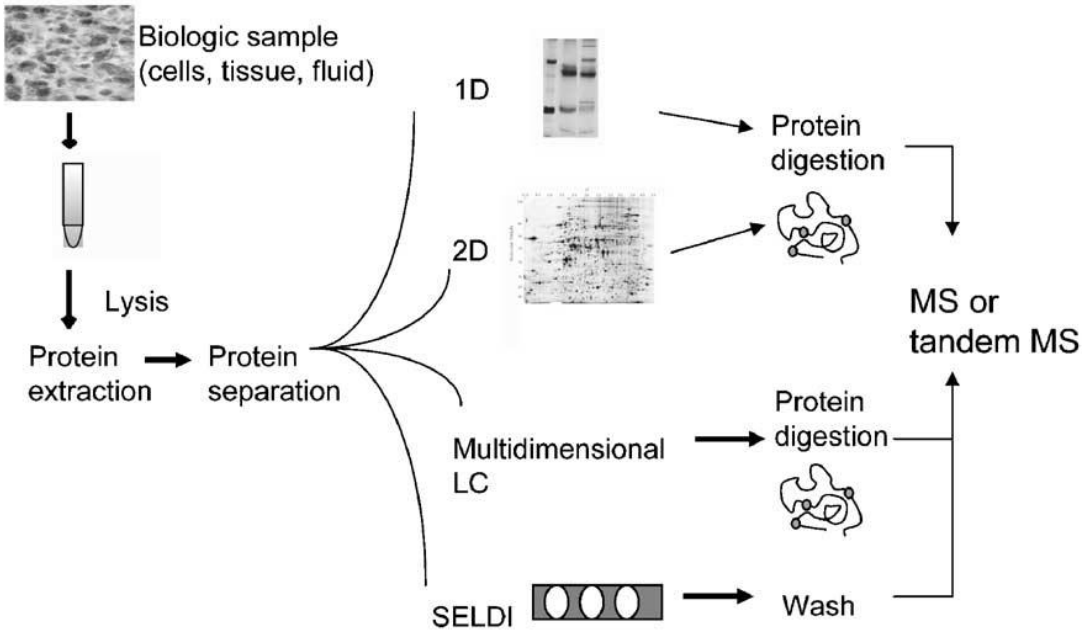

Figure 2.15 Overview of experimental design for mass spectrometry-based proteomic studies [98].

Moreover, protein samples from mass spectrometry are further advanced of searchable sequence databases, and complemented by virtual experiments performed on computers, namely bioinformatics.

2.8.1 Gel electrophoresis

Gel electrophoresis is a method for separation and analysis of macromolecules such as DNA, RNA and proteins based on their size, electric charge, and other physical properties. Once separated, gels are usually detected by staining either with silver salts or with Coomassie brilliant blue. Gel electrophoresis can be performed within one dimensional or two dimensional according to the objective and limitation of the work [100].

2.8.1.1 One-dimensional gel electrophoresis technique

One-dimensional gel electrophoresis technique or SDS-PAGE is popular and well known method for over 40 years. It was first known as the Laemmli method, after it was invented by Laemmli since 1970 [101]. It is used to separate proteins through a polyacrylamide gel matrix by helping an electrical field. With SDS-PAGE, proteins are denatured prior to electrophoresis, and separation is based on a protein's mass or molecular weight. SDS (sodium dodecyl sulphate) is an anionic detergent which denatures proteins from complex structure to linear structure by binding to the hydrophobic core of the protein, and gives each protein a negative charge proportionate to its mass. The proteins may be further treated with reducing agents, for example, dithiothreitol (DTT) or β-mercaptoethanol to break any reformed disulfide bonds [102, 103]. This leaves only the linear primary amino acid structure of the protein which will contain an overall negative charge proportional to its mass. Therefore, the proteins are separated on the basis of their molecular mass or molecular weight.

2.8.1.2 Two-dimensional gel electrophoresis technique

Two-dimensional gel electrophoresis technique or 2D-PAGE is widely used method for the analysis of complex protein mixtures extracted from cells, tissues, or other biological specimens. In 2D-PAGE, proteins are initially separated by isoelectric focusing which occurs across a pH gradient. The protein band will stop moving across the gel at its isoelectric point when the charge associated with the different amino groups is nullified by the pH. After that, the gel is turned 90° and the second electrophoresis occur using SDS to separate the proteins by molecular weight. This second dimension of focusing gives a series of spots across the gel and each spot is a specific protein [104, 105]. Therefore, with this technique, proteins are separated according to two different physical properties: the first-dimension is isoelectric focusing (IEF), which separates proteins on the basis of their

isoelectric points (pI) or net charge; the second-dimension is SDS-PAGE which further separates the proteins by their molecular weight or mass.

2.8.2 Mass spectrometry (MS)

Mass spectrometry is also known as mass spectrometer (MS). It is an analytical technique to measure the mass to charge ratio (m/z) of molecules with high accuracy [98]. Recently, mass spectrometry has become the method of choices for the rapid identification of proteins and the characterization of post-translational modifications [15, 106]. Generally, a typical mass spectrometer consists of three parts: an ionization source, the mass analyzer and the detector as shown in Figure 2.16.

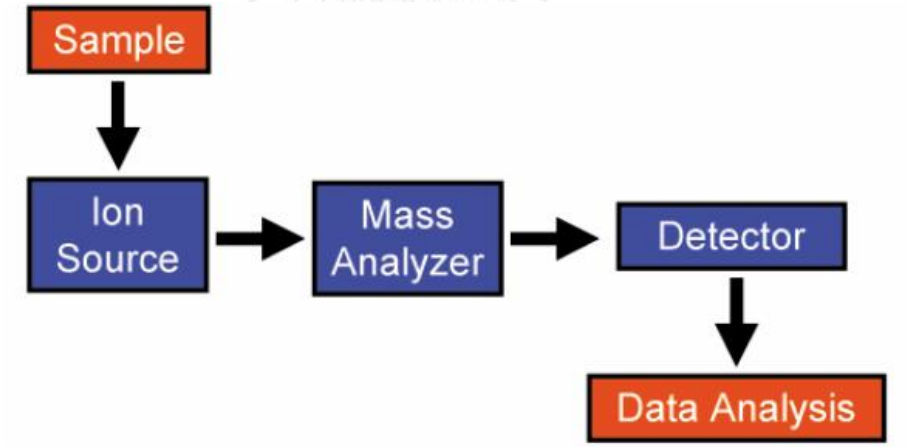

Figure 2.16 Schematic graph of mass spectrometry (MS) [107].

The function of the ionization source (i.e., electrospray ionization, MALDi) is to create ions from the sample. The function of the mass analyzer (i.e., quadrupoles, time-of-flight (TOF), ion-trap) is to separate ions with different mass to charge ratios (m/z). Then the numbers of different ions or mass are detected by the detector. Finally, the mass spectrum is generated after all the data have been collected [108].

2.8.2.1 Tandem mass spectrometry (MS/MS or Tandem MS)

Tandem mass spectrometer (MS/MS or Tandem MS) involves multiple steps of mass spectrometry, usually it is used for structural and sequencing studies [109]. It provides the same concept with the same composition and function as mass spectrometer; however, it has more than one analyzer, in practice usually two. After the molecules especially proteins pass through the ionization source, the first analyzer stabilizes the peptide ions while they collide with an inert gas (i.e., argon, xenon), causing them to fragment by collision-induced dissociation (CID) [110]. After that the second analyzer sorts the fragments produced from the peptides. Finally, the detector detects ions or mass to generate the mass spectrum (Figure 2.17).

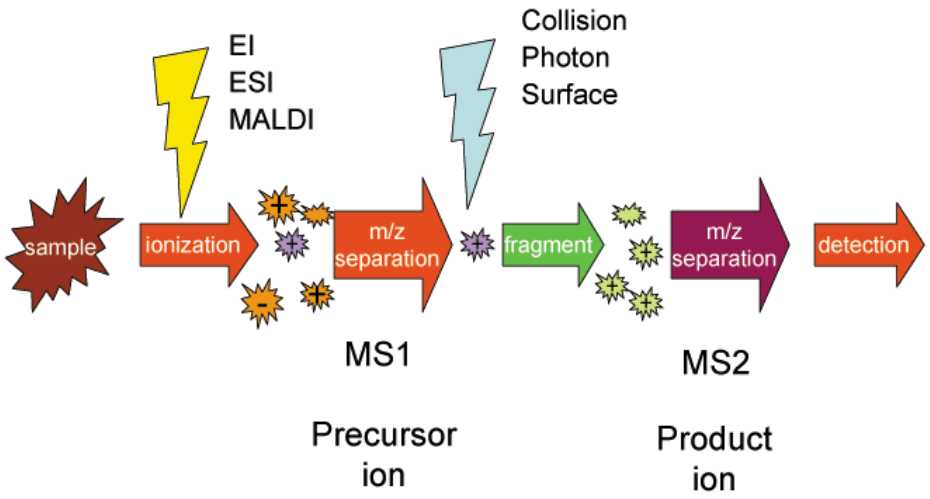

Figure 2.17 Schematic of tandem mass spectrometry (MS/MS) [107].

Tandem MS can also be done in a single mass analyzer over time, as in a quadrupole ion trap. Moreover, tandem MS is commonly combined with chromatographic techniques such as liquid chromatography (LC) in order to enhance the mass resolving and mass determining capabilities [111]. The combination between tandem mass spectrometry (MS/MS) together with liquid chromatography

(LC) called liquid chromatography-tandem mass spectrometry (LC-MS/MS). Therefore, LC-MS/MS is a method where a sample mixture is first separated by liquid chromatography (mobile phase is liquid) before being ionized and characterized by mass to charge ratios (m/z) and relative abundance using two mass spectrometers in series [107, 112].

2.8.3 Bioinformatics

Bioinformatics is related with development and improvement upon methods for storing, retrieving, organizing and analyzing biological data (biological information and biological systems) [113]. Bioinformatics is a virtual experiments performed on computer, usually comes later after protein information done in a real laboratory.

Recently, bioinformatics has become tremendous development of various areas of biology. There are even increasing needs for good understanding of quantitative methods in the study of proteins. In experimental molecular biology, bioinformatics techniques such as image and signal processing allow extraction of useful results from large amounts of raw data. For the genetics and genomics field, it aids in sequencing and annotating genomes and their observed mutations. Also, bioinformatics plays a role in the analysis and understanding of gene and protein expression, regulation, and evolution of molecular biology. For more integrative level, it analyzes and catalogues the biological pathways and networks which are an important part of biology systems. Ultimately, it helps researchers in simulation and modeling of DNA, RNA, and protein structures as well as molecular interactions in structural biology [114-116].

CHAPTER III

EXPERIMENTAL

3.1 Preparation of silver nanoparticles

3.1.1 Chemicals and materials

1. Silver nitrate ($AgNO_3$, (CARLO ERBA REAGENTS, Italy))
2. Sodium borohydride ($NaBH_4$, (Fisher scientific, USA))
3. Poly (4-styrenesulfonic acid – co – maleic acid) or PSSMA (Aldrich, USA)
4. Alginic acid or alginate (Aldrich, USA)
5. I-Carrageenan, type II (Sigma, USA)
6. Ultrapure water
7. Ice

3.1.2 Synthesis of silver nanoparticles

Silver nanoparticles (AgNPs) were synthesized with a chemical reduction method. Silver nitrate was used as a metal precursor and sodium borohydride as a reducing agent. The AgNPs were prepared without capping agents, as well as with different kinds of capping agents, i.e., PSSMA, alginate, and carrageenan.

3.1.2.1 Non-capping agents

AgNPs were prepared according to the description of Solomon and coworkers [117]. All solutions of reacting materials were prepared in ultrapure water. In a typical experiment, 10 mL of 1 mM silver nitrate was added drop by drop to 30 mL of 2 mM sodium borohydride solution that was chilled in an ice bath. The

reaction mixture was stirred vigorously on a magnetic stir plate (Lab-Line, Pyro-Magnestir No. 1267, Lab-Line Instruments, Inc.) at room temperature until the solution became yellow color as shown in Figure 3.1.

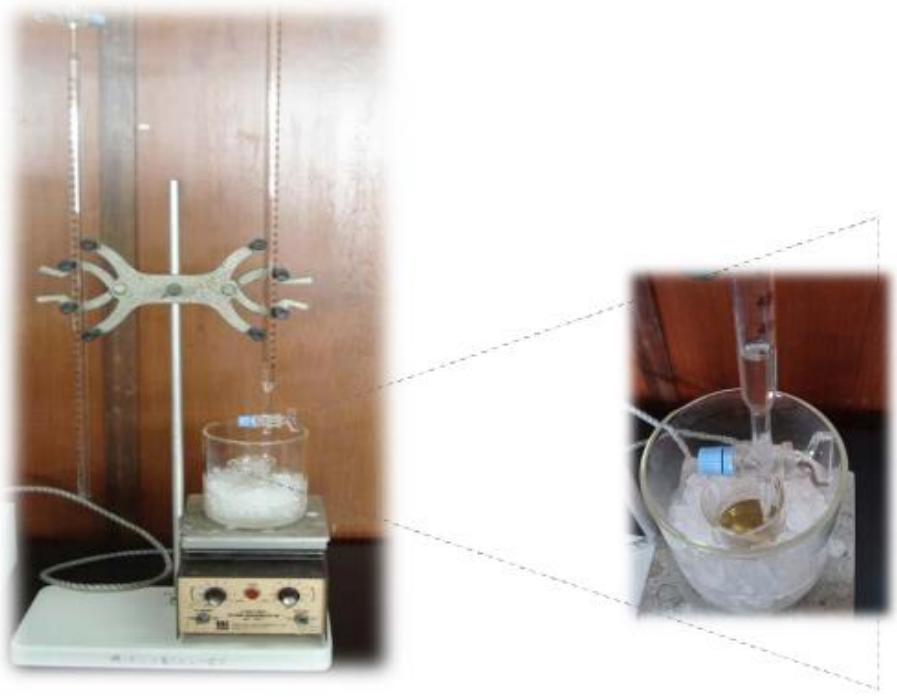

Figure 3.1 Experimental setup for AgNPs synthesis with non-capping agents.

3.1.2.2 Capping agents (PSSMA, alginate and carrageenan)

AgNPs were also synthesized by using sodium borohydride for the chemical reduction of silver salt. However, three kinds of capping agents were used to prevent the aggregation and prolong the stability of AgNPs (Figure 3.2).

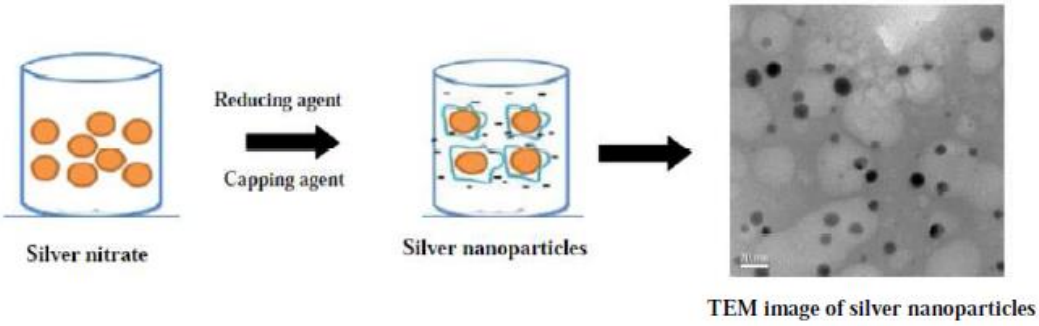

Figure 3.2 Schematic of synthesis of silver nanoparticles by the chemical reduction method.

The steps to synthesize AgNPs can be described as follows: 100 mL of 10 mM silver nitrate was mixed with each 100 mL of 1 mM capping agent (PSSMA, alginate and carrageenan) solution respectively. Then, 100 mL of 10 mM sodium borohydride was rapidly added and rated with 1 drop per second into the mixture solution to reduce silver ion. The mixture solution was kept for 3 h at room temperature to obtain a dark brown solution of AgNPs. The colloidal AgNPs were used after overnight incubation.

3.1.3 Characterization of silver nanoparticles

The synthesized AgNPs with capping agents and without capping agents were characterized and confirmed with the following techniques as shown in Table 3.1.

Table 3.1 Characterization techniques of AgNPs.

No.	Characterization techniques	Nanoparticles characteristics
1.	Ultraviolet-visible spectroscopy (Specord S 100 Analytikjena, Germany)	Surface plasmon resonance (SPR)
2.	Zetasizer (Zetasizer NanoZS, Malvern Instruments, UK)	Size and surface charge (Zeta potential)
3.	Transmission electron microscopy (TEM) (JEM-2100, Jeol, Japan)	Size and morphology

3.1.3.1 Ultraviolet-visible spectroscopy

The localized surface plasmon absorbance band of the colloidal AgNPs was tested by a Specord S 100 UV–vis spectrophotometer with a 1 cm optical path quartz cuvette (ultrapure water was used for setting up as blank before testing). UV–vis spectra were recorded and analyzed with SpectraSuite program. The spectral data in the range between 360 nm – 600 nm were plotted into a graph using Microsoft Excel.

3.1.3.2 Zetasizer

The surface charges or zeta potential and the average sizes of the synthesized AgNPs were analyzed using Zetasizer NanoZS, Malvern Instruments. The surface charges of the particles were measured by laser Doppler velocimetry (LDV) with no effective limitations of zeta potential range using disposable capillary cell (DTS1061) whereas the average sizes of the particles were characterized by dynamic light scattering (DLS) with size range (diameter) between 0.30 nm - 10 microns. Operating system was set up by selecting material as silver, dispersal solvent as water, and temperature as 25°C.

3.1.3.3 Transmission electron microscopy (TEM)

The size and morphology of the particles were characterized by JEM-2100 Transmission Electron Microscope, Jeol. Samples were prepared by dropping a small amount of the colloidal AgNPs onto carbon-coated TEM grids. The solution was air-dried at room temperature or in a desiccator overnight before testing. SemAfore 5.21 program was used to obtain the particle size histogram from TEM images in each sample.

3.2 Investigation of the antibacterial activity of silver nanoparticles

3.2.1 Chemicals and materials

1. Colloidal AgNPs capped with PSSMA, alginate, and carrageenan
2. Ultrapure water
3. Sterile water
4. 70% Alcohol (Carlo Erba (Rodano, Milano, Italy))
5. *Staphylococcus aureus* ATCC 25923
6. *Staphylococcus aureus* ATCC 6538P
7. *Staphylococcus aureus* ATCC 43300
8. *Staphylococcus epidermidis* ATCC 12228
9. *Escherichia coli* ATCC 25922
10. *Lactobacillus salivarius* ATCC 11741
11. *Kocuria rhizophila* ATCC 9341
12. *Bacillus subtilis* ATCC 6633
13. *Enterobacter aerogenes* ATCC 13048
14. *Pseudomonas aeruginosa* ATCC 27853
15. Ice
16. Glycerol
17. Tryptic (trypticase) soy broth (TSB, (Difco, USA))
18. Tryptic (trypticase) soy agar (TSA, (Difco, USA))
19. de Man, Rogosa and Sharpe agar (MRS, (Difco, USA))
20. Saline (0.85% NaCl)
21. Blank paper discs (Whatman, USA)

3.2.2 Disc diffusion method

The synthesized AgNPs capped with PSSMA, alginate, carrageenan, and without capping agents were preliminary tested of antibacterial susceptibility compared to silver nitrate ($AgNO_3$) by using the Kirby Bauer diffusion method or disc diffusion method. Disposable plates inoculated with the tested bacteria, i.e.; *E. coli* ATCC 25922, *S. aureus* ATCC 25923, *L. salivarius* ATCC 11741, and *K. rhizophila* ATCC 9341 with approximate the same concentration of cells in a suspension at 0.5 McFarland were used for the tests. The prepared paper discs of colloidal AgNPs and $AgNO_3$ were then inoculated in the disposable plates containing bacteria, each in triplicate. The diameters of clear zones or inhibition zones (mm) were measured after 24 h of incubation of bacteria at $37^{\circ}C$.

3.2.3 Bacterial growth curve

Based on the results from previous session, the most effective AgNPs, AgNPs capped with PSSMA, were selected for further study on bacterial growth of eight bacterial strains that are *S. aureus* ATCC 25923, *S. aureus* ATCC 6538P, *S. aureus* ATCC 43300, *S. epidermidis* ATCC 12228, *B. subtilis* ATCC 6633, *E. coli* ATCC 25922, *En. aerogenes* ATCC 13048, and *Ps. aeruginosa* ATCC 27853 compared with ultrapure water (control).

3.2.3.1 Preparation of bacteria

Bacterial strains were transferred 1 loop respectively from their glycerol stock in -80°C freezer to streak on TSA agar plate and then incubated at 37°C for 24 h. One bacterial colony was inoculated into TSB broth and further incubated for 24 h (at 37°C, shaked at 200 rpm). The bacteria were then centrifuged (High Speed Refrigerated Micro Centrifuge, Model MX-301, Tomy) at 5000 rpm for 3 min. The supernatant was discarded, and the pellet was resuspended with TSB media for testing.

3.2.3.2 Preparation of silver nanoparticles

TSB powder was separately dissolved in ultrapure water and colloidal 360 ppm AgNPs solution (proportion 30 g: 1000 mL). The solutions were sterilized by filtration with Acrodisc® 25 nm syringe filter (with 0.20 um Super® membrane) before testing.

The experiments were preliminary performed in 96-well plates. Bacterial cells (*S. aureus* ATCC 25923, *S. aureus* ATCC 6538P, *S. aureus* ATCC 43300, *S. epidermidis* ATCC 12228, *B. subtilis* ATCC 6633, *E. coli* ATCC 25922, *En. aerogenes* ATCC 13048, *and Ps. aeruginosa* ATCC 27853) with the OD value at 600 nm of each well-being 0.05 were exposed and unexposed to prepared AgNPs. The bacterial growth curve were obtained and determined for the antibacterial susceptibility towards AgNPs.

3.3 Studying of protein expression by sodium dodecyl sulfate polyacrylamide gel electrophoresis (SDS-PAGE)

3.3.1 Chemicals and materials

1. Bovine serum albumin (BSA, (Sigma, USA))
2. Sodium dodecyl sulfate (SDS, (Sigma-Aldrich, USA))
3. Sterile water
4. Distilled water
5. *Staphylococcus aureus* ATCC 25923
6. *Escherichia coli* ATCC 25922
7. Acrylamide (monomer, (GE Healthcare, Sweden))
8. Tris-Hydrochloride (Tris-HCl)
9. Glycerol
10. Tryptic (trypticase) soy broth (TSB, (Difco, USA))
11. Tryptic (trypticase) soy agar (TSA, (Difco, USA))
12. Dithiothreitol (DTT)
13. Bromophenol blue
14. Ammonium persulfate (APS, (Bio Basic, Canada))
15. Tetramethylethylenediamine (TEMED, (USB Corporation, USA)
16. Glycine

Silver stainning

17. Methanol (MeOH, (RCI Labscan, Thailand))
18. Acetic acid (Mallinckrodt, USA)
19. Formaldehyde (Sigma, Germany)
20. Ethanol (EtOH, (J.T.Baker, Netherland))
21. Sodium thiosulfate (Sigma-Aldrich, Germany)
22. Silver nitrate ($AgNO_3$, (AppliChem, Germany))
23. Sodium carbonate (VWR/BDH Prolabo, Italy)

24. Ethylenediaminetetraacetic acid (EDTA, (USB Corporation, Netherland))

Coomassie brilliant blue G staining

25. Coomassie stock
26. Ammonium sulfate
27. Phosphoric acid
28. Acetic acid (Mallinckrodt, USA)
29. Methanol (RCI Labscan, Thailand)

3.3.2 Collection and extraction of bacterial proteins

Bacterial strains and AgNPs were prepared according from the previous session. In order to collect enough proteins for proteomics study, bacterial cells with 0.1 OD (OD 600 nm) (Microplate Reader, VersaMax, USA) were up-scaled by using beakers instead of 96-well plates.

For the proteomics study of *S. aureus* ATCC 25923 and *E. coli* ATCC 25922, both of bacterial cells exposed and unexposed to AgNPs were immediately collected at different time intervals, i.e.; 0 min, 15 min, 30 min, 45 min, 1 h, 2 h and 3 h (data were recorded in quadruplicate). Collected bacterial cells were centrifuged (Scientific Inc., USA) at 5000 rpm for 5 min and then supernatants were discarded. The pellet cells were re-suspended with 0.5% SDS solution, vortexed vigorously, and frozen in -80°C freezer overnight. The bacterial cells exposed and unexposed to AgNPs were broken with pipetting, and then centrifuged at 5000 rpm for 5 min. The supernatants containing total proteins were collected in order to determine protein concentration using Lowry assay.

3.3.3 Protein determination by Lowry assay

The bacterial proteins of *S. aureus* ATCC 25923 and *E. coli* ATCC 25922 after exposed or unexposed to AgNPs were determined by Lowry assay [118] using bovine serum albumin (BSA) as standard. The absorbance at 750 nm (OD_{750}) (Microplate Reader, VersaMax, USA) was measured and the protein concentrations were calculated using the standard curve, which was plotted with OD_{750} as Y-axis and concentration (μg/μL) of BSA as X-axis.

3.3.4 Protein separation by SDS-PAGE

3.3.4.1 Preparation of samples for SDS-PAGE analysis

Samples with appropriate protein concentrations (40 μg protein per well) were mixed with 6 μL of 5x loading buffer or loading dye (0.125 M Tris-HCl pH 6.8, 20% glycerol, 5% SDS, 0.2 M DTT, 0.02% bromophenol blue). The 0.5% SDS solution was added until the final volume was 18 μL (2x vol.). The mixture was heated at 100°C for 5 min before loaded onto 12.5% SDS-PAGE.

3.3.4.2 Preparation of SDS-PAGE slab gel

The mixture of proteins was separated by their molecular weights on SDS-PAGE mini slab gel (miniPAGE chamber AE-6530, ATTO, Japan). There were two gels for bacterial cells exposed and unexposed (control) to AgNPs. The polyacrylamide gels were prepared following the method of Laemmli [119]. The preparation of separating and stacking gel was shown in Table 3.2.

Table 3.2 Preparation of SDS-PAGE separating and stacking gel for 90 x 80 x 1 mm mini-slab format gel size (proportion for 2 gels).

Reagent	**Separating gel (12.5%)**	**Stacking gel (5%)**
40% acrylamide (mL)	6.25	1.14
1.5 M Tris-HCl pH 8.8 (mL)	5.00	-
0.5 M Tris-HCl pH 6.8 (mL)	-	2.23
10% SDS (µL)	250.00	90.00
Sterile water (mL)	8.39	5.47
10% APS (µL)	100.00	69.00
TEMED (µL)	6.60	5.10

3.3.4.3 Running condition

Electrophoresis will be performed in SDS electrophoresis buffer (25 mM Tris-HCl pH 8.3, 192 mM glycine, 0.1% SDS). SDS-PAGE was carried out at 50 volts for stacking gel and 70 volts for separating gel using an electrophoresis power supply (Electrophoresis Power Supply, GE Healthcare Bio-Sciences AB, Sweden) until the blue line of loading dye (tracking dye) reached the bottom of the gel. Both of two gels were then put into fixing solution for gel staining.

3.3.4.4 Gel staining

The fixed gels were visualized by silver staining and Coomassie brilliant blue G staining before stained gels were scanned with Image Scanner (Bio-Rad, USA).

3.3.4.4.1 Silver staining

In addition to Coomassie blue staining, silver staining was also used, which can provide a higher sensitivity with approximate 1 ng of protein in a detected single band. The gels were stained according to Blum and coworkers [120] as shown in Table 3.3.

Table 3.3 Silver staining procedure for 90 x 80 x 1 mm gel.

Step	Solution	Time
Fixing (200 mL)	Methanol 100 mL Acetic acid 24 mL 37% Formaldehyde 100 µL Distilled water 75.90 mL	Overnight
Washing (300 mL)	Ethanol 105 mL Distilled water 195 mL	2x5 min
Sensitizing (200 mL)	Sodium thiosulfate 0.04 g Distilled water 200 mL	2 min
Washing	Distilled water	2x5 min
Staining (200 mL)	Silver nitrate 0.40 g Distilled water 200 mL	20 min
Washing	Distilled water	1 min
Developing (200 mL)	Sodium carbonate 12 g 0.02% Sodium thiosulfate 4 mL 37% Formaldehyde 100 µL Distilled water 195.90 mL	The reaction can be stopped when all of protein bands appear
Stopping (100 mL)	EDTA 1.46 g Distilled water 100 mL	20 min
Washing	Distilled water	3x5 min
Storing	0.1% Acetic acid	Until used

3.3.4.4.2 Coomassie brilliant blue G staining

Coomassie brilliant blue G staining is a popular and routine procedure to visualize protein bands, which is simple, fast, and consistent. Also, its staining sensitivity approximates 50 ng of protein in a single band. Gels were stained with Coomassie brilliant blue G as described in Table 3.4 [121].

Table 3.4 Coomassie brilliant blue G staining procedure for 90 x 80 x 1 mm gel.

Step	Solution	Time
Fixing	10% Acetic acid 35% Methanol	Overnight
Staining (500 mL)	Ammonium sulfate 40 g 85% Phosphoric acid 4.80 mL 5% Coomassie stock 0.40 g Distilled water 395.20 mL Methanol 100 mL	Overnight
Washing	Distilled water	Until background of the gel becomes clear, and bands are explicitly observed
Storing	0.1% Acetic acid	Until used

3.4 Protein identification by liquid chromatography tandem mass spectrometry (LC-MS/MS)

3.4.1 Chemicals and materials

1. Acetic acid (Mallinckrodt, USA)
2. Gel plugs of BSA
3. Sterile water
4. Acetonitrile (ACN), AR Grade (RCI Labscan, Thailand)
5. Dithiothreitol (DTT, (USB Corporation, USA))
6. Ammonium bicarbonate (Ambic, (Sigma-Aldrich, USA))
7. Iodoacetamide (IAA, (GE Healthcare, UK))
8. Trypsin (Promega, USA)
9. Acetonitrile (ACN), LC Grade (J.T.Baker, USA)
10. Formic acid (FA, (AppliChem, Germany))

3.4.2 Excision of protein bands

Protein bands from the silver and Coomassie blue stained SDS-PAGE gels were first horizontally excised, and then gradually vertically excised from left to right side (Figure 3.3) in order to acquire the entire population of proteins in the gel.

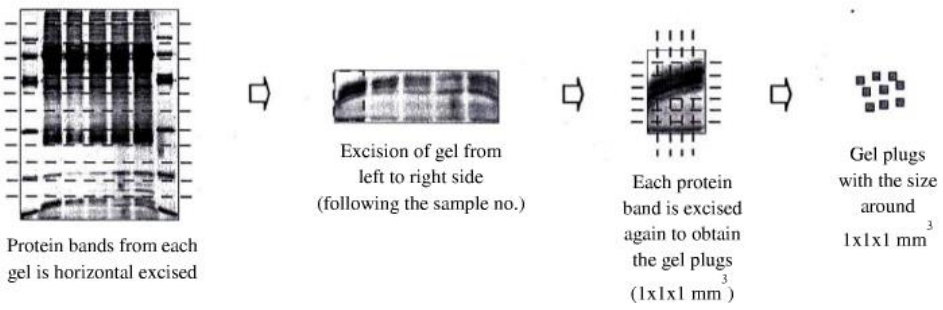

Figure 3.3 Excision of protein bands.

Each protein band (gel slice) was excised again to obtain gel plugs with the size around 1x1x1 mm^3 using scalpel and forcep. The gel plugs were placed in 96-well plates (8 pieces per well), destained, and washed with sterilized water for the in-gel digestion.

3.4.3 In-gel digestion

The gel plugs were subjected to in-gel tryptic digestion by using an in-house method developed in Proteomics Research Laboratory, Genome Institute, National Center for Genetic Engineering and Biotechnology (BIOTEC), National Science and Technology Development Agency (NSTDA), Thailand [122].

To perform in-gel digestion of proteins, the gel plugs in each well were washed one time with 200 µL of sterilized water, and dehydrated twice with 200 µL of 100% acetonitrile (ACN) for 5 min each time in a shaker (Mx2, Micromixer, Korea). The proteins in gel plugs were reduced with 50 µL of 10 mM dithiotreitol (DTT) in 10 mM ammonium bicarbonate (Ambic) at room temperature for 1 h and alkylated in the dark with 50 µL of 100 mM iodoacetamide (IAA) in 10 mM ammonium bicarbonate (Ambic) at room temperature for 1 h. After that, the gel plugs were dehydrated three times with 200 µL of 100% ACN for 5 min each time. Then, 10 µL of trypsin solution (10 ng/µL trypsin in 50% ACN containing 10 mM Ambic) was added followed by incubation at room temperature for at least 20 min, and 20 µL of 30% ACN was added to keep the gels immersed throughout digestion. The gels were then incubated at room temperature overnight. To extract peptide digestion products, 30 µL of 50% ACN with 0.1% formic acid (FA) and 30 µL of 70% ACN with 0.1% FA were used twice and once, respectively. Each time, the gel plugs were incubated at room temperature for 10 min in a shaker. Extracted peptides were collected and pooled together. The pooled extracted peptides were dried at 40 °C in an incubator (Incubator, Memmert, Germany) overnight and kept at -80 °C for further LC-MS/MS analysis.

3.4.4 LC-MS/MS analysis

To analyse peptides by LC-MS/MS, the extracted peptides from in-gel digestion were resuspended with 0.1% FA and centrifuged (Scientific Inc., USA) at 10,000 rpm for 5 min. The extracted protein were injected to Ultimate 3000 LC system (Dionex) coupled with ESI-Ion Trap MS (HCT ultra PTM Discovery System, BrukerDaltonics Ltd., UK) with electrospray at a flow rate of 20 µL/min to µ-precolumn (Monolithic Trap Column, 200 µm i.d. x 5 cm). The peptides were separated on a nanocolumn (PepSwift Monolithic Nanocolumn, 100 µm i.d. x 50 mm) at a flow rate of 1 µL/min. A solvent gradient (solvent A: H_2O, 0.1% formic acid; solvent B: 50% H_2O, 50% ACN, 0.1% formic acid) was run in 20 min.

3.4.5 Protein quantitation and identification

For protein quantitation, DeCyder MS Differential Analysis software (DeCyderMS, GE Healthcare) was used. The analyzed MS/MS data from DeCyderMS were submitted for database search using the Mascot software (Matrix Science Ltd., London, U.K.). The data were searched in the National Center for Biotechnology Information (NCBI) database for protein identification.

3.4.5.1 Protein quantitation

The MS/MS spectra of all samples were analyzed by DeCyder MS 2.0 Differential Analysis Software (GE Healthcare) [123, 124]. This software consists of two analysis features, i.e.; the PepDetect module and the PepMatch module. It starts from PepDetect module which provides consistent and accurate peptide detection, background subtraction, isotope and charge-state deconvolution, and peak volume calculations using novel imaging algorithms. Also, the software's visualization tools offer the new capabilities for user to optimize chromatography and MS/MS settings. Then, Pepmatch module supports a wide range of experimental

designs, such as control/treated experiments as well as time-dose studies. It even detects small quantitative differences between peptides across multiple runs with high statistical confidence at p value < 0.05.

3.4.5.2 Protein identification and gene ontology

Differential tandem mass spectra of peptides from protein quantitation using DeCyder MS Differential Analysis software (DeCyderMS, GE Healthcare) were identified by Mascot software (Matrix Science Ltd., London, U.K.) [106], a search engine that uses mass spectrometry data to identify proteins from primary sequence databases. The database was obtained from the NCBI (http://www.ncbi.nlm.nih.gov) for protein identification. Database interrogation was used as follows: taxonomy = bacteria, enzyme = trypsin, max. missed cleavages = 1; fixed modifications = carbamidomethyl (C); variable modifications = oxidation (M); peptide mass tolerance ±1.2 Da; MS/MS or fragment mass tolerance ±0.6 Da; peptide charge state = 1+, 2+ and 3+; instrument = ESI-TRAP. Data normalization and quantification of the changes in protein abundance between *S. aureus* ATCC 25923 and *E. coli* ATCC 25922 cells exposed and unexposed to AgNPs were visualized using Venn Diagram.

To better understand the antibacterial mechanism of AgNPs, the free areas of *E. coli* (control), *E. coli* (AgNPs), *S. aureus* (control), *S. aureus* (AgNPs), as well as intersection areas of free areas of *E. coli* (control and AgNPs) and *S. aureus* (control and AgNPs) were analyzed. The protein functions of interested proteins were further searched based on the UniProt (http://www.uniprot.org), enabling their gene ontology (GO) prediction. The identified proteins were simultaneously submitted to The Search Tool for the Retrieval of Interacting Genes (STRING) (http://string-db.org) to search for understanding of cellular functions and annotate all functional interactions among proteins in the bacterial cells [125].

CHAPTER IV
RESULTS & DISCUSSIONS

4.1 Synthesis and characterization of silver nanoparticles

Silver nanoparticles (AgNPs) with non-capping agent and with anionic capping agents, i.e.; PSSMA, alginate, and carrageenan were synthesized. The colloidal solution turned dark yellow and then turned clear yellow upon dilution, indicating that the AgNPs were presented. AgNPs were then characterized by ultraviolet-visible spectroscopy, zetasizer, and transmission electron microscopy.

4.1.1 Ultraviolet-visible Spectroscopy

The synthesized AgNPs were first characterized by UV-vis spectroscopy. The UV-vis absorbance spectra of AgNPs capped with three kinds of capping agents (PSSMA, alginate, carrageenan) and without capping agents is shown in Figure 4.1. The colloids AgNPs showed λ_{max} as 407.33 nm, 395.01 nm, 385.15 nm and 391.72 nm with non-capping agents, PSSMA, alginate and carrageenan, respectively. The result demonstrated that all prepared colloids of AgNPs were formed, which can be explained from the surface plasmon resonance (SPR) properties. Solutions of colloidal AgNPs have distinctive color arising from their tiny dimensions. Especially, at nanometer dimensions the SPR phenomena are occurred owing to the oscillation of electrons on the surface of nanoparticles induced by electromagnetic radiation [50].

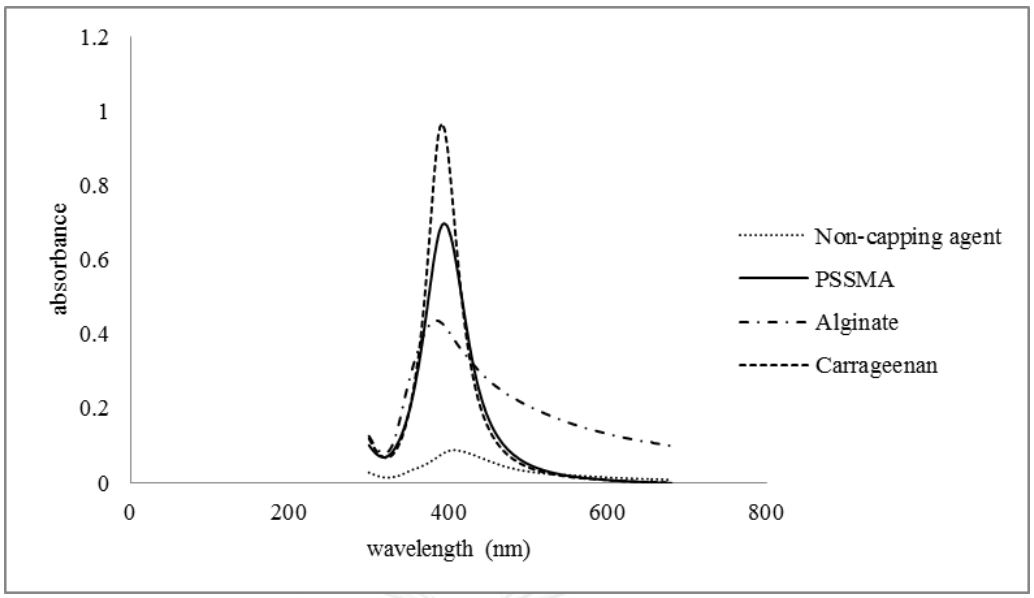

Figure 4.1 UV-vis absorbance spectra of AgNPs capped with three kinds of capping agents (PSSMA, alginate, carrageenan) and without capping agents.

Normally, the optical absorption spectrum of metal nanoparticles is dominated by the SPR which exhibits blue or red shift depending upon the shape, particle size, state of aggregation and the surrounding dielectric medium [51]. Figure 4.1 showed that the colloidal AgNPs with capping agents had narrow adsorption bands which were an indication of well-dispersity and small size of particles, especially in AgNPs capped with carrageenan and PSSMA. On the other hand, the colloidal AgNPs without capping agents had a broader absorption band which indicated the colloids had a larger particle size and tended to become aggregation easily [126, 127] (Table 4.1). The size of colloidal AgNPs without any capping agents from DLS were distinctive large size of particles around 73.20 ± 1.09 nm. This is in agreement with TEM observations that showed the aggregation of AgNPs (see Figure 4.2).

4.1.2 Zetasizer

Colloidal AgNPs were also characterized by using Zetasizer to measure the size and surface charge or zeta potential of the nanoparticles. This can indicate the potential stability of the colloidal system. The zeta potential values of AgNPs capped with three anionic polymers showed the zeta potential ranged from -35.50 to -43.40 mV as shown in Table 4.1.

Table 4.1 Effect of capping agents on zeta potential and average size of AgNPs (mean ± S.D., n =3).

Sample name	ZP (mV)	Z-Ave (d.nm)
AgNPs without capping agent	-24.90 ± 0.58	73.20 ± 1.09
AgNPs capped with PSSMA	-35.50 ± 0.96	13.81 ± 0.06
AgNPs capped with alginate	-41.00 ± 2.34	52.29 ± 0.24
AgNPs capped with carrageenan	-43.40 ± 1.06	58.03 ± 0.13

The negative surface properties of AgNPs were observed because capping agents surrounding AgNPs were anionic polymers. Makino and coworkers revealed that nanoparticles with a zeta potential above (±) 30 mV have been shown to be stable in suspension, as the surface charge prevents aggregation of the particles [128]. These all of the zeta potential were more than (±) 30 mV; therefore, colloidal AgNPs with capping agents were found to have high stability. However, AgNPs without capping agent showed the zeta potential around -24.90 mV, which was less than (±) 30 mV, and easy to form aggregates.

4.1.3 Transmission electron microscopy (TEM)

The transmission electron microscope (TEM) is currently the imaging technique of choice for the characterization of the shape and size distribution of all materials. The sizes of the observed particles in TEM are in good agreement with the values obtained by dynamic light scattering (DLS) (Table 4.1). However, the particle size obtained using DLS is significantly larger than that determined by TEM because DLS measures the equivalent-sphere hydrodynamic diameters of nanoparticles in solutions [129, 130].

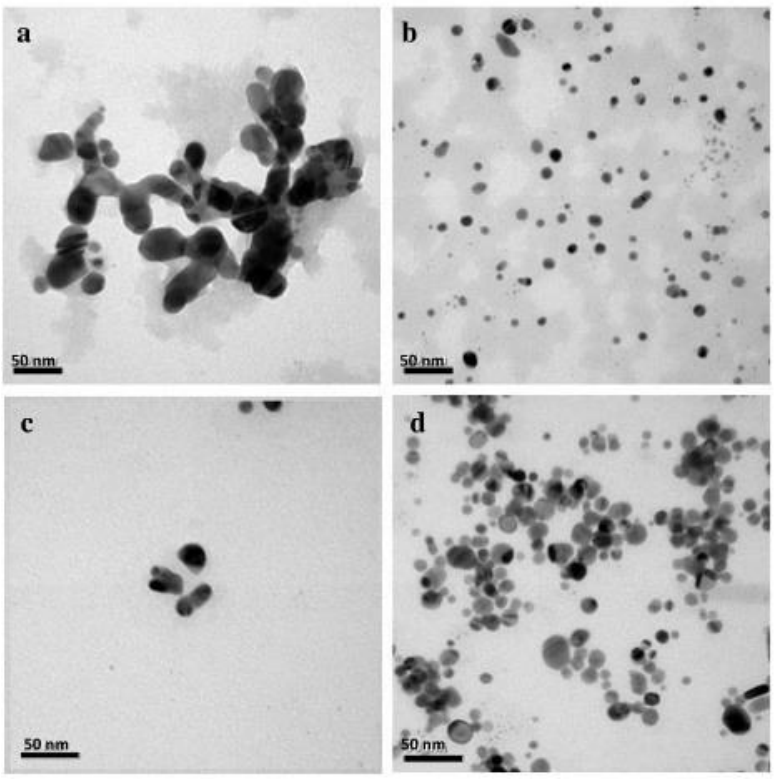

Figure 4.2 Transmission electron micrograph of the AgNPs with difference kinds of capping agents: (a) non-capping agent, (b) PSSMA, (c) alginate, and (d) carrageenan. Scale bar: 50 nm.

TEM images in Figure 4.2 present the size and morphology of spherical AgNPs with and without capping agents. The AgNPs without capping agents had larger sizes of nanoparticles and agglomeration, whereas all the AgNPs with capping agents were well dispersed with relative small sizes. TEM micrographs showed very small sizes of spherical nanoparticles with the best homogeneous and size distributions at room temperature for the AgNPs coated with PSSMA as well as with carrageenan.

4.1.4 Particle size distribution

To obtain the particle size histogram, TEM images from each sample were analyzed by SemAfore 5.21 program. For each capping agent, 250 nanoparticles from their TEM images were randomly selected, and their sizes were measured in order to obtain particle size distributions (Figure 4.3). However, non-capping agent could not show with the particle size histogram because there were a lot of particle aggregates.

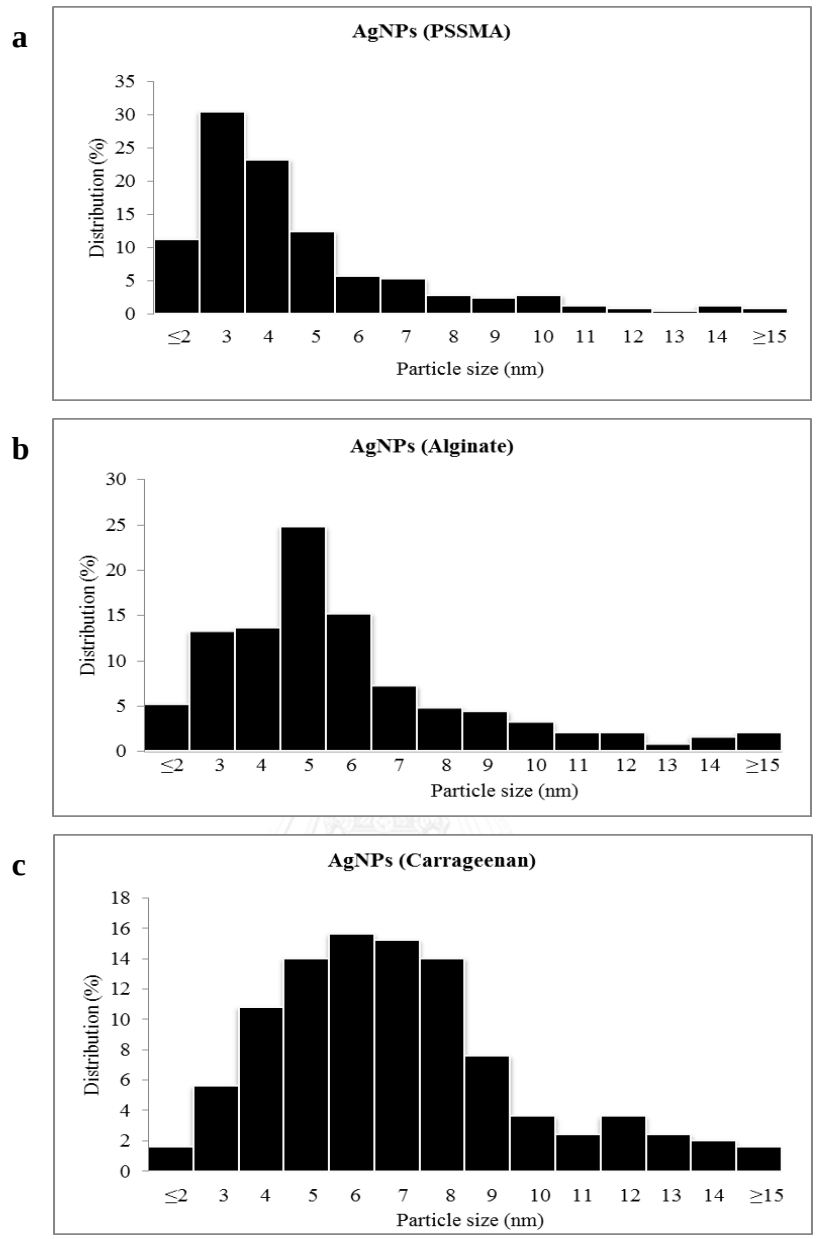

Figure 4.3 Particle size distributions of the AgNPs with three kinds of capping agents: (a) PSSMA, (b) alginate, (c) carrageenan, (n = 250, of each sample).

Figure 4.3 showes the size distributions of the AgNPs ranging from smaller than or equal to 2 nm to larger than or equal to 15 nm (≤ 2 nm - ≥ 15 nm) in each kind of capping agent. The analysis revealed that the average size of AgNPs capped with PSSMA, alginate and carrageenan were 4.67 ± 2.79 nm, 5.91 ± 2.96 nm and 7.03 ± 2.83 nm, respectively.

4.2 Investigation of antibacterial activity of silver nanoparticles

4.2.1 Disc diffusion method

The preliminary test of antibacterial susceptibility of AgNPs by the Kirby-Bauer diffusion method found that AgNPs exhibited the antibacterial susceptibility against all of tested bacterial strains.

The bargraph of antibacterial susceptibility of AgNPs capped with three kinds of capping agents versus inhibition zone (mm) is shown in Figure 4.4. Figure 4.4 shows the effective antibacterial susceptibility of $AgNO_3$ and capped AgNPs with capping agents (PSSMA, alginate, and carrageenan) in tested bacteria that are *E. coli* ATCC 25922, *S. aureus* ATCC 25923, *L. salivarius* ATCC 11741, and *K. rhizophila* ATCC 9341.

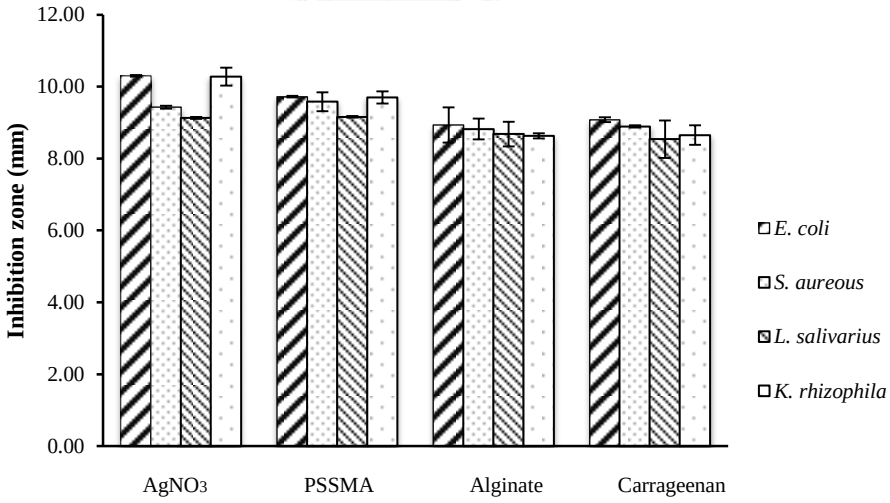

Figure 4.4 The antibacterial susceptibility of *E. coli* ATCC 25922, *S. aureus* ATCC 25923, *L. salivarius* ATCC 11741, and *K. rhizophila* ATCC 9341 after tested with $AgNO_3$ (control) and AgNPs with capping agents, i.e., PSSMA, alginate, and carrageenan. Each bar represents mean ± S.D. of inhibition zone (mm) in each group.

The antibacterial property of colloidal AgNPs capped with PSSMA showed the radial diameter of the inhibition zones of *E. coli* ATCC 25922, *S. aureus* ATCC 25923, *L. salivarius* ATCC 11741, and *K. rhizophila* ATCC 9341 as 9.72 ± 0.02, 9.58 ± 0.26, 9.16 ± 0.02, 9.70 ± 0.17 mm, respectively (see Figure 4.4). The antibacterial susceptibility of colloidal AgNPs capped with PSSMA seem to be higher than colloidal AgNPs capped with alginate, which showed the inhibition zones as 8.93 ± 0.49, 8.82 ± 0.29, 8.68 ± 0.34, 8.63 ± 0.07 mm, respectively, and carrageenan, which showed the inhibition zones as 9.08 ± 0.07, 8.89 ± 0.03, 8.54 ± 0.52, 8.65 ± 0.27 mm, respectively.

Guzman and coworkers [131] revealed that the antibacterial activity of AgNPs was influenced by the size of particles. Smaller particles usually present a greater antibacterial effect [9, 131]. Thereby in Figure 4.4, the antibacterial effect of colloidal AgNPs capped with PSSMA was higher than that with alginate because of the smaller size and less nanoparticles aggregation. Meanwhile, the sizes of AgNPs capped with alginate and carrageenan were larger than that with PSSMA, probably because alginate and carrageenan covering around particles affect less antibacterial properties. Although an average size of colloidal AgNPs capped with alginate was less than colloidal AgNPs capped with carrageenan, AgNPs capped with carrageenan tended to have higher antibacterial activity. This was because of colloidal AgNPs capped with carrageenan had less aggregation when compared that with alginate (Figures 4.2-4.3). Probably, there was a relationship between the size, aggregation and the bacterial susceptibility.

The antibacterial susceptibility of the capping agents coated AgNPs was also comparable with those of $AgNO_3$ which showed the inhibition zones of *E. coli* ATCC 25922, *S. aureus* ATCC 25923, *L. salivarius* ATCC 11741, *and K. rhizophila* ATCC 9341 as 10.30 ± 0.02, 9.43 ± 0.04, 9.13 ± 0.03, 10.28 ± 0.25 mm, respectively (see Figure 4.4). This is well-known that $AgNO_3$ is a good antibacterial agent. The antibacterial activity of the $AgNO_3$ and complexes (ionic silver) is generally based on the bonding of metallic ions to various biomacromolecular components

[10, 132] and then its effect could destroy the DNA replication ability and cellular proteins activation [27, 133, 134].

4.2.2 Bacterial growth curve

According to the previous results, colloidal AgNPs capped with PSSMA had the highest antibacterial effect. Therefore it was selected for further study on bacterial growth of 0.05 OD (OD 600 nm) of *S. aureus* ATCC 25923 (Figure 4.5) and *E. coli* ATCC 25922 (Figure 4.6) compared with ultrapure water (control).

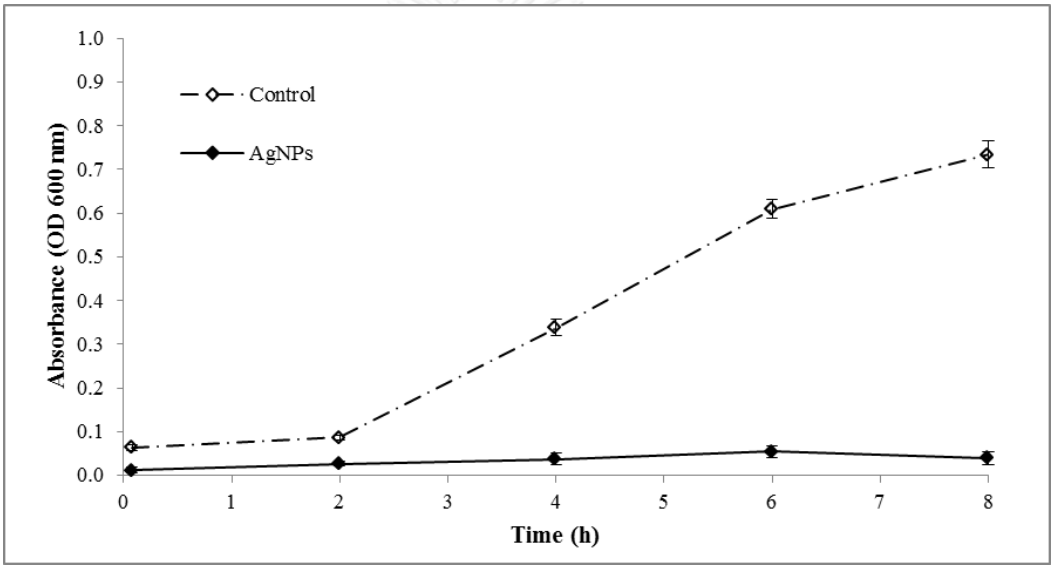

Figure 4.5 The bacterial growth of 0.05 OD (OD 600 nm) of *S. aureus* ATCC 25923 after exposed to AgNPs (solid line) compared with control (dashed line). The values for bacterial growth curve are the means of 6 replicates. Error bars indicate standard deviations of the means.

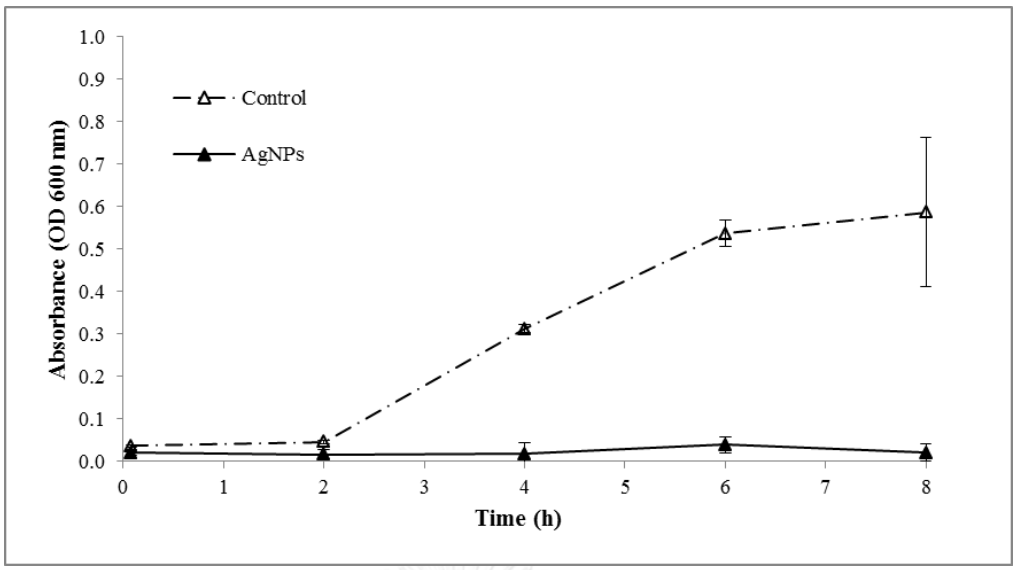

Figure 4.6 The bacterial growth of 0.05 OD (OD 600 nm) of *E. coli* ATCC 25922 after exposed to AgNPs (solid line) compared with control (dashed line). The values for bacterial growth curve are the means of 6 replicates. Error bars indicate standard deviations of the means.

In this antibacterial testing, not only *S. aureus* ATCC 25923 and *E. coli* ATCC 25922, but also *S. aureus* ATCC 6538p, *S. aureus* ATCC 43300, *S. epidermidis* ATCC 12228, *B. subtilis* ATCC 6633, *En. aerogenes* ATCC 13048, *Ps. aeruginosa* ATCC 27853 were tested on the bacterial growth exposed and unexposed to AgNPs (Figures 4.7-4.9).

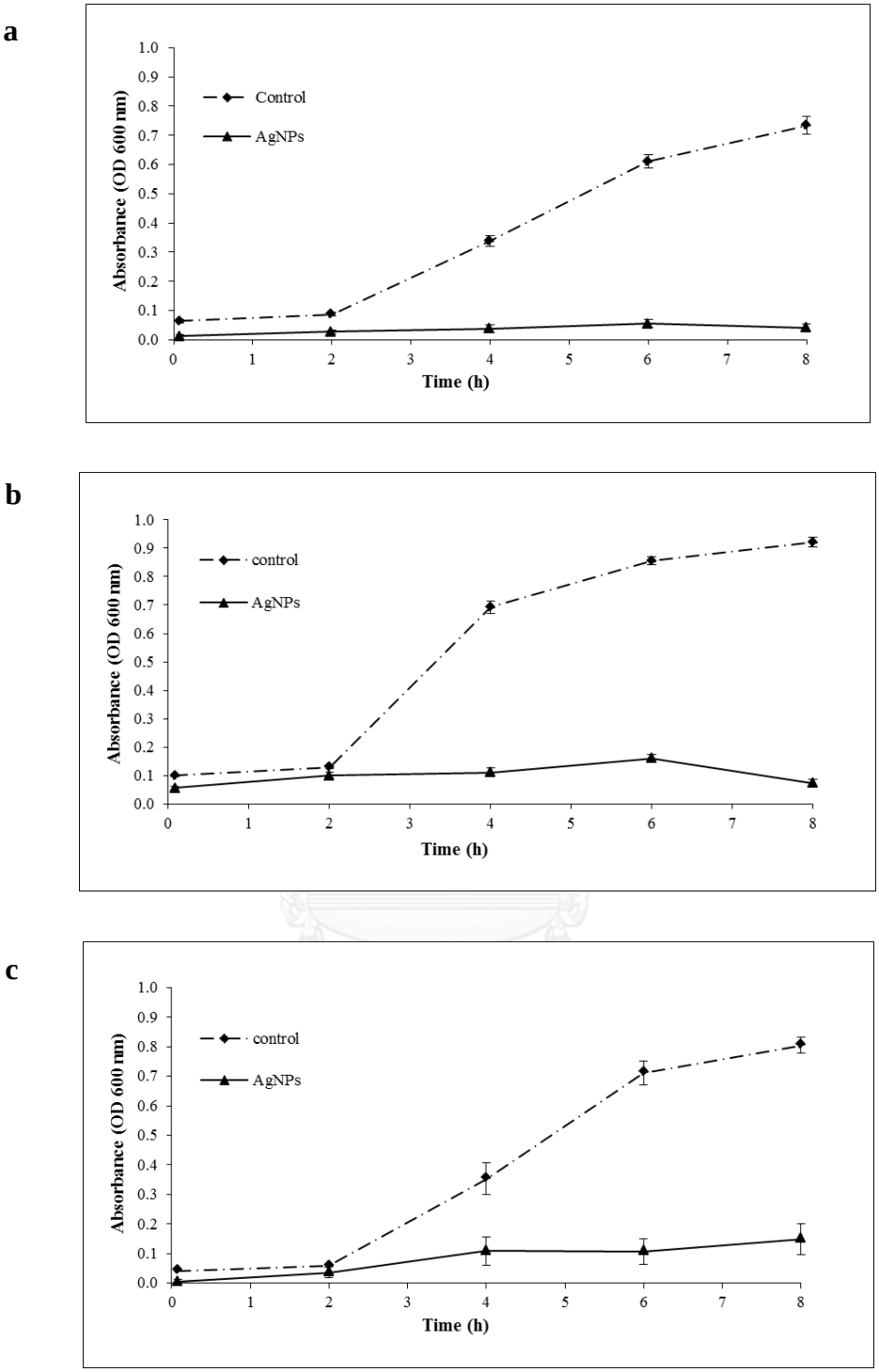

Figure 4.7 The antibacterial susceptibility of *Staphylococcus aureus* strains, (a) *S. aureus* ATCC 25923, (b) *S. aureus* ATCC 6538p and (c) *S. aureus* ATCC 43300, after exposed to AgNPs (solid line) compared with untreated control (dashed line).

The values for bacterial growth curve are the means of 6 replicates. Error bars indicate standard deviations of the means.

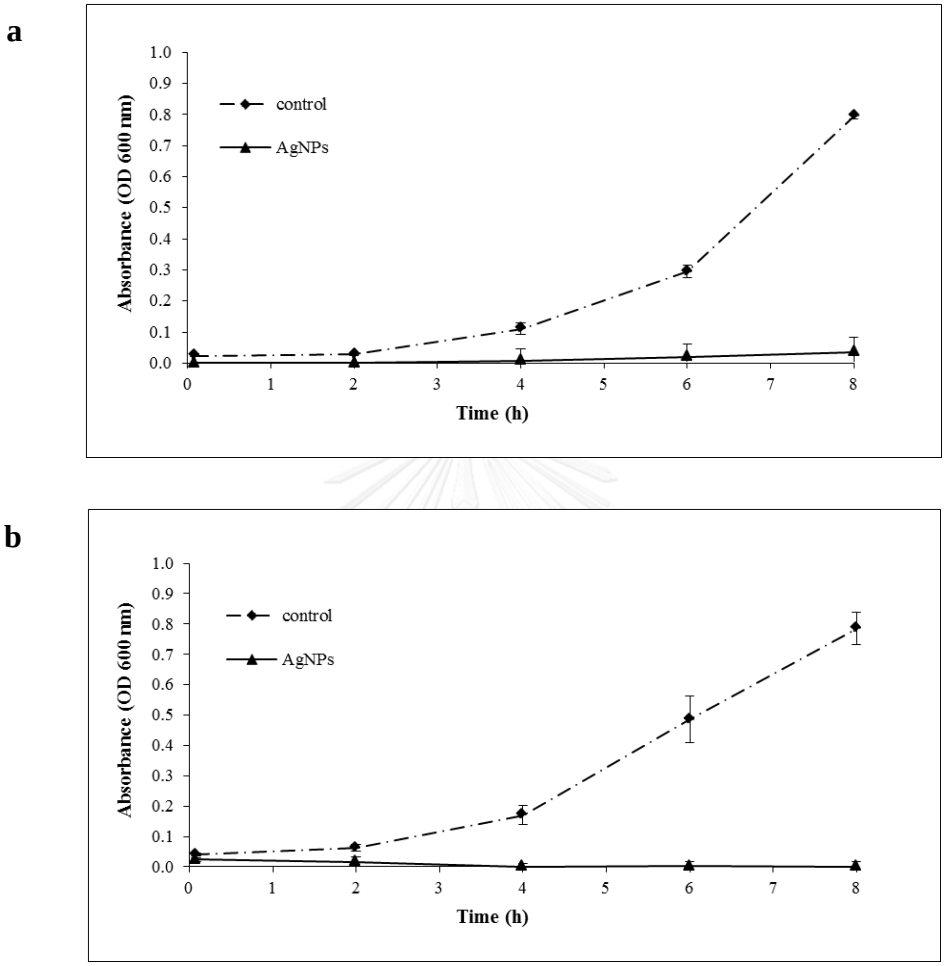

Figure 4.8 The antibacterial susceptibility of Gram-positive bacteria, (a) *S. epidermidis* ATCC 12228 and (b) *B. subtilis* ATCC 6633, after exposed to AgNPs (solid line) compared with untreated control (dashed line). The values for bacterial growth curve are the means of 6 replicates. Error bars indicate standard deviations of the means.

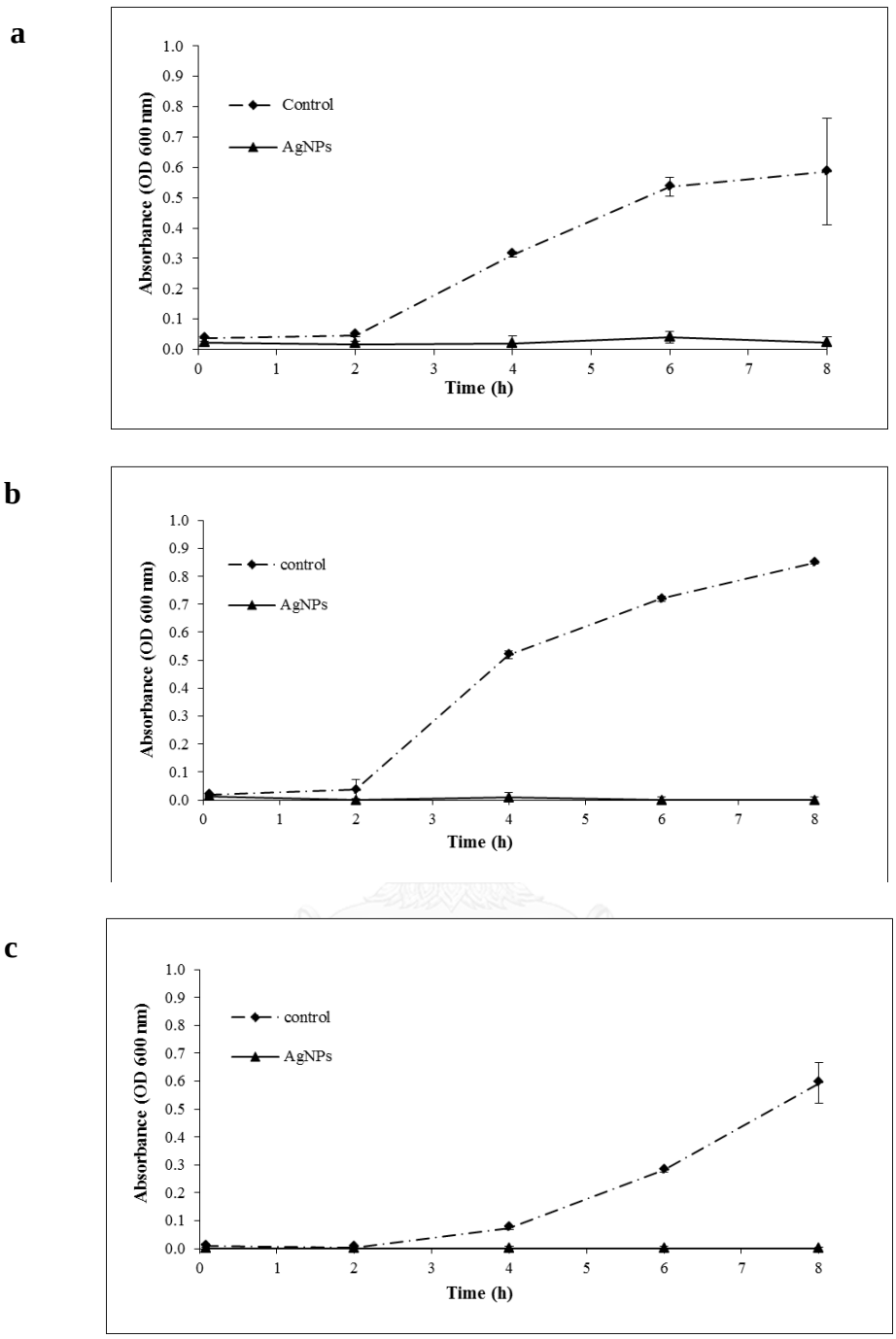

Figure 4.9 The antibacterial susceptibility of Gram-negative bacteria, (a) *E. coli* ATCC 25922, (b) *En. aerogenes* ATCC 13048 and (c) *Ps. aeruginosa* ATCC 27853, after exposed to AgNPs (solid line) compared with untreated control (dashed line). The values for bacterial growth curve are the means of 6 replicates. Error bars indicate standard deviations of the means.

It was found that synthesized AgNPs was capable of inhibiting all of tested bacterial strains; Gram-positive bacteria (*S. aureus* ATCC 25923, *S. aureus* ATCC 6538p, *S. aureus* ATCC 43300, *S. epidermidis* ATCC 12228, *B. subtilis* ATCC 6633) and Gram-negative bacteria (*E. coli* ATCC 25922, *En. aerogenes* ATCC 13048, *Ps. aeruginosa* ATCC 27853) within a couple hours. Therefore it could be concluded that synthesized AgNPs has the bactericidal effect.

In order to study the effects of AgNPs on *S. aureus* ATCC 25923 and *E. coli* ATCC 25922 protein profiles, both of their proteins were collected much enough for proteomics study. Therefore, *S. aureus* ATCC 25923 and *E. coli* ATCC 25922 cells were up-scaled experiment by using bacterial cells with 0.1 OD (OD 600 nm). The result of bacterial growth after up-scaled study has shown in Figure 4.10.

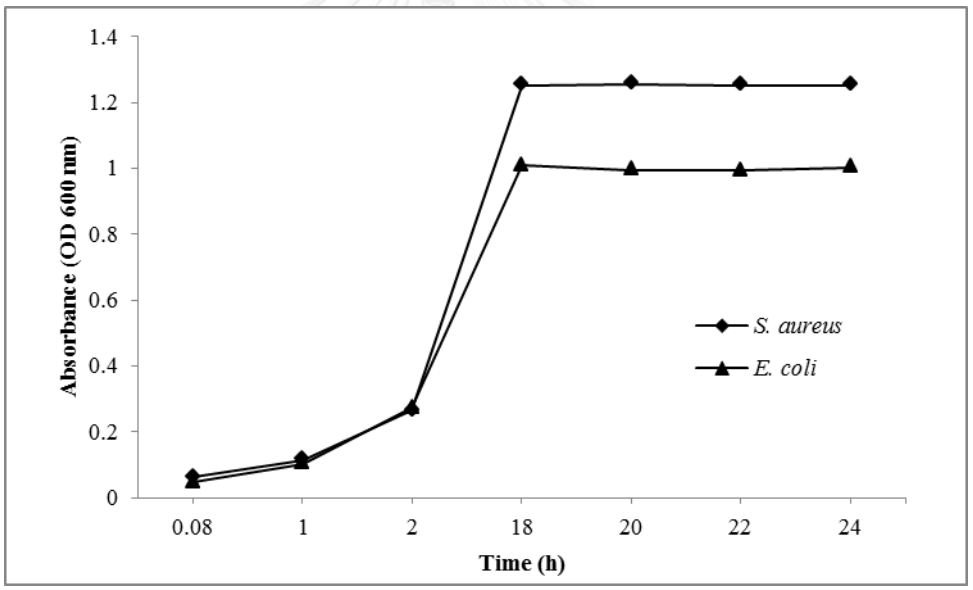

Figure 4.10 The S-shaped growth of 0.1 OD (OD 600 nm) of *S. aureus* ATCC 25923 and *E. coli* ATCC 25922 after up-scaled study.

Figure 4.10 shows the growth curve of *S. aureus* ATCC 25923 and *E. coli* ATCC 25922 which both are S-shaped. Up-scaled method influenced bacteria by decreasing of each time phase, and it was even shorten stationary phase. Probably, these are because of the extreme conditions from bacterial media and oxygen (compared with 96-well plates: small scaled).

S. aureus ATCC 25923 and *E. coli* ATCC 25922 cells with 0.1 OD (OD 600 nm) exposed and unexposed to AgNPs were studied bacterial growth at different time intervals (0 min, 15 min, 30 min, 45 min, 1 h, 2 h and 3 h).

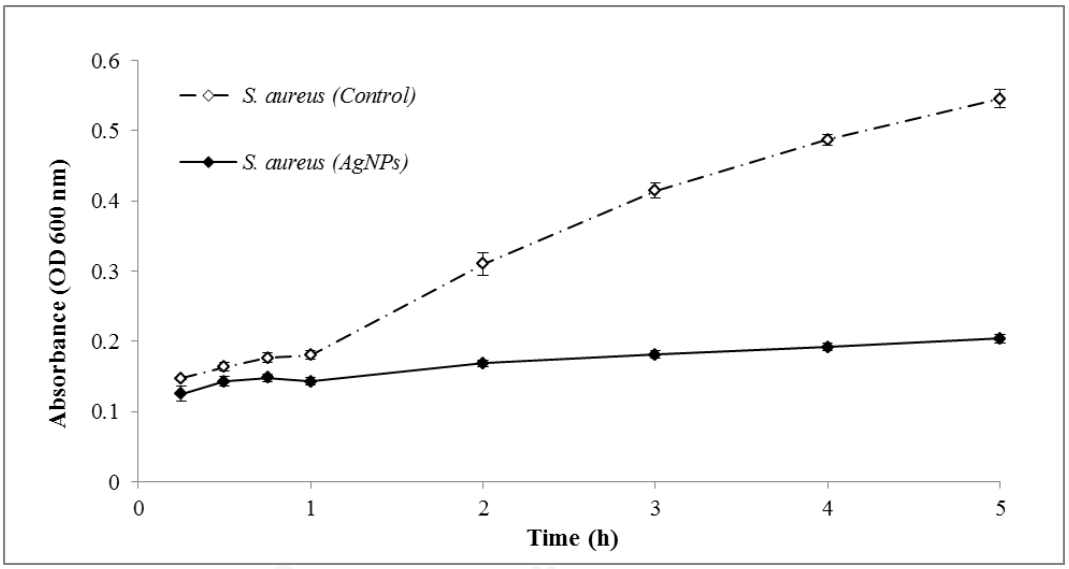

Figure 4.11 The bacterial growth of 0.1 OD (OD 600 nm) of *S. aureus* ATCC 25923 after exposed (solid line) and unexposed (dashed line) to AgNPs. The values for bacterial growth curve are the means of 4 replicates. Error bars indicate standard deviations of the means.

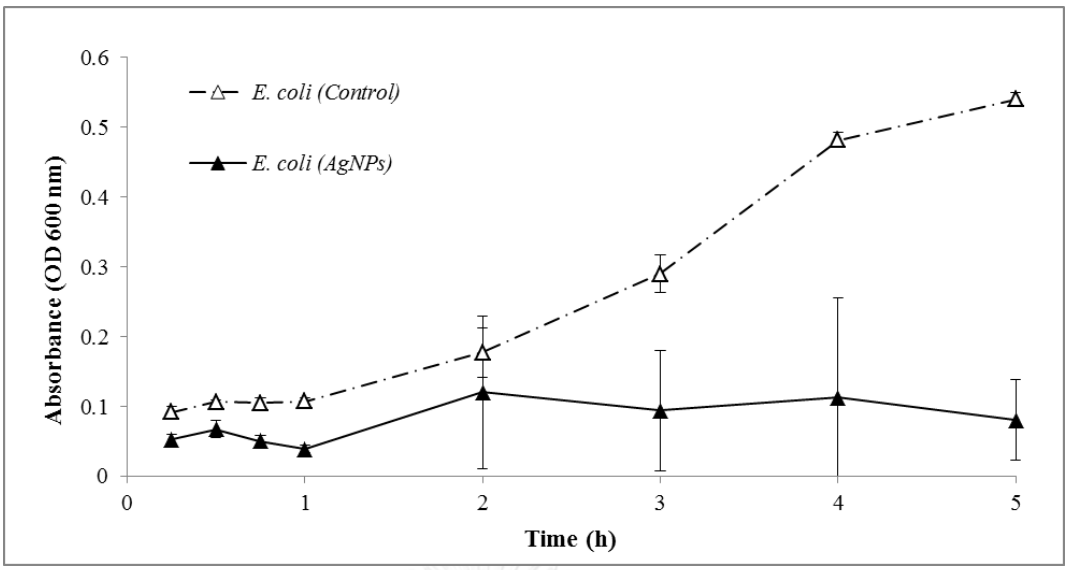

Figure 4.12 The bacterial growth of 0.1 OD (OD 600 nm) of *E. coli* ATCC 25922 after exposed (solid line) and unexposed (dashed line) to AgNPs. The values for bacterial growth curve are the means of 4 replicates. Error bars indicate standard deviations of the means.

From the antibacterial testing, AgNPs showed the bactericidal effect on *S. aureus* ATCC 25923 (Figure 4.11) and *E. coli* ATCC 25922 (Figure 4.12). Interestingly, AgNPs presented more antibacterial effect on *E. coli* ATCC 25922 cells than *S. aureus* ATCC 25923 cells. This is because *S. aureus* ATCC 25923 has a thicker peptidoglycan cell wall than *E. coli* ATCC 25922 [13, 135]. This thicker cell wall protects the cell from the penetration of AgNPs in the cytoplasm.

4.3 Protein separation by sodium dodecyl sulfate polyacrylamide gel electrophoresis (SDS-PAGE)

The SDS-PAGE analysis was used to observe the protein patterns of total protein extracted from different time intervals (0 min, 15 min, 30 min, 45 min, 1 h, 2 h and 3 h) of both *S. aureus* ATCC 25923 and *E. coli* ATCC 25922 after exposed and unexposed to AgNPs. After that it was followed by LC-MS/MS analysis for protein quantification and identification. The protein samples were analyzed by 12.5% gel SDS-PAGE, and the gel was visualized by silver staining and Coomassie brilliant blue G staining as shown in Figure 4.13 and Figure 4.14.

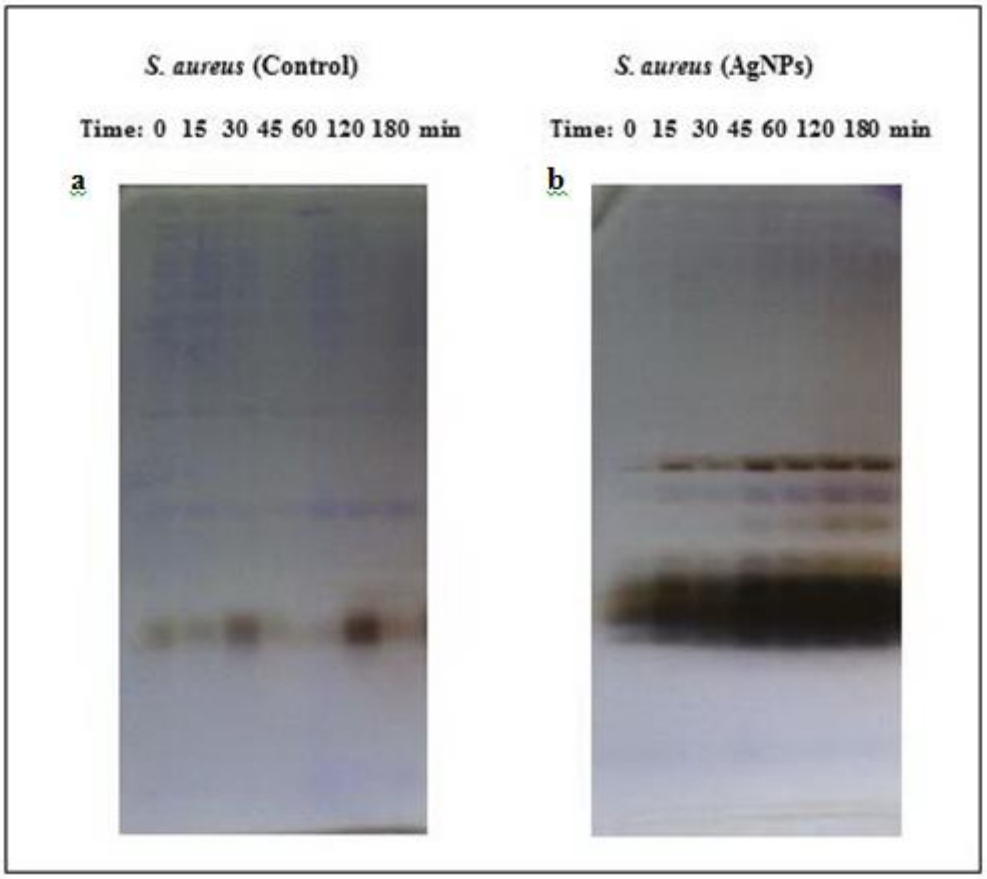

Figure 4.13 Pattern of total protein extracted from *S. aureus* ATCC 25923 after (a) unexposed and (b) exposed to AgNPs at 7 different incubation times.

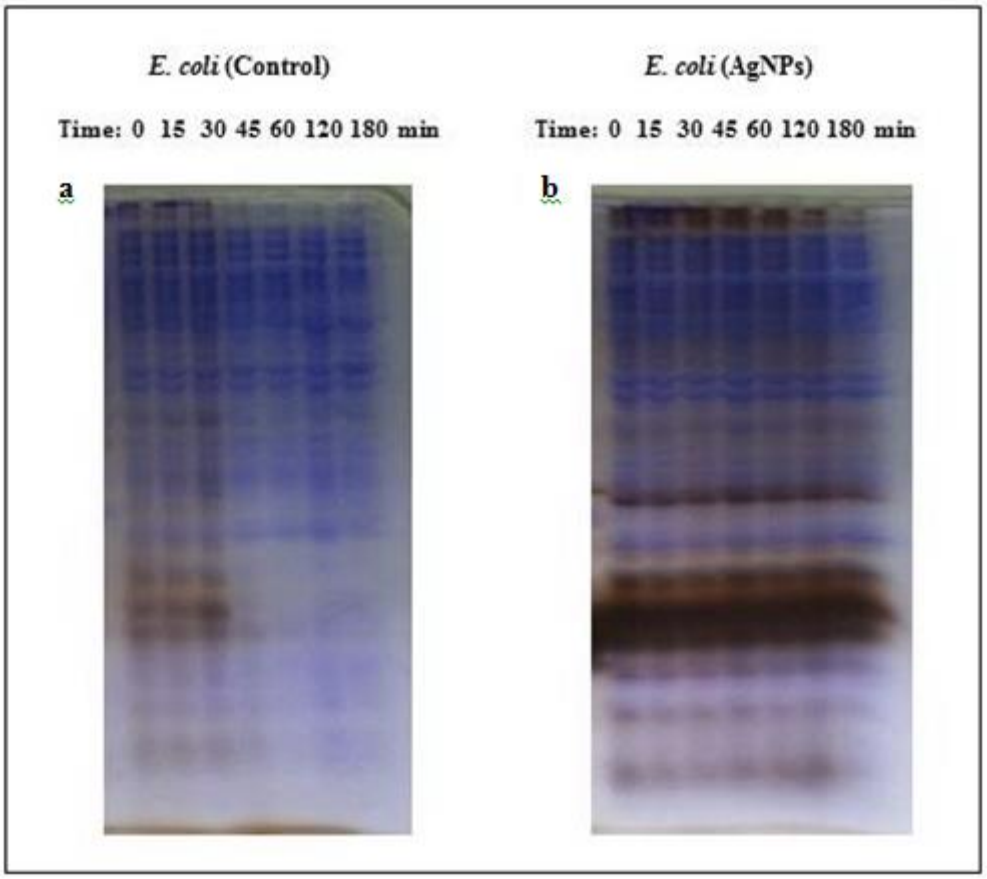

Figure 4.14 Pattern of total protein extracted from *E. coli* ATCC 25922 after (a) unexposed and (b) exposed to AgNPs at 7 different incubation times.

The double staining (silver staining and Coomassie brilliant blue G staining) is working well for protein patterns detection. This is because each dye has different staining mechanism. Although the mechanism of silver staining is not yet completely known [136], Coomassie brilliant blue G stains proteins by binding to the aromatic amino acids (arginine, histidine, etc.) based on physical adsorption [137]. Hence, AgNPs may affect to the aromatic acids inside the *S. aureus* ATCC 25923 cells. In contrast, the blue color of Coomassie dye is almost disappeared when compared with unexposed to AgNPs (Figure 4.13). Meanwhile, the blue staining color of the protein patterns from *E. coli* ATCC 25922 exposed and unexposed to AgNPs is almost the same (Figure 4.14). The different color intensity of bacterial protein after exposed to AgNPs reveals the increased (up-regulation) and decreased (down-regulation) protein expression in both bacteria (Figure 4.13, Figure 4.14).

4.4 Protein identification by liquid chromatography tandem mass spectrometry (LC-MS/MS)

4.4.1 LC-MS/MS analysis

Each protein band was excised separately as shown in Figure 4.15 and Figure 4.16. After that, the tryptic in-gel digestion was performed in 96-well plates. All extracted peptides sample were individually injected to LC-MS/MS.

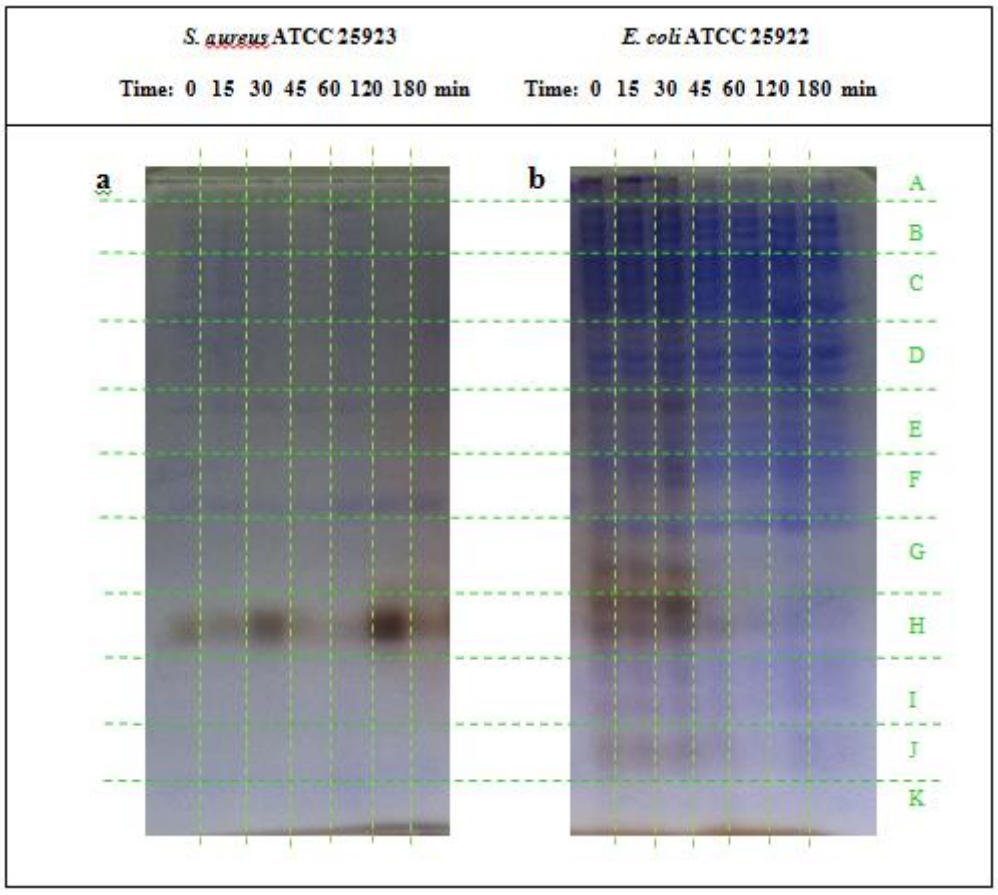

Figure 4.15 The 11 excised ranges (follow the horizontal lines) of protein expression extracted from (a) *S. aureus* ATCC 25923 and (b) *E. coli* ATCC 25922 after unexposed to AgNPs (control).

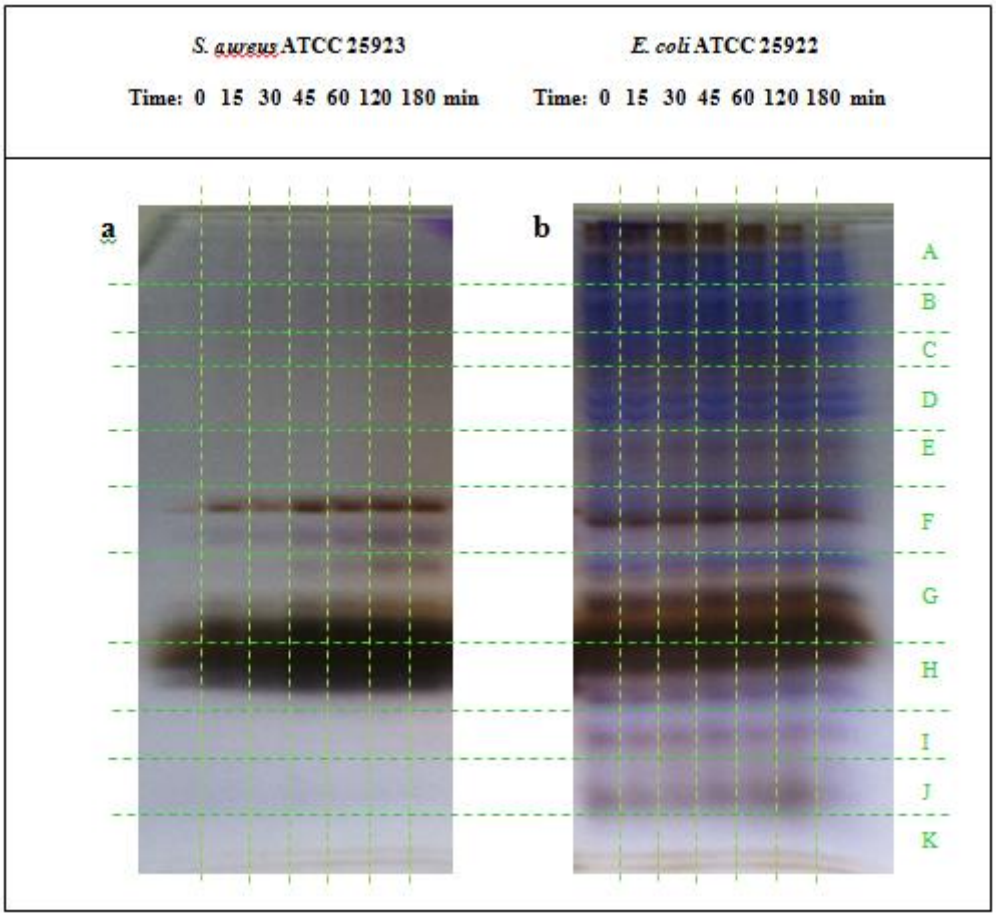

Figure 4.16 The 11 excised ranges (follow the horizontal lines) of protein expression extracted from (a) *S. aureus* ATCC 25923 and (b) *E. coli* ATCC 25922 after exposed to AgNPs.

4.4.2 Protein identification and gene ontology

With the proteomics analysis, the synthesized AgNPs showed different effects on the protein patterns of *S. aureus* ATCC 25923 and *E. coli* ATCC 25922 compared with control samples. Among protein quantitation and protein identification, there were 2,475 proteins that were matched with the proteins deposited in National Center for Biotechnology Information (NCBI) database. The proteins data were imported into Microsoft Excel. Proteins with the same name was once selected based on the maximum score, the minimum t-test and ANOVA, the minimum mass, and the minimum MH^+ (Da), respectively before protein

normalization. Intensity data with different time intervals in each protein was individually sorted from the maximum to the minimum. The maximum intensity of each protein sample in Excel table was selected for Venn diagram expression; an interested part selected with the intensity value while another uninterested part selected with zero value. The number of proteins from each part was counted and further expressed in the Venn diagram. Four main protein expression categories, *E. coli* (control), *E. coli* (AgNPs), *S. aureus* (control) and *S. aureus* (AgNPs), of the total matched proteins are shown in Venn diagram (Figure 4.17).

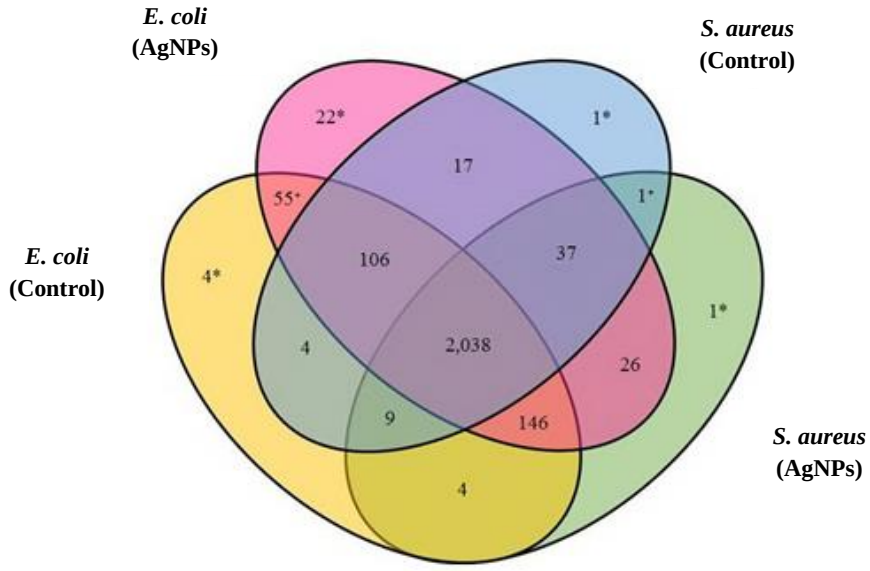

Figure 4.17 Identified proteins from *E. coli* ATCC 25922 and *S. aureus* ATCC 25923 after exposed to AgNPs analyzed by LC-MS/MS (*: free areas of *E. coli*_control, *E. coli*_AgNPs, *S. aureus*_control, *S. aureus*_AgNPs, and $^{+}$: intersection areas of free areas of *E. coli*_control and AgNPs, and *S. aureus*_control and AgNPs).

To better understand the antibacterial mechanism of AgNPs, free areas of *E. coli*_control (*: yellow color), *E. coli*_AgNPs (*: pink color), *S. aureus*_control (*: blue color), *S. aureus*_AgNPs (*: green color), as well as intersection areas of free areas of *E. coli*_control and AgNPs ($^{+}$: coral color) and *S. aureus*_control and AgNPs ($^{+}$: teal color) were focused. The significant proteins from above 6 interested parts were further searched the protein symbols and protein functions by the UniProt database. The Uniprot can identify proteins that only represent in the database. Therefore, if the identified proteins from LC-MS/MS have no functions or symbols, those proteins were automatically diminished. According to Figure 4.17, the identified proteins were reduced, for example the reduction of the number of proteins from 4 proteins to 2 proteins, 22 proteins to 8 proteins, and 55 proteins to 16 proteins in the free area of *E. coli* (Control), *E. coli* (AgNPs), and the intersection area of free areas between them as can be shown in the Table 4.2 and Figure 4.18.

Table 4.2 The identified proteins by LC-MS/MS with known functions.

Protein accession number	Protein name	Protein symbol	Function
***S. aureus* (Control)**			
gi|170081960	Long-chain fatty acid transport protein	fadL	Molecular transport
***S. aureus* (AgNPs)**			
gi|326798469	3-deoxy-D-manno-octulosonic-acid transferase	waaA	Metabolic process
***S. aureus* (Control and AgNPs)**			
gi|1786970	2,3-bisphosphoglycerate-dependent phosphoglycerate mutase	gpmA	Metabolic process
***E. coli* (Control)**			
gi|1786964	Quinolinate synthase A	nadA	Metabolic process
gi|153844091	Protein YhgF	yhgF	Metabolic process

Protein accession number	Protein name	Protein symbol	Function
***E. coli* (AgNPs)**			
gi|146319043	Threonine dehydrogenase and related Zn-dependent dehydrogenase	srlB	Metabolic process
gi|283778629	DNA topoisomerase type IA Zn finger domain-containing protein	yrdD	Transcription
gi|1787018	Probable ATP-dependent helicase DinG	dinG	DNA replication
gi|1789715	50S ribosomal protein L4	rplD	Translation
gi|308050024	Flagellar hook-basal body protein	fliE	Metabolic process
gi|156973219	UDP-N-acetylmuramoyl-L-alanyl-D-glutamate synthetase	murD	Metabolic process
gi|197103203	Peptide transport system ATP-binding protein SapF	sapF	Molecular transport
gi|323524861	Enoyl-CoA hydratase/isomerase	tdcF	Signal transduction
***E.coli* (Control and AgNPs)**			
gi|260893293	Alanyl-tRNA synthetase	alaS	Translation
gi|331007050	Colicin V production protein	cvpA	Molecular transport
gi|312196358	IclR family transcriptional regulator	iclR	Transcription
gi|227357988	Siderophore biosynthesis IucA / IucC family protein	iucA	Metabolic process

Protein accession number	Protein name	Protein symbol	Function
gi|226943115	Isopropylmalate isomerase large subunit	leuC	Metabolic process
gi|227495901	Leucine--tRNA ligase	leuS	Translation
gi|384412003	NusA antitermination factor	nusA	Transcription
gi|325067458	Oligopeptide ABC transporter periplasmic protein	oppA	Molecular transport
gi|225010785	PhoH family protein	phoH	Metabolic process
gi|261854682	Phosphoribosylaminoimidazolecarboxamide formyltransferase/IMP cyclohydrolase	purH	Metabolic process
gi|85860692	ATP-dependent RNA helicase	rhlB	Transcription
gi|29653579	50S ribosomal protein L1	rplA	Translation
gi|257459944	Putative TonB dependent receptor	tonB	Signal transduction
gi|333984533	TonB-dependent siderophore receptor	yncD	Signal transduction
gi|319762019	HAD-superfamily hydrolase	yqaB	Metabolic process
gi|320353100	OmpA/MotB domain-containing protein	motB	Molecular transport

Figure 4.18 showed the Venn diagram of significantly identified proteins that were grouped from Table 4.2. *S. aureus* (control) had 1 gene ontology (GO) category like *S. aureus* (AgNPs) and 1 shared GO category between them (Figure 4.18a). *E. coli* (control) had 2 GO categories while *E. coli* (AgNPs) had 8 GO categories. Although *E. coli* (AgNPs) had 6 more proteins than *E. coli* (control), there were 16 shared GO categories between *E. coli* (control) and *E. coli* (AgNPs) (Figure 4.18b).

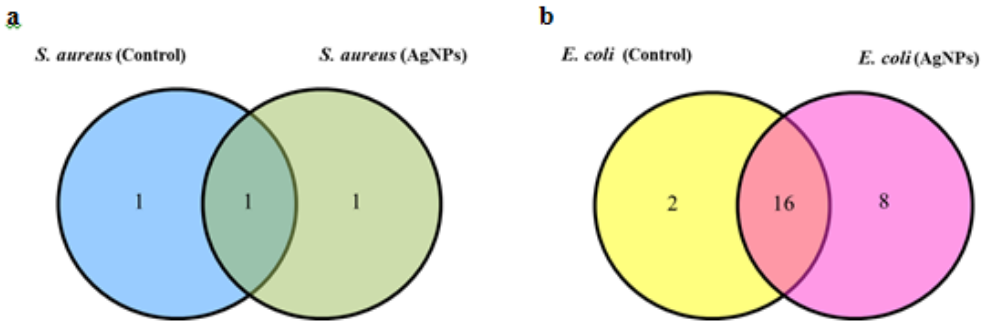

Figure 4.18 Significant identified proteins from (a) *S. aureus* ATCC 25923 and (b) *E. coli* ATCC 25922 after exposed to AgNPs (excluding unknown protein symbols and functions).

From the identified protein results, AgNPs would affect to the bacterial system by 6 main functions that are 1) signal transduction, 2) molecular transport, 3) metabolic process, 4) DNA replication, 5) transcription, and 6) translation.

4.4.3 Bioinformatics pathways analysis

Protein candidate found in free areas and intersection areas of *S. aureus* ATCC 25923 and *E. coli* ATCC 25922 samples were searched for their protein symbols by using Uniprot (http://www.uniprot.org) (Table 4.2, Figure 4.18). Protein symbols were futher analyzed with the help of the Search Tool for the Retrieval of Interacting Genes/Proteins (String), the pathway analysis independent software. Integration of proteins into biological association networks was done on String database (http://string-db.org), which is based on known and predicted protein interactions [138]. Data upload in the String software tools resulted in the pathway cartoons shown in Figure 4.19 (*S. aureus* ATCC 25923) and Figure 4.20 (*E. coli* ATCC 25922).

Three genes (gmpA, waaA, and fadL) of *S. aureus* ATCC 25923 were directly inputted into String software. 2,3-bisphosphoglycerate-dependent phosphoglycerate mutase (gmpA gene) is a protein in cytoplasm which catalyzes the

interconversion of 2-phosphoglycerate and 3-phosphoglycerate in glycolysis pathway [139]. 3-deoxy-D-manno-octulosonic acid transferase (waaA gene) is a protein located at cell membrane and cell inner membrane, usually involved in lipopolysaccharide (LPS) biosynthesis, and catalysis of the transfer of two 3-deoxy-D-manno-octulosonate (Kdo) residues from CMP-Kdo to lipid IV(A), the tetraacyldisaccharide-1,4'-bisphosphate precursor of lipid A [140, 141]. Long-chain fatty acid transport protein (fadL gene) is a protein at cell outer membrane and membrane [142]. It is associated in translocation of long-chain fatty acids across the outer membrane, protein receptor, and specific channel. The fadL gene was found to be down-regulated expression after exposed to AgNPs.

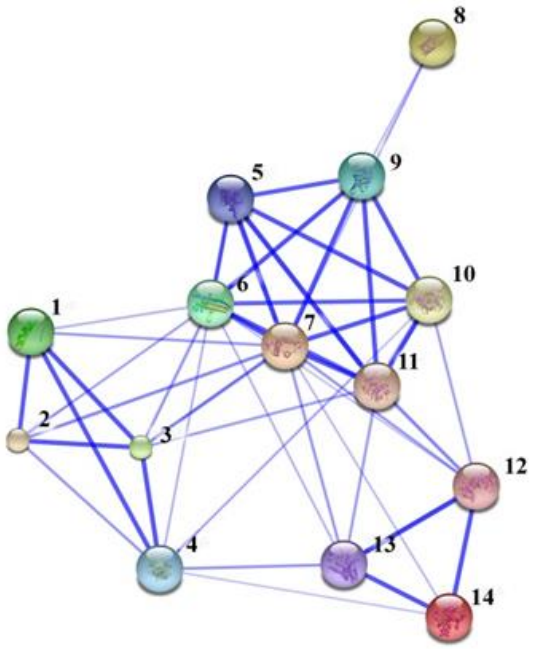

1: lpxK, 2: htrB, 3: waaA, 4: kdsB, 5: fabF, 6: acpS, 7: acpP, 8: fadL, 9: fabB, 10: fabI, 11: fabH, 12: pgk, 13: eno, 14: gpmA

Figure 4.19 Interaction network of matched categories for *S. aureus* ATCC 25923. Thicker lines indicate higher confidence and higher number of interactions described by String database.

When bacterial cells were treated with AgNPs, the outer membrane proteins are the first part to confront with AgNPs (antibiotic agent). This was in agreement with the study by Cottingham [143] whom presented that fadL gene of *E. coli* was down-regulated after it grew resistance to streptomycin (SM), an antibiotic drug [143]. Some studies showed an aberrant morphology of bacterial cells after AgNPs treatment. TEM electron micrographs from previous studies showed the cell membrane was fragmentary and membrane components became disorganized and scattered [144-146]. With this case, protein receptors or specific channels on the surface of *S. aureus* cells perhaps have a conformational change which has effect on the lipid transport deficiency and finally leads to cells death. Li and coworkers [144] revealed that there were expression alterations of proteins in *S. aureus* cells treated with AgNPs. Up-regulated expression was observed in the gene encoding for formate acetyltransferase, and down-regulated expression in the genes encoding for aerobic glycerol-3-phosphate dehydrogenase, ABC transporter ATP-binding protein and recombinase A protein [144]. Moreover, the whole connection among the differently expressed proteins investigated by String software (Figure 4.19) revealed that *S. aureus* ATCC 25923 (representative bacteria of Gram-positive bacteria) represented genes implicated in lipid and carbohydrate metabolisms.

Meanwhile, 26 genes (nadA, yhgF, srlB, yrdD, dinG, rplD, fliE, murD, sapF, tdcF, alaS, cvpA, iclR, iucA, leuC, leuS, nusA, oppA, phoH, purH, rhlB, rplA, tonB, yncD, yqaB, and motB) of *E. coli* ATCC 25922 were directly inputted into String database. However, there were matched with String software for 25 genes (nadA, yhgF, srlB, yrdD, dinG, rplD, fliE, murD, sapF, tdcF, alaS, cvpA, iclR, leuC, leuS, nusA, oppA, phoH, purH, rhlB, rplA, tonB, yncD, yqaB, and motB), and another iucA gene was absent. A previous study on *E. coli* cells with AgNPs treatment by Lok and coworkers [147] showed up-regulated expression of a panel of envelope protein precursors (i.e., OmpA, OmpC, OmpF, OppA, MetQ), which was a direct evidence of dissipation of proton motive force [147]. Heat shock proteins (IbpA, IbpB, and 30S ribosomal subunit S6) were also up-regulated, which had chaperone functions against stress-induced protein denaturation [148]. Interestingly, for *E. coli* ATCC 25922 exposed to AgNPs, the expression of nadA and yhgF genes was down-regulated,

whereas the expression of other genes such as srlB, yrdD, dinG, rplD, fliE, murD, sapF, and tdcF genes was up-regulated.

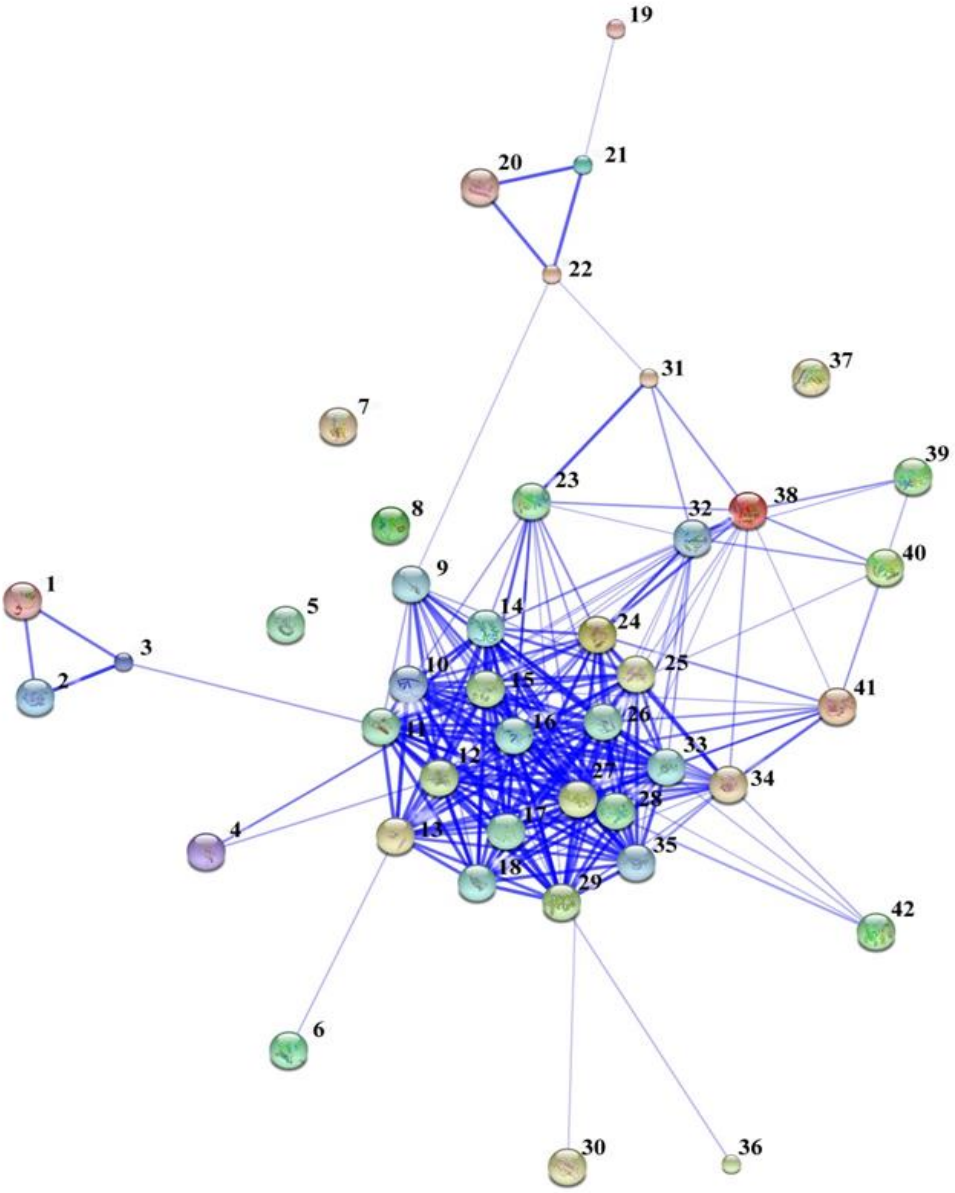

1: sapF, 2: oppA, 3: oppB, 4: tonB, 5: iclR, 6: phoH, 7: yqaB, 8: dinG, 9: secE, 10: rpsG, 11: rpsR, 12: secY, 13: rpsU, 14: rpsF, 15: rpsL, 16: rpsE, 17: rplB, 18: rplW, 19: yncD, 20: motB, 21: flgI, 22: fliE, 23: purH, 24: leuS, 25: nusA, 26: rplK, 27: rplM, 28: rplA, 29: rplD, 30: tdcF, 31: cvpA, 32: leuD, 33: rplC, 34: alaS, 35: rplV, 36: yrdD, 37: srlB, 38: leuC, 39: yhgF, 40: nadA, 41: murD, 42: rhlB

Figure 4.20 Interaction network of matched categories for *E. coli* ATCC 25922. Thicker lines indicate higher confidence and higher number of interactions described by String database.

Down-regulation defines as the process of reducing or suppressing a response to an external variable, by which a cell decreases the quantity of a cellular component (RNA, protein, etc.). Quinolinate synthase A (nadA gene) is a protein in cytoplasm that catalyzes the condensation of iminoaspartate with dihydroxyacetone phosphate to form quinolinate (pyridine nucleotide biosynthesis) [149-151]. Protein YhgF (yhgF gene) is related to nucleobase-containing compound metabolic process, RNA binding, and hydrolase activity. After down-regulation of nadA and yhgF genes after exposed to AgNPs, the synthesis of the NAD and NADP is decreased. A decrease affects the redox reactions and cellular metabolic processes such as interaction of nucleic acids and their compounds, hydrolysis of ester bond, and posttranslational modifications, which are important for cell survival. Therefore, the AgNPs treatment results in the down-regulation of the two proteins which further induces the cell death.

On the other hand, up-regulation defines as the process of increasing of a cellular component after response to an external variable. Probable ATP-dependent helicase DinG (dinG gene) is a vital enzyme to all living organisms. Its function is involved in DNA repair and possibly replication [152]. 50S ribosomal protein L4 (rplD gene) is a primary rRNA binding proteins at ribosome. Protein L4 is a transcriptional repressor as well as a translational repressor protein [153], which antagonizes conversion of DNA segment into RNA, and ribosome-mediated translation of mRNA into a polypeptide. Moreover, this protein shows antibiotic resistance in biological process, which is the ability to withstand antibiotics (in terms of movement, secretion, enzyme production, gene expression, etc.) as a result of an antibiotic stimulus (AgNPs). Peptide transport system ATP-binding protein SapF (sapF gene) is a protein in plasma membrane and involved in a peptide intake transport system that plays a role in the resistance to antimicrobial peptides [154]. After exposed to AgNPs, the above genes were up-regulated to prevent the damage from AgNPs. For example, the increasing of dinG gene expression after exposed to AgNPs can help DNA repair to resist the antibacterial effect from AgNPs. However, if bacterial cells get much damaged effect from AgNPs and DNA repair process could not repair or recover cells in time, AgNPs may finally interrupt cellular process and

lead to cell death. Furthermore, the whole connection among the differently expressed proteins investigated by String database (Figure 4.20) revealed that *E. coli* ATCC 25922 (representative bacteria of Gram-negative bacteria) represented genes implicated mainly in transporter system, metabolic activity, transcription and translation. Moreover, 4 novel biomarkers, i.e.; yqaB, iclR, dinG, and srlB were investigated in this study. These novel biomarkers could refer to or expect for antibacterial activity of AgNPs.

Overall, the proposed pathway for AgNPs to affect *S. aureus* ATCC 25923 and *E. coli* ATCC 25922 bacterial growth and bacterial protein profiles in this study are based on 6 main functions i.e., signal transduction, molecular transport, metabolic process, DNA replication, transcription, and translation (Table 4.2).

These correspond with the action of silver ions ($AgNO_3$) and antibacterial drugs which the effect ranges from outside to inside of bacterial cells. Besides, Ag^+ in the form of $AgNO_3$ solution, Ag^+ also probably releases from AgNPs. Schreurs and Rosenberg [155] presented the effect of Ag^+ on *E. coli* that Ag^+ inhibits phosphate uptake and causes efflux of accumulated phosphate as well as of mannitol, succinate, glutamine, and proline [155]. Although, the mechanism for the antibacterial action of silver ions is not well understood, the effect of silver ions on bacteria can be observed by the structural and morphological changes. Feng and coworkers [13] revealed that similar morphological changes occurred in both *E. coli* and *S. aureus* cells after Ag^+ treatment. DNA was condensed, clearly visible in the center of the electron-light region in both strains after $AgNO_3$ treatment. $AgNO_3$ also creates a big gap between the cytoplasm membrane and the cell wall and then leads to cell damage and cell death of bacteria [13].

Furthermore, several categories of antibiotics target the bacterial cell wall by inhibition of the activity of enzymes involved in the synthesis, maturation and layer formation of peptidoglycan. For example, daptomycin inhibits membrane function by inducing membrane pore formation and leading to bacterial death due to imbalance in transmembrane ion fluxes [156]. β-Lactams target bacterial cell wall and then affect metabolic processes, which are associated with fatty acid biosynthesis, the pentose phosphate pathway, glycolysis and stress-related

responses. Tetracyclines are broad-spectrum agents exhibiting the inhibition of bacterial protein synthesis by preventing the association of aminoacyl-tRNA with the bacterial ribosome [157]. Macrolides create an antibacterial property by binding to the 50S subunit of the bacterial ribosomes thus inhibiting protein synthesis [158]. Moreover, DNA and RNA synthesis were inhibited by antibacterial drugs. The proteomics data indicated that ciprofloxacin-induced down-regulation of metabolic pathways produced NADH and imbalanced synthesis of dNTPs in *Streptococcus uberis* [159] meanwhile rifampicin inhibited a DNA-dependent bacterial RNA polymerase, blocked mRNA synthesis and inhibited protein synthesis [160].

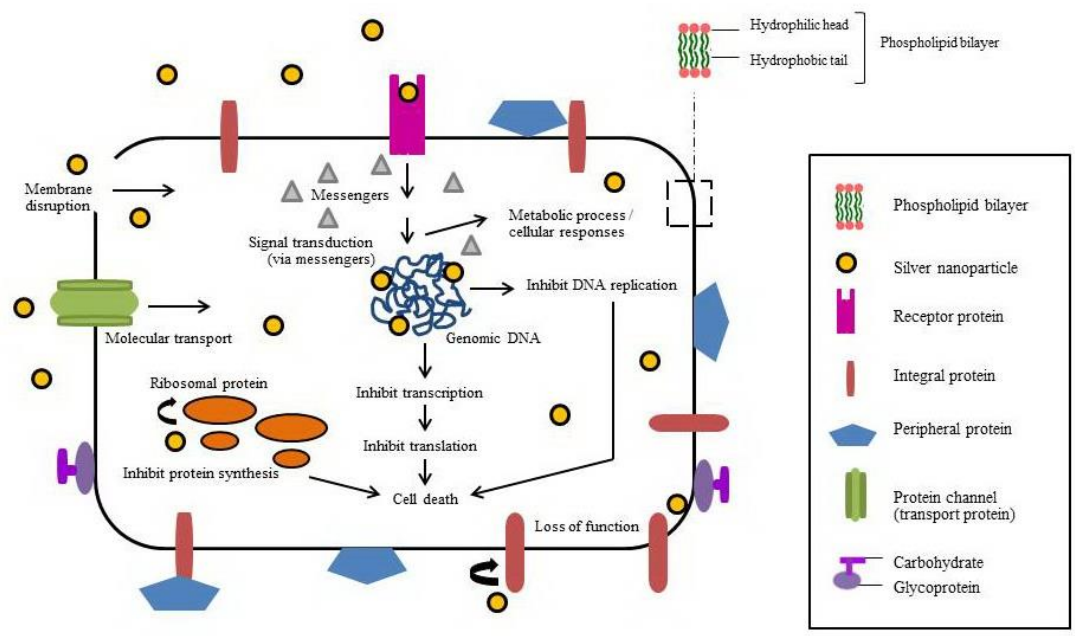

Figure 4.21 Proposed schematic representation of antibacterial mechanism of AgNPs.

Based on this study, the antibacterial mechanism of AgNPs is proposed as following: AgNPs start on an antibacterial effect by triggering at bacterial membrane. This activates a specific receptor protein on the cell membrane and then lets a messenger transmits the signal into the cell. AgNPs also directly enter into the bacterial cell because of its small size. Whether AgNPs creates an effect on signal transduction or self-transport into bacterial cells, both have an effect on molecular

transport and metabolism activity. Moreover, the effect from AgNPs tends to interfere with DNA replication, transcription, and translation by disruption of nucleic acid and protein synthesis. The proposed pathways elicit a physiological response and lead to cell death of bacteria (Figure 4.21). Although, the proposed antibacterial mechanism of AgNPs above can be used as the target mechanism for the antibiotics development, the results should be once confirmed by western blot or real-time polymerase chain reaction (RT-PCR).

The full potential of antibacterial mechanism of AgNPs has not been discovered, though it has been gradually clarified. This may be due to only a few strains of bacteria that have been studied. Moreover, the study is time consuming and costliness, which results in the report of incomplete protein profiles of overall bacterial perspective. This leaves a room for future research in AgNPs modification and their antibacterial applications.

CHAPTER V
CONCLUSIONS

Metallic silver nanoparticles (AgNPs) with and without capping agents were synthesized by the chemical reduction method in form of hydrocolloid-capped AgNPs. Silver nitrate ($AgNO_3$) was used as a metal precursor and sodium borohydride ($NaBH_4$) as a reducing agent. AgNPs with capping agents (4-styrenesulfonic acid – co – maleic acid (PSSMA), alginate, carrageenan) had a small size and high stability compared to AgNPs without capping agents which were prone to aggregate. The results demonstrated that capping agents affect the size and stability, and further affect the antibacterial susceptibility of AgNPs. Hydrocolloid-capped AgNPs served as a potent antibacterial agent against a broad spectrum of bacteria. Especially, PSSMA capped AgNPs presented a promising antibacterial susceptibility based on characterization techniques (UV-vis spectroscopy, laser Doppler electrophoresis (LDE), dynamic light scattering (DLS), transmission electron microscopy (TEM) and antibacterial susceptibility tests (Kirby-Bauer method, bacterial growth curves).

In order to gain insight into the antibacterial mechanism of AgNPs, comparative proteomics approach was used to annotate the differently expressed proteins between *S. aureus* ATCC 25923 and *E. coli* ATCC 25922 (representative for Gram-positive and Gram-negative bacteria, respectively) cells after exposed to PSSMA capped AgNPs compared with their control. The bacterial growth curves of both representative strains after exposed to AgNPs showed bactericidal effect within a few hours. Moreover, the sodium dodecyl sulfate polyacrylamide gel electrophoresis (SDS-PAGE) have shown that AgNPs affected the protein expression profiles differently in *S. aureus* ATCC 25923 and *E. coli* ATCC 25922, which was further confirmed by protein identification and gene ontology based on NCBI and UniProt databases.

After exposure to AgNPs, *S. aureus* ATCC 25923 showed the down-regulated and up-regulated expression in fadL gene and waaA gene, respectively. Meanwhile *E. coli* ATCC 25922 after exposure to AgNPs showed the down-regulated expression in nadA and yhgF genes, while the up-regulated expression in srlB, yrdD, dinG, rplD, fliE, murD, sapF, and tdcF genes was observed. Further study on bioinformatics pathways analysis using String software revealed that *S. aureus* ATCC 25923 represented genes implicated in lipid and carbohydrate cycles, meanwhile *E. coli* ATCC 25922 represented genes implicated mainly in transporter system, metabolic activity, transcription and translation. The novel biomarkers for antibacterial activity of AgNPs were investigated.

From this work, the proposed antibacterial mechanism of AgNPs were based on 6 main functions i.e., signal transduction, molecular transport, metabolic process, DNA replication, transcription, and translation. The results provide an understanding on AgNPs affected bacterial growth and possibly antibacterial mechanism. The study also provides a number of promising targets of antibacterial mechanism of AgNPs, which could be further applied on the design of nanoparticles for antibacterial purposes.

REFERENCES

[1] Gao, Y., Gopee, N. V., Howard, P. C., and Yu, L. R. Proteomic analysis of early response lymph node proteins in mice treated with titanium dioxide nanoparticles. Journal of Proteomics 74 (2011): 2745-2759.

[2] Abou El-Nour, K. M. M., Eftaiha, A., Al-Warthan, A., and Ammar, R. A. A. Synthesis and applications of silver nanoparticles. Arabian Journal of Chemistry 3 (2010): 135-140.

[3] Khan, Z., Al-Thabaiti, S. A., Obaid, A. Y., and Al-Youbi, A. O. Preparation and characterization of silver nanoparticles by chemical reduction method. Colloids and Surfaces B: Biointerfaces 82 (2011): 513–517.

[4] Harada, M., Kimura, Y., Saijo, K., Ogawa, T., and Isoda, S. Photochemical synthesis of silver particles in Tween 20/water/ionic liquid microemulsions. Journal of Colloid and Interface Science 339 (2009): 373-381.

[5] Wani, I. A., Ganguly, A., Ahmed, J. and Ahmad, T. Silver nanoparticles: Ultrasonic wave assisted synthesis, optical characterization and surface area studies. Materials Letters 65 (2011): 520-522.

[6] Mukherjee, P., et al. Fungus-mediated synthesis of silver nanoparticles and their immobilization in the mycelial matrix: A novel biological approach to nanoparticle synthesis. Nano Letters 1 (2001): 515-519.

[7] Li, W. R., et al. Antibacterial effect of silver nanoparticles on *Staphylococcus aureus*. Biometals 24 (2011): 135–141.

[8] Navarro, E., et al. Toxicity of silver nanoparticles to *Chlamydomonas reinhardtii.* Environmental Science and Technology 42 (2008): 8959-8964.

[9] Panacek, A., et al. Silver colloid nanoparticles: synthesis, characterization, and their antibacterial activity. The Journal of Physical Chemistry B 110 (2006): 16248-16253.

[10] Rai, M., Yadav, A., and Gade, A. Silver nanoparticles as a new generation of antimicrobials. Biotechnology Advances 27 (2009): 76–83.

[11] Guzman, M., Dille, J., and Godet, S. Synthesis and antibacterial activity of silver nanoparticles against Gram-positive and Gram-negative bacteria. Nanomedicine: Nanotechnology, Biology, and Medicine 8 (2012): 37-45.

[12] Tenover, F. C. Mechanisms of antimicrobial resistance in bacteria. The American Journal of Medicine 119 (2006): 3-10.

[13] Feng, Q. L., Wu, J., Chen, G. Q., Cui, F. Z., Kim, T. N., and Kim, J. O. A mechanistic study of the antibacterial effect of silver ions on *Escherichia coli* and *Staphylococcus aureus.* Journal of Biomedical Materials Research 52 (2000): 662-668.

[14] Patti, G. J., Yanes, O., and Siuzdak, G. Innovation: Metabolomics: The apogee of the omics trilogy. Nature Reviews Molecular Cell Biology 13 (2012): 263-269.

[15] Blackstock, W. P., and Weir, M. P. Trends in biotechnology proteomics: Quantitative and physical mapping of cellular proteins. vol. 17. Netherlands: Springer, 1999.

[16] Park, O. K. Proteomic studies in plants. Journal of Biochemistry and Molecular Biology 37 (2004): 133-138.

[17] Salekdeh, G. H., Siopongco, J., Wade, L. J., Ghareyazie, B., and Bennet, J. Proteomic analysis of rice leaves during drought stress and recovery. Proteomics 2 (2002): 1131-1145.

[18] Ali, G. M., and Komatsu, S. Proteomic analysis of rice leaf sheath during drought stress. Journal of Proteome Research 5 (2006): 396-403.

[19] Banks, R. E., et al. Proteomics: New perspectives, new biomedical opportunities. The Lancet 356 (2000): 1749-1756.

[20] Lok, C. N., et al. Proteomic analysis of the mode of antibacterial action of silver nanoparticles. Journal of Proteome Research 5 (2006): 916-924.

[21] Khademhosseini, A., and Langer, R. Nanobiotechnology—applications in drug delivery and tissue engineering. Centre for Economic Performance Magazine 102 (2006): 38–42.

[22] U.S. FDA. U.S. Food and Drug Administration [Online]. 2010. Available from: http://www.fda.gov/ScienceResearch/SpecialTopics/Nanotechnology/ucm153723.htm [February, 2010]

[23] Nowack, B., Krug, H. F., and Height, M. 120 years of nanosilver history: Implications for policy makers. Environmental Science and Technology 45 (2011): 1177–1183.

[24] Buzea, C., Pacheco, I. I., and Robbie, K. Nanomaterials and nanoparticles: Sources and toxicity. Biointerphases 2 (2007): 17-71.

[25] ASTM International. Standard terminology relating to Nanotechnology [Online]. 2006. Available from: http://www.astm.org/Standards/E2456.htm [April, 2013]

[26] Wijnhoven, S. W. P., et al. Nanosilver – a review of available data and knowledge gaps in human and environmental risk assessment. Nanotoxicology 3 (2009): 109-138.

[27] Morones, J. R., et al. The bactericidal effect of silver nanoparticles. Nanotechnology 16 (2005): 2346-2353.

[28] Baker, C., Pradhan, A., Pakstis, L., Pochan, D. J., and Shah, S. I. Synthesis and antibacterial properties of silver nanoparticles. Journal of Nanoscience and Nanotechnology 5 (2005): 244-249.

[29] El-Badawy, A., Feldhake, D., and Venkatapathy, R. State of the science, literature review: Everything nanosilver and more. Washington: U.S. Environmental Protection Agency, Office of Research and Development, 2010.

[30] Kumlangdudsana, P. Fabrication and development of silver nanoparticles microelectrode for lab on a chip application by flow deposition technique. Doctoral dissertation, Nanoscience and Technology Program, Graduate School, Chulalongkorn University, 2011.

[31] Korbekandi, H., and Iravani, S. The delivery of nanoparticles: Silver nanoparticles. Croatia: In Tech, 2012.

[32] Lei, G. Synthesis of nano-silver colloids and their antimicrobial effects. Master's Thesis, Materials Science & Engineering, The Virginia Polytechnic Institute and State University Blacksburg, 2007.

[33] Tolaymat, T., El Badawy, A., Genaidy, A., Scheckel, K., Luxton, T., and Suidan, M. An evidence-based environmental perspective of manufactured silver nanoparticle in syntheses and applications: A systematic review and critical appraisal of peer-reviewed scientific papers. Science of The Total Environment 408 (2010): 999-1006.

[34] Merga, G., Wilson, R., Lynn, G., Milosavljevic, B., and Meisel, D. Redox catalysis on "naked" silver nanoparticles. The Journal of Physical Chemistry C 111 (2007): 12220–12226.

[35] Wiley, B., Sun, Y., Mayers, B., and Xi, Y. Shape-controlled synthesis of metal nanostructures: The case of silver. Chemistry: A European Journal 11 (2005): 454-463.

[36] Amendola, V., Polizzi, S., and Meneghetti, M. Free silver nanoparticles synthesized by laser ablation in organic solvents and their easy functionalization. Langmuir 23 (2007): 6766-6770.

[37] Kim, J. S., et al. Antimicrobial effects of silver nanoparticles. Nanomedicine 3 (2007): 95-101.

[38] Nikolaj, L., Kildeby, O. Z., Andersen, R. E., Roge, T. L., Petersen, R., and Riis, J. F. Silver nanoparticles. Denmark: Institute for Physics and Nanotechnology - Aalborg University, 2006.

[39] Oliveira, M., Ugarte, D., Zanchet, D., and Zarbin, A., Influence of synthetic parameters on the size, structure, and stability of dodecanethiol-stabilized silver nanoparticles. Journal of Colloid and Interface Science 292 (2005): 429-435.

[40] Olenin, A. Y., Krutyakov, Y. A., Kudrinskii, A. A., and Lisichkin, G. V. Formation of surface layers on silver nanoparticles in aqueous and water-organic media. Colloid Journal 70 (2008): 71–76.

[41] Si, S., and Mandal, T. K. Tryptophan-based peptides to synthesize gold and silver nanoparticles: A mechanistic and kinetic study. Chemistry: A European Journal 13 (2007): 3160–3168.

[42] Wacharanad, S. Controlled release of Ag^{+} from silver nanoparticles deposited into polyelectrolyte multilayers and their antibacterial and anticancer activities. Doctoral dissertation, Nanoscience and Technology Program, Graduate School, Chulalongkorn University, 2012.

[43] Gong, X., Han, L., Gao, J., and Gao, C. Stability of polyelectrolyte multilayer micropatterns in response to post-treatments. Colloids and Surfaces A: Physicochemical and Engineering Aspects 396 (2012): 299-304.

[44] Adikwu, M. U. Biopolymers in drug delivery: Recent advances and challenges. Netherlands: Bentham Science Publishers, 2009.

[45] Mattern, R. The molecular structures of different types of carrageenan [Online]. 2009. Available from: http://de.academic.ru/dic.nsf/dewiki/752005 [July, 2013]

[46] Gauglitz, G., and Vo-Dinh, T. Handbook of spectroscopy: UV/VIS spectrometers. Germany: WILEY-VCH Verlag GmbH & Co. KGaA, 2003.

[47] Michigan State University. UV-Visible spectroscopy [Online]. 2013. Available from: http://www2.chemistry.msu.edu/faculty/reusch/VirtTxtJml/Spectrpy/UV-Vis/uvspec.htm#uv1 [May, 2013]

[48] Mehta, A. Ultraviolet-Visible (UV-Vis) spectroscopy – principle [Online]. 2011. Available from: http://pharmaxchange.info/press/2011/12/ultraviolet-visible-uv-vis-spectroscopy-principle/ [May, 2013]

[49] Ball, D. W. The basics of spectroscopy. Washington: SPIE—The International Society for Optical Engineering, 2001.

[50] Warisnoicharoen, W., Hongpiticharoen, P., and Lawanprasert, S. Alteration in enzymatic function of human cytochrome P450 by silver nanoparticles. Research Journal of Environmental Toxicology 5 (2011): 58-64.

[51] Smitha, S. L., Nissamudeen, K. M., Philip, D., and Gopchandran, K. G. Studies on surface plasmon resonance and photoluminescence of silver nanoparticles. Spectrochimica Acta Part A 71 (2008): 186–190.

[52] Malvern Instruments Ltd. Zetasizer Nano Series [Online]. 2004. Available from: http://www.biophysics.bioc.cam.ac.uk/files/Zetasizer_Nano_user_manual_Man0317-1.1.pdf [May, 2013]

[53] Peternelj, A. Charge and size of particles in surface waters. Master's Thesis, Department of Chemical Engineering, Lunds University, 2009.

[54] Arzensek, D. Dynamic light scattering and application to proteins in solutions. Slovenia: University of Ljubljana, 2010.

[55] McNaught, A. D., and Wilkinson, A. Compendium of chemical terminology: definition of electrokinetic potential. Oxford: Blackwell Scientific Publications, 1997.

[56] Freire, J. M., et al. Using zeta-potential measurements to quantify peptide partition to lipid membranes. European Biophysics Journal 40 (2001): 481-487.

[57] Sjoblom, J. Emulsions and emulsion stability. vol. 132. Florida: Taylor & Francis Group, CRC Press, 2006.

[58] Duzgunes, N. Nanomedicine: Infectious diseases, immunotherapy, diagnostics, antifibrotics, toxicology and gene medicine. vol. 509. Massachusetts: Elsevier, 2012.

[59] Mendez-Vilas, A. and Diaz, J. Investigation of nanostructured organic solar cells with transmission electron microscopy. vol. 3. Spain: Formatex, 2010.

[60] Orlova, E. V., and Saibil, H. R. Structural analysis of macromolecular assemblies by electron microscopy. Chemical Reviews 111 (2011): 7710–7748.

[61] Alberts, B., Johnson, A., Lewis, J., Raff, M., Roberts, K., and Walter, P. Molecular biology of the cell: Looking at the structure of cells in the microscope. New York: Garland Science, Taylor & Francis Group, 2007.

[62] Ciccarelli, F. D., Doerks, T., von Mering, C., Creevey, C. J., Snel, B., and Bork, P. Toward automatic reconstruction of a highly resolved tree of life. Science 311 (2006): 1283 - 1287.

[63] Hooke, R. Microbiology: Bacteria [Online]. 2013. Available from: http://www.microbiologyonline.org.uk/about-microbiology/introducing-microbes/bacteria [May, 2013]

[64] Anderson, R. J., Groundwater, P. W., Todd, A. and Worsley, A. J. Antibacterial agents: Chemistry, mode of action, mechanisms of resistance and clinical applications. New York: John Wiley & Sons, Ltd., 2012.

[65] Ramphal, R., Gulig, P. A., and Schain, D. Bacterial classification and disease [Online]. 2013. Available from: http://old.mgm.ufl.edu/~gulig/mmid/lectures/classification_and_disease_revised.pdf. [May, 2013]

[66] Davies, J. A., Anderson, G. K., Beveridge, T. J., and Clark, H. C. Chemical mechanism of the Gram stain and synthesis of a new electron-opaque marker for electron microscopy which replaces the iodine mordant of the stain. Journal of Bacteriology 156 (1983): 837-845.

[67] Plata, K., Rosato, A. E., and Wegrzyn, G. *Staphylococcus aureus* as an infectious agent: Overview of biochemistry and molecular genetics of its pathogenicity. Acta Biochimica Polonica 56 (2009): 597–612.

[68] Carr, J. H. *Staphylococcus aureus* VISA [Online]. 2001. Available from: http://en.wikipedia.org/wiki/File:Staphylococcus_aureus_VISA_2.jpg [May, 2013]

[69] Tambe, Y. Microscopic image of *Staphylococcus aureus*, gram staining [Online]. 2005. Available from: http://en.wikipedia.org/wiki/File:Staphylococcus_aureus_Gram.jpg [May, 2013]

[70] Kornacki, J. L. Principles of microbiological troubleshooting in the industrial food processing environment food microbiology and food safety. New York: Springer, 2010.

[71] Al-Hamdani, M. A., and Hamad, I. G. Study of plasmid profile, susceptibility patterns of clinical *Staphylococcus aureus* isolated from patients with otitis media in Basrah. Journal of Basrah Researches ((Sciences)) 38 (2012): 79-89.

[72] Carr, J. H. *Escherichia coli* [Online]. 2012. Available from: http:// drtummy.com/ index.php?option=com_content&view=article&catid=54:headers&id=144:escherichia-coli&Itemid=57 [May, 2013]

[73] Tambe, Y. Microscopic image of *Escherichia coli*, gram staining [Online]. Available from: http://commons.wikimedia.org/wiki/File:Escherichia_coli_Gram.jpg [May, 2013]

[74] Tchobanoglous, G. and Schroeder, E. D. Water quality: Characteristics, modeling, modification. vol. 1. Boston: Addison-Wesley, 1985.

[75] Moder, J. *Escherichia coli* [Online]. 2008. Available from: http://bioweb.uwlax.edu/bio203/s2008/moder_just/about%20the%20author.htm [May, 2013]

[76] Gross, R. J. The pathogenesis of *Escherichia coli* diarrhoea. Reviews in Medical Microbiology (1991): 37-44.

[77] Angert, E. R. Alternatives to binary fission in bacteria. Nature Reviews Microbiology 3 (2005): 214-224.

[78] Zwietering, M. H., Jongenburger, I. Rombouts, F. M., and van't Riet, K. Modeling of the bacterial growth curve. Applied and Environmental Microbiology 56 (1990): 1875–1881.

[79] Koch, A. L. Turbidity measurements of bacterial cultures in some available commercial instruments. Analytical Biochemistry 38 (1970): 252–259.

[80] Pearson Education, Inc., publishing as Benjamin Cummings. Bacterial growth curve [Online]. 2007. Available from: http://www.professorcrista.com/files/animations/posted_animations/bacterial_growth_curve.html [May 2014]

[81] Todar, K. The growth of bacterial populations [Online]. 2012. Available from: http://textbookofbacteriology.net/growth_3.html [May 2014]

[82] Becker, R. O. Silver ions in the treatment of local infections. Metal-Based Drugs 6 (1999): 297-300.

[83] Monafo, W. W, and Freedman, B. Topical therapy for burns. The Surgical Clinics of North America 67 (1987): 133-145.

[84] Sampath, L. A., Chaowdhury, N., Caraos, L., and Modak, S. M. Infection resistance of surface modified catheters with either short-lived or prolonged activity. The Journal of Hospital Infection 30 (1995): 201-210.

[85] Mendez-Vilas, A. and Diaz, J. Science against microbial pathogens: Communicating current research and technological advances. Spain: Formatex, 2011.

[86] Dallas, P., Sharma, V. K., and Zboril, R. Silver polymeric nanocomposites as advanced antimicrobial agents: Classication, synthetic paths, applications, and perspectives. Advances in Colloid and Interface Science 166 (2011): 119-135.

[87] Yin, H. Q., Langford, R., and Burrell, R. E. Comparative evaluation of the antimicrobial activity of Acticoat antimicrobial barrier dressing. The Journal of Burn Care & Rehabilitation 20 (1999): 195-200.

[88] Percival, S. L., Bowler, P. G., and Dolman, J. Antimicrobial activity of silver containing dressings on wound microorganisms using an in vitro biofilm model. International Wound Journal 4 (2007): 186-191.

[89] Wright, J. B., Lam, K., and Burrell, R. E. Wound management in an era of increasing bacterial antibiotic resistance: A role for topical silver treatment. American Journal of Infection Control 6 (1998): 572-577.

[90] Zhao, G. and Stevens, S. J. Multiple parameters for the comprehensive evaluation of the susceptibility of *Escherichia coli* to the silver ion. Biometals 11 (1998): 27-32.

[91] Slawson, R. M., Van Dyke, M. I., Lee, H., and Trevors, J. T. Germanium and silver resistance, accumulation, and toxicity in microorganisms. Plasmid 27 (1992): 72-79.

[92] Sondi, I. and Salopek-Sondi, B. Silver nanoparticles as antimicrobial agent: A case study on *E. coli* as a model for Gram-negative bacteria. Journal of Colloid and Interface Science 275 (2004): 177-182.

[93] Pal, G., et al. Effect of low intensity laser interaction with human skin fibroblast cells using fiber-optic nano-probes. Journal of Photochemistry and Photobiology. B, Biology 86 (2007): 252-261.

[94] Dastjerdi, R., and Montazer, M. A review on the application of inorganic nano-structured materials in the modification of textiles: Focus on anti-microbial properties. Colloids and Surfaces. B, Biointerfaces 79 (2010): 5-18.

[95] Percival, S. L., Bowler, P. G., and Russell, D. Bacterial resistance to silver in wound care. The Journal of Hospital Infection 60 (2005): 1-7.

[96] Yang, W., et al. Food storage material silver nanoparticles interfere with DNA replication fidelity and bind with DNA. Nanotechnology 20 (2009): 85102-85102.

[97] Patterson, S. D., and Aebersold, R. H. Proteomics: The first decade and beyond. Nature Genetics 33 (2003): 311-323.

[98] Lim, M. S., and Elenitoba-Johnson, K. S. Proteomics in pathology research. Laboratory Investigation 84 (2004): 1227-1244.

[99] Wilkins, M. R., et al. From proteins to proteomes: Large scale protein identification by two-dimensional electrophoresis and amino acid analysis. Biotechnology 14 (1996): 61-65.

[100] Gallagher, S. R. Current protocols in cell biology: One-dimensional SDS gel electrophoresis of proteins. New York: John Wiley and Sons, Inc., 2007.

[101] Pederson, T. Turning a PAGE: The overnight sensation of SDS-polycrylamide gel electrophoresis. The FASEB Journal 22 (2008): 949-953.

[102] Bay Area Biotechnology Education Consortium. SDS polyacrylamide gel electrophoresis (SDS-PAGE): Analysis of purified fluorescent protein. San Francisco: BABEC, 2012.

[103] Wikibooks. Protein separations-one dimensional gel electrophoresis [Online]. 2011. Available from: http://en.wikibooks.org/wiki/Proteomics/Protein_Separations-_Electrophoresis/One_Dimensional_Gel_Electrophoresis [May 2013]

[104] Issaq, H. J., and Veenstra, T. D. Two-dimensional polyacrylamide gel electrophoresis (2D-PAGE): Advances and perspectives. BioTechniques 44 (2008): 697-700.

[105] Randox Research and Development. Gel electrophoresis and blotting techniques [Online]. 2009. Available from: http://www.randoxlifesciences.com/Content/useruploads/Support/Catalogue/Gel_Electrophoresis.pdf [May, 2013]

[106] Perkins, D. N., Pappin, D. J., Creasy, D. M., and Cottrell, J. S. Probability-based protein identification by searching sequence databases using mass spectrometry data. Electrophoresis 20 (1999): 3551-3567.

[107] Prasain, J. Tandem mass spectrometry - applications and principles. Croatia: InTech, 2012.

[108] Barker, G., Want, E. J., Boydston, J. and Siuzdak, G. Analytics of synthetic peptides: Mass spectrometry. New York: John Wiley & Sons, Ltd., 2003.

[109] Hoffmann, E. Tandem mass spectrometry: A primer. Journal of Mass Spectrometry 31 (1996): 129-137.

[110] Jones, C. M. Characterization of macromolecular protein assembies by collision-induced and surfaceinduced dissociation: Expanding the role of mass spectrometry in structural biology. Doctoral dissertation, Department of Chemistry, The University of Arizona, 2008.

[111] Halket, J. M., Waterman, D., Przyborowska, A. M., Patel, R. K., Fraser, P. D., and Bramley, P. M. Chemical derivatization and mass spectral libraries in metabolic profiling by GC/MS and LC/MS/MS. Journal of Experimental Botany 56 (2005): 219-243.

[112] Pitt, J. J. Principles and applications of liquid chromatography-mass spectrometry in clinical biochemistry. The Clinical Biochemist Reviews 30 (2009): 19-34.

[113] Keet, C. M. and Franconi, E. Computer science & IT with/for biology. Italy: CSBio Reader, 2005.

[114] Wingender, E., Crass, T., Hogan, J. D., Kel, A. E., Kel-Margoulis, O. V., and Potapov, A. P. Integrative content-driven concepts for bioinformatics “beyond the cell”. Journal of Biosciences 32 (2007): 169-180.

[115] Wikipedia. Bioinformatics [Online]. 2013. Available from: http://en.wikipedia.org/wiki/Bioinformatics [May, 2013]

[116] Edwards, Y. J., and Cottage, A. Bioinformatics methods to predict protein structure and function. A practical approach. Molecular Biotechnology 23 (2003): 139-166.

[117] Solomon, S. D., Bahadory, M., Jeyarajasingam, A. V., Rutkowsky, S. A., and Boritz, C. Synthesis and study of silver nanoparticles. Journal of Chemical Education 84 (2007): 322-325.

[118] Lowry, O. H., Rosebrough, N. J., Fair, A. L., and Randall, R. J. Protein measurement with the Folin phenol reagent. The Journal of Biological Chemistry 193 (1951): 265-275.

[119] Laemmli, U. K. Cleavage of structural proteins during the assembly of the head of bacteriophage T4. Nature 227 (1970): 680-685.

[120] Blum, H., Beier, H., and Gross, H. J. Improved silver staining of plant protein, RNA and DNA in polyacrylamide gels. Electrophoresis 8 (1987): 93-99.

[121] Sambrook, J., Fritsch, E. F., and Maniatis, T. Molecular cloning: A laboratory manual. New York: Cold Spring Harbor Laboratory Press, 1989.

[122] Jaresitthikunchai, J., Phaonakrop, N., Kittisenachai, S., and Roytrakul, S. Rapid in-gel digestion protocol for protein identification by peptide mass fingerprint. In The 2nd Biochemistry and Molecular Biology Conference: Biochemistry and Molecular Biology for Regional Sustainable Development. Khon Kaen, Thailand, 2009.

[123] Johansson, C., Samskog, J., Sundstrom, L., Wadensten, H., Bjorkesten, L., and Flensburg, J. Differential expression analysis of *Escherichia coli* proteins using a novel software for relative quantitation of LC-MS/MS data. Proteomics 6 (2006): 4475-4485.

[124] Thorsell, A., Portelius, E., Blennow, K., and Westman-Brinkmalm, A. Evaluation of sample fractionation using microscale liquid-phase isoelectric focusing on mass spectrometric identification and quantitation of proteins in a SILAC experiment. Rapid Communications in Mass Spectrometry 21 (2007): 771-778.

[125] Szklarczyk, D., et al. The STRING database in 2011: Functional interaction networks of proteins, globally integrated and scored. Nucleic Acids Research 39 (2011): 561–568.

[126] Yamamoto, S., Fujiwara, K., and Watari, H. Surface-enhanced raman scattering from oleate-stabilized silver colloids at a liquid/liquid interface. Analytical Sciences 20 (2004): 1347–1352.

[127] Sileikaite, A., Prosycevas, I., Puiso, J., Juraitis, A., and Guobiene, A. Analysis of silver nanoparticles produced by chemical reduction of silver salt solution. Materials Science 12 (2006): 287-291.

[128] Sonavane, G., Tomoda, K., and Makino, K. Biodistribution of colloidal gold nanoparticles after intravenous administration: Effect of particle size. Colloids and Surfaces B: Biointerfaces 66 (2008): 274–280.

[129] Jang, S. P., Lee, J. H., Hwang, K. S., Moon, H. J., and Choi, S. U. Response to "comment on 'particle concentration and tube size dependence of viscosities of Al_2O_3-water nanofluids flowing through microand minitubes'". Applied Physics Letters 94 (2009): 066102.

[130] Khlebtsov, B. N., and Khlebtsov, N. G. On the measurement of gold nanoparticle sizes by the dynamic light scattering method. Colloid Journal 73 (2011): 118–127.

[131] Guzman, M. G., Dille, J., and Godet, S. Synthesis of silver nanoparticles by chemical reduction method and their antibacterial activity. International Journal of Chemical and Biological Engineering 2 (2009): 104-111.

[132] Dallas, P., Sharma, V. K., and Zboril, R. Silver polymeric nanocomposites as advanced antimicrobial agents: Classification, synthetic paths, applications, and perspectives. Advances in Colloid and Interface Science 166 (2011): 119-135.

[133] Kumar, A., Vemula, P. K., Ajayan, P. M., and John, G., Silver-nanoparticle embedded antimicrobial paints based on vegetable oil. Nature Materials 7 (2008): 236-41.

[134] Gupta, P., Bajpai, M., and Bajpai, S. K. Investigation of antibacterial properties of silver nanoparticle-loaded poly (acrylamide-co-itaconic acid)-grafted cotton fabric. The Journal of Cotton Science 12 (2008): 280-286.

[135] Singh, V., Pande, P. C., and Jain, D. K. A text book of botany. India: Rakesh Kumar Rastogi, 2009.

[136] Winkler, C., Denker, K., Wortelkamp, S., and Sickmann, A. Silver- and Coomassie-staining protocols: Detection limits and compatibility with ESI MS. Electrophoresis 28 (2007): 2095–2099.

[137] Chauhan, A. K., and Varma, A. Textbook of Molecular Biotechnology. India: I. K. International Pvt Ltd., 2009.

[138] Li, Q. W., et al. Comparative proteomic analysis suggests that mitochondria are involved in autosomal recessive polycystic kidney disease. Proteomics 12 (2012): 2556-2570.

[139] Fraser, H. I., Kvaratskhelia, M., and White, M. F. The two analogous phosphoglycerate mutases of *Escherichia coli*. FEBS Letters 455 (1999): 344-348.

[140] Belunis, C. J., and Raetz, C. R. Biosynthesis of endotoxins. Purification and catalytic properties of 3-deoxy-D-manno-octulosonic acid transferase from *Escherichia coli*. The Journal of Biological Chemistry 267 (1992): 9988-9997.

[141] Brabetz, W., Lindner, B., and Brade, H. Comparative analyses of secondary gene products of 3-deoxy-D-manno-oct-2-ulosonic acid transferases from Chlamydiaceae in *Escherichia coli* K-12. European Journal of Biochemistry 267 (2000): 5458-5465.

[142] Kumar, G. B, and Black, P. N. Bacterial long-chain fatty acid transport. Identification of amino acid residues within the outer membrane protein FadL required for activity. The Journal of Biological Chemistry 268 (1993): 15469-15476.

[143] Cottingham, K. Network of proteins involved in antibiotic resistance. Journal of Proteome 7 (2008): 3640–3640.

[144] Li, W. R., Xie, X. B., Shi, Q. S., Duan, S. S., Ouyang, Y. S., and Chen, Y. B. Antibacterial effect of silver nanoparticles on *Staphylococcus aureus*. Biometals 24 (2011): 135-141.

[145] Li, W. R., Xie, X. B., Shi, Q. S., Zeng, H. Y., Ou-Yang, Y. S., and Chen, Y. B. Antibacterial activity and mechanism of silver nanoparticles on *Escherichia coli*. Applied Microbiology and Biotechnology 85 (2010): 1115–1122.

[146] Jung, W. K., Koo, H. C., Kim, K. W., Shin, S., Kim, S. H., and Park, Y. H. Antibacterial activity and mechanism of action of the silver ion in *Staphylococcus aureus* and *Escherichia coli*. Applied and Environmental Microbiology 74 (2008): 2171–2178.

[147] Lok, C. N., et al. Proteomic analysis of the mode of antibacterial action of silver nanoparticles. Journal of Proteome Research 5 (2006): 916-924.

[148] Rizzello, L. and Pompa, P. P. Nanosilver-based antibacterial drugs and devices: Mechanisms, methodological drawbacks, and guidelines. Chemical Society Reviews 43 (2014): 1501-1518.

[149] Ceciliani, F., Caramori, T., Ronchi, S., Tedeschi, G., Mortarino, M., and Galizzi, A. Cloning, overexpression, and purification of *Escherichia coli* quinolinate synthetase. Protein Expression and Purification 18 (2000): 64-70.

[150] Ollagnier-de Choudens, S., Loiseau, L., Sanakis, Y., Barras, F., and Fontecave, M. Quinolinate synthetase, an iron-sulfur enzyme in NAD biosynthesis. FEBS Letters 579 (2005): 3737-3743.

[151] Cicchillo, R. M., Tu, L., Stromberg, J. A., Hoffart, L. M., Krebs, C., and Booker, S. J. *Escherichia coli* quinolinate synthetase does indeed harbor a [4Fe-4S] cluster. Journal of the American Chemical Society 127 (2005): 7310-7311.

[152] Koonin, E. V. *Escherichia coli* dinG gene encodes a putative DNA helicase related to a group of eukaryotic helicases including Rad3 protein. Nucleic Acids Research 21 (1993): 1497-1497.

[153] Freedman, L. P., Zengel, J. M., Archer, R. H., and Lindahl, L. Autogenous control of the S10 ribosomal protein operon of *Escherichia coli*: genetic dissection of transcriptional and posttranscriptional regulation. Proceedings of The National Academy of Sciences of The United States of America 84 (1987): 6516-6520.

[154] Lange, P. F., Huesgen, P. F., and Overall, C. M. TopFIND 2.0—linking protein termini with proteolytic processing and modifications altering protein function. Nucleic Acids Research 40 (2012): 351-361.

[155] Schreurs, W. J. A., and Rosenberg, H. Effect of silver ions on transport and retention of phosphate by *Escherichia coli*. Journal of Bacteriology 152 (1982): 7-13.

[156] Baltz, R. H. Daptomycin: Mechanisms of action and resistance and biosynthetic engineering. Current Opinion in Chemical Biology 13 (2009): 144-151.

[157] Chopra, I., Hawkey, P. M., and Hinton, M. Tetracyclines, molecular and clinical aspects. The Journal of Antimicrobial Chemotherapy 29 (1992): 245-277.

[158] Monteiro, R., et al. Proteome of a methicillin-resistant *Staphylococcus aureus* clinical strain of sequence type ST398. Journal of Proteomics 75 (2012): 2892-2915.

[159] Poutanen, M., Varhimo, E., Kalkkinen, N., Sukura, A., Varmanen, P., and Savijoki, K. Two-dimensional difference gel electrophoresis analysis of *Streptococcus uberis* in response to mutagenesis-inducing ciprofloxacin challenge. Journal of Proteome Research 8 (2009): 246–255.

[160] Neri, A., et al. *Neisseria meningitidis* rifampicin resistant strains: Analysis of protein differentially expressed. BMC Microbiology 10 (2010): 246-253.

.

APPENDICES

1. Preliminary test of antibacterial susceptibility by Kirby Bauer diffusion method

Table A-1 Zone of inhibition (mm) of colloidal AgNPs prepared at different conditions against various kind of bacteria. (mean ± S.D., n= 3).

Microorganisms	Inhibition zone (mm)			
	10 mM $AgNO_3$	AgNPs		
		PSSMA	Alginate	Carrageenan
1. *E. coli* ATCC 25922	10.30 ± 0.02	9.72 ± 0.02	8.93 ± 0.49	9.08 ± 0.07
2. *S. aureous* ATCC 25923	9.43 ± 0.04	9.58 ± 0.26	8.82 ± 0.29	8.89 ± 0.03
3. *L. salivarius* ATCC 11741	9.13 ± 0.03	9.16 ± 0.02	8.68 ± 0.34	8.54 ± 0.52
4. *K. rhizophila* ATCC 9341	10.28 ± 0.25	9.70 ± 0.17	8.63 ± 0.07	8.65 ± 0.27

2. Preparation of bacteria for bacterial growth curve study

For example: Preparation 0.1 OD (OD 600 nm) of *S. aureus* ATCC 25923 5 mL for bacterial growth study

$$OD_1V_1 = OD_2V_2$$

OD_1 = OD of the broth culture, inoculated the previous day

V_1 = volume of this broth culture to be added to the inoculums

OD_2 = OD of the inoculum (as a standard, this value was adjusted to 0.1)

V_2 = volume of the inoculums (in this experiment, 5 mL)

If OD_1 after measurement at OD 600 nm is 1.38

and OD of blank at OD 600 nm is 0.07.

From

$$OD_1V_1 = OD_2V_2$$

$$(1.38-0.07)V_1 = (0.1)(5\ mL)$$

$$V_1 = \frac{0.1\times5}{1.31}$$

$$= 0.38\ mL \text{ or } 380\ \mu L$$

Therefore, 380 µL of the *S. aureus* ATCC 25923 broth culture will be added, and then continued adding with TSB broth until 5 mL to obtain inoculum of 0.1 OD *S. aureus* ATCC 25923 5 mL.

3. The effect of PSSMA on bacterial growth curve

Table A-2 The effect of PSSMA on *S. aureus* ATCC 25923 growth

Time (h)	Control	PSSMA	Synthesized AgNPs
0.08	0.06	0.05	0.02
1	0.09	0.09	0.01
2	0.16	0.17	0.08
4	0.30	0.34	0.10
6	0.48	0.47	0.09
24	1.01	1.17	0.05

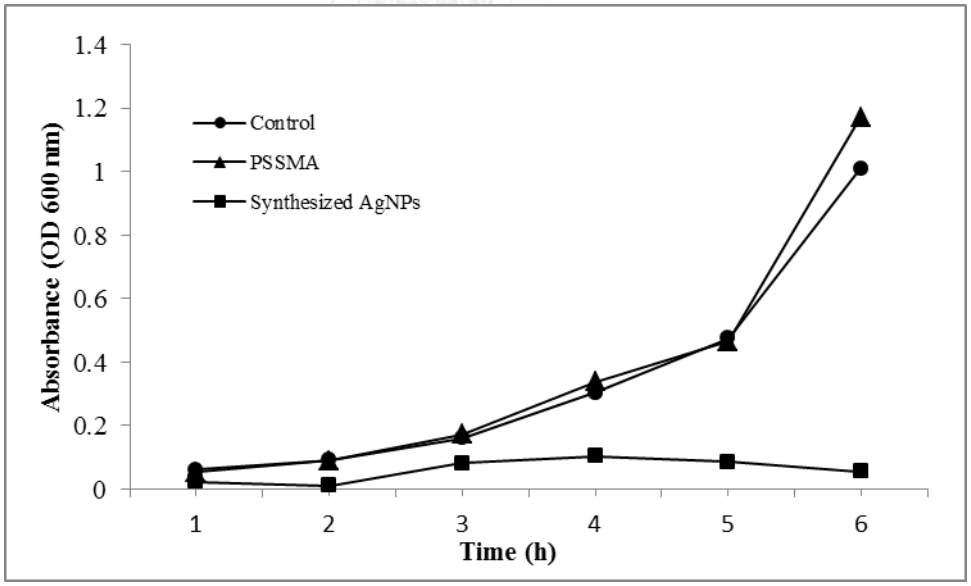

Figure A-1 The bacterial growth curve of *S. aureus* ATCC 25923 after exposed to PSSMA and AgNPs compared with control.

Table A-3 The effect of PSSMA on *E. coli* ATCC 25922 growth

Time (h)	Control	PSSMA	Synthesized AgNPs
0.08	0.05	0.03	0.02
1	0.06	0.05	0.03
2	0.11	0.08	0.02
4	0.39	0.29	0.02
6	0.53	0.40	0.04
24	0.67	0.67	0.04

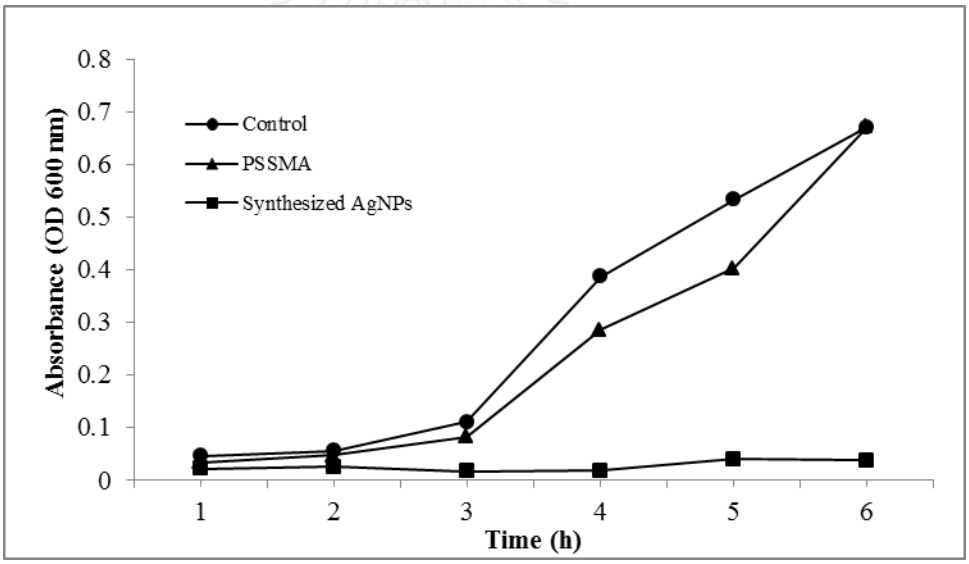

Figure A-2 The bacterial growth curve of *E. coli* ATCC 25922 after exposed to PSSMA and AgNPs compared with control.

4. Protein determination by Lowry assay

4.1 Standard curve

The total proteins were extracted from the *S. aureus* ATCC 25923 and *E. coli* ATCC 25922 cells after exposed and unexposed to AgNPs. The proteins concentrations were determined according to the method of Lowry. BSA standard curve, plotted between OD_{750} on Y-axis and BSA concentration (µg/µL) on X-axis has R^2 = 0.9985, is shown in Figure A-3.

Table A-4 Standard curve using BSA (OD 750 nm) by Lowry assay

0.5% SDS	5 µL	4 µL	3 µL	2 µL	1 µL	0 µL
BSA	0 µL	1 µL	2 µL	3 µL	4 µL	5 µL
OD 750 (Average)	0.07	0.10	0.13	0.15	0.19	0.21

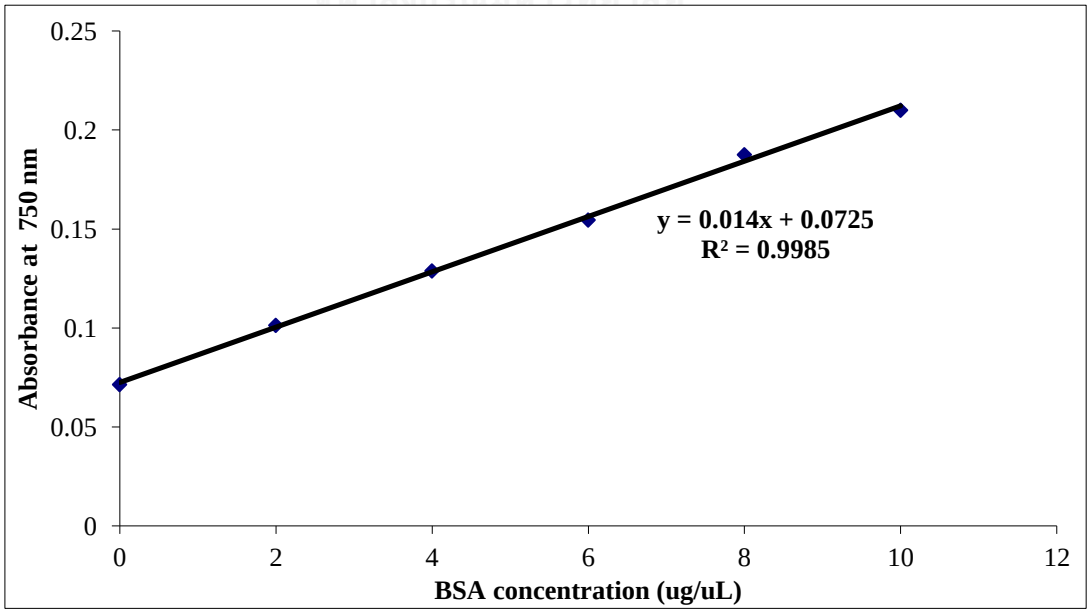

Figure A-3 The BSA standard curve (OD 750 nm)

4.2 Protein concentration

Protein concentration (µg protein/µL) of collected *S. aureus* ATCC 25923 and *E. coli* ATCC 25922 cells after exposed and unexposed to AgNPs with different time intervals were calculated using the standard curve and demonstrated in Table A-5.

$$Y = mx + c$$

Y = Readable OD 750 nm, m = Slope or gradient

x = Protein concentration, c = The Y intercept

Therefore;

Protein concentration (µg/µL) = $x = \frac{Y-c}{m}$

Table A-5 Protein concentrations of *S. aureus* ATCC 25923 and *E. coli* ATCC 25922 after unexposed (control) and exposed to AgNPs with different time intervals.

	Time intervals	µg protein/µL	
		Protein concentration after exposure to AgNPs	Protein concentration after unexposure to AgNPs
S. aureus	0 min	3.36	4.95
	15 min	3.67	3.97
	30 min	4.19	4.78
	45 min	5.16	3.52
	1 h	3.73	4.27
	2 h	5.82	4.09
	3 h	6.98	3.95
E. coli	0 min	10.56	7.69
	15 min	10.65	7.87
	30 min	8.84	8.63
	45 min	9.36	7.83
	1 h	11.09	8.80
	2 h	11.46	8.11
	3 h	10.46	8.06

Table A-6 Protein concentration of *S. aureus* ATCC 25923 and *E. coli* ATCC 25922 after unexposed to AgNPs (control) and amount of each component for SDS-PAGE analysis

Protein concentration and amount of each component for SDS-PAGE analysis (Prepare 40 µg for 9 µL (2x vol = 18 µL))						
Bacterial strains	**Time (min)**	**Average OD750**	**Protein Concentration (µg/µL)**	**Bacterial protein unexposed to AgNPs (µL)**	**0.5%SDS (µL)**	**Loading dye (µL)**
S. aureus	0	0.12	3.36	11.90	0.10	6.00
	15	0.12	3.67	10.90	1.10	6.00
	30	0.13	4.19	9.50	2.50	6.00
	45	0.14	5.16	7.80	4.20	6.00
	60	0.12	3.73	10.70	1.30	6.00
	120	0.15	5.82	6.90	5.10	6.00
	180	0.17	6.98	5.70	6.30	6.00
E. coli	0	0.22	10.56	3.80	8.20	6.00
	15	0.22	10.65	3.80	8.20	6.00
	30	0.20	8.84	4.50	7.50	6.00
	45	0.20	9.36	4.30	7.70	6.00
	60	0.23	11.09	3.60	8.40	6.00
	120	0.23	11.46	3.50	8.50	6.00
	180	0.22	10.46	3.80	8.20	6.00

Table A-7 Protein concentration of *S. aureus* ATCC 25923 and *E. coli* ATCC 25922 after exposed to AgNPs and amount of each component for SDS-PAGE analysis

Protein concentration and amount of each component for SDS-PAGE analysis (Prepare 40 µg for 9 µL (2x vol = 18 µL))						
Bacterial strains	**Time (min)**	**Average OD750**	**Protein Concentration (µg/µL)**	**Bacterial protein exposed to AgNPs (µL)**	**0.5%SDS (µL)**	**Loading dye (µL)**
S. aureus	0	0.14	4.95	8.10	3.90	6.00
	15	0.13	3.97	10.10	1.90	6.00
	30	0.14	4.78	8.40	3.60	6.00
	45	0.12	3.52	11.40	0.60	6.00
	60	0.13	4.27	9.40	2.60	6.00
	120	0.13	4.09	9.80	2.20	6.00
	180	0.13	3.95	10.10	1.90	6.00
E. coli	0	0.18	7.69	5.20	6.80	6.00
	15	0.18	7.87	5.10	6.90	6.00
	30	0.19	8.63	4.60	7.40	6.00
	45	0.18	7.83	5.10	6.90	6.00
	60	0.20	8.80	4.50	7.50	6.00
	120	0.19	8.11	4.90	7.10	6.00
	180	0.19	8.06	5.00	7.00	6.00

VITA

Miss Hathaichanok Tamiyakul was born on June 30, 1987 in Singburi, Thailand. She received Bachelor's Degree in Biological Science with First Class Honours from Kasetsart University in 2009. After that, she continued her Doctorate's Degree in Nanoscience and Technology Program, Faculty of Graduate School, Chulalongkorn University in 2010. During her graduate study, she also received a research scholarship from The 90th Anniversary of Chulalongkorn University Fund (Ratchadaphiseksomphot Endowment Fund), Center of Innovative Nanotechnology (CIN) Research Fellowship, and Nanoscience and Technology Research Fund. She has completed her study leading to a Doctor of Philosophy (Ph.D.) in Nanoscience and Technology Program in Academic Year 2014.

VITA (CONT.)

Publications

Tamiyakul, H., Dubas, S. T., and Warisnoicharoen, W. Preparation and characterization of hydrocolloid stabilized silver nanoparticles. Advanced Materials Research 1060 (2015): 115-118.

Tamiyakul, H., Tanasupawat, S., Dubas, S. T., and Warisnoicharoen, W. Antibacterial potential of silver nanoparticles capped with poly(4-styrenesulfonic acid-co-maleic acid) polymer. Advanced Materials Research (accepted)

Tamiyakul, H., Roytrakul, S., Jaresitthikunchai, J., Phaonakrop, N., Tanasupawat, S., and Warisnoicharoen, W. Antibacterial activity and mechanism of silver nanoparticles on *Staphylococcus aureus* and *Escherichia coli*. Applied Microbiology and Biotechnology (in preparation)

Conference Presentations

Tamiyakul, H., and Warisnoicharoen, W. Silver nanoparticles down-regulate cellular proteins of *Escherichia coli*. Nanoscience and Nanomedicine Workshop (NTU MSE, IGS & CU), September 2014, Singapore

Tamiyakul, H., Roytrakul, S., Jaresitthikunchai, J., Phaonakrop, N., Tanasupawat, S., and Warisnoicharoen, W. Early response to silver nanoparticles on protein expression of *Escherichia coli*. The 7th Asia Oceania Human Protein Organization Congress and 9th International Symposium of the Protein Society of Thailand (AOHUPO), August 2014, Bangkok, Thailand